The roles of RAS in controlling cell fate – a yeast model of oncogenic potential

A thesis submitted to the University of Kent for the degree of

M.Sc. Cell Biology in the Faculty of Science

2021

Fiona Dresel

School of Biosciences

University of Kent

I Declaration

No part of this thesis has been submitted in support of an application for any degree or qualification of the University of Kent or any other University or institute of learning.

Fiona Dresel

September 2021

II Acknowledgements

Firstly, my sincere gratitude goes to my supervisor, Dr Campbell Gourlay, without whom this project would not have been possible. I would like to thank him for his kindness, constant support and guidance, patience, and for sharing his vast knowledge in science.

I would also like to express my special thanks to Kevin Doyle and Jack Davis and all the members of the Gourlay lab and the KFG for your constant support and advise, but also for making this year a wonderful experience outside the laboratory. An additional thanks to my fellow Master student Jamie T. who made long days in the laboratory appear shorter than they were. Finally, I would like to thank my wonderful family for their support.

III Contents

Table of Contents

IV List of Figures and Tables

List of Tables

V Abbreviations

AC	**Adenyl cyclase**
ADP	**Adenosine diphosphate**
Amp	**Ampicillin**
AntA	**Antimycin A**
APS	**Ammonium persulfate**
ATP	**Adenosine triphosphate**
ATPase	**Protein hydrolysing Adenosine triphosphate**
C. elegans	**Caenorhabditis elegans**
cAMP	**Cyclic adenosine monophosphate**
Cdks	**cyclin-dependent kinases**
Clns	**cyclins**
D. melanogaster	***Drosophila melanogaster***
Da	**Dalton**
DMSO	**Dimethyl sulphoxide**
DNA	**Deoxyribonucleic acid**
E. coli	**Escherichia coli**
ECL	**Enhanced chemiluminescence**
EDTA	**EDTA**
eIF2α	**eukaryotic initiation factor 2 alpha**
ER	**Endoplasmic reticulum**
Et al	**Et allia**
ETC	**Electron transport chain**

ETS	**Electron transport system**
FCCP	**carbonyl cyanide p-trifluoromethoxy phenylhydrazone**
G1	**Gap1**
G2	**Gap2**
GAPs	**GTPase activating proteins**
GDIs	**Guanine nucleotide dissociation inhibitors**
GDP	**Guanosine diphosphate**
GEFs	**Guanine exchange factors**
GFP	**Green fluorescent protein**
GO	**Gene ontology**
GPCR	**G-protein coupled receptor**
GRD	**GAP-related domain**
GTP	**Guanosine triphosphate**
GTPase	**Guanosine triphosphate hydrolases**
HVR	**hypervariable regions**
IMS	**Intermembrane space of mitochondria**
kDa	**Kilo Dalton**
L	**Litre**
LB	**Lysogeny broth**
Leu	**Leucine**
LiAc	**Lithium acetate**
M	**Molar**
M Phase	**Phase of mitosis or cell division**

MAPK	**mitogen-activated protein-kinase**
MAPKKK	**mitogen activated protein kinase kinase kinase**
mRNA	**Messenger RNA**
mTOR	**mammalian target of rapamycin**
NMT	**Non-mitochondrial respiration**
OD_{600}	**Optical density measured at 600 nm**
OPT	**tetra/penta-peptide system**
PBS	**Phosphate buffered saline**
PCR	**Polymerase chain reaction**
PEG	**Polyethylene glycol**
PI3K	**phosphatidylinositol-3-kinase**
Pip3	**phosphatidylinositol-3, 4-triphosphate**
PKA	**Protein Kinase A**
PKC	**protein kinase C**
PLCε	**phospholipase Cε**
PTMs	**Posttranslational modifications**
PTR	**di/tri-peptide system**
PVDF	**Polyvinylidene fluoride**
RAD	**RAS-association domain**
RALGDS	**RAL guanine nucleotide-dissociation stimulator**
RNA	**Ribose nucleic acid**

RNA-Seq	**Ribose nucleic acid sequencing**
S phase	**Phase of replication of DNA**
S. cerevisiae	***Saccharomyces cerevisiae***
SD	**Synthetic Dropout**
SDS	**Sodium dodecyl sulphate**
SSRs	**Sugar-sensing receptors**
TEMED	**N, N, N', N'-Tetramethyl ethylenediamine**
TET	**Triethiltyn bromide**
TFs	**Transcription factors**
Tiam1	**T-lymphoma invasion and metastasis-inducing 1**
TKRs	**Tyrosine kinase receptors**
TOR	**Target of rapamycin**
Tris	**Tris(hydroxymethyl)aminomethane**
tRNAs	**Transfer ribonucleic acid**
URA	**Uracil**
WT	**Wild type**
YPD	**YPD**
µ	**Micron**
µg	**Microgram (10^{-6} gram)**
µl	**Microliter (10-6 litre)**

VI Abstract

The small GTPase Ras plays an important role in cell growth and proliferation. Human diseases, like cancer, can be caused by mutations leading to constantly activated Ras proteins. Post-translational modifications ensure Ras localisation and thus its proper function. However, the precise mechanisms of those modifications in controlling the localisation of Ras are still poorly understood. Our previous studies have shown that phosphorylation of the Serine^{225} residue of Ras is important in cell growth and proliferation in the yeast *S. cerevisiae*. Serine^{225} modifications have resulted in mislocalisation of Ras2 within the cell driving the cells towards a quiescent state of growth through aberrant Ras/cAMP/PKA signalling. In this study we show that the combination of an increased copy number and mutation leads to an altered cell fate supporting evidence that both Ras mutation and gene duplication are often necessary to cause cancer. We also show that the deletion of *CUP9* could rescue the toxic effects of *Ras2*^{S225} mutant alleles including growth, viability, and respiratory defects. In addition, MET-auxotrophy could be overcome in *Ras2*^{S225} mutants. Our results demonstrate that the Serine^{225} residue is important in regulating Ras2 localisation and its activity co-ordinating nutrient sensing with cell growth and proliferation. We highlight the importance of post-translational modifications of Ras2 but also other regions outside the Ras GTPase domain e.g. other nutritional pathways controlled or modulated by Ras in yeast in cell fate. Our findings have implications for the development of novel therapeutic approaches for cancers driven by oncogenic Ras proteins.

1 Introduction

1.1 *S. cerevisiae* as a model organism

The use of model organisms is fundamental for the discovery and understanding of molecular processes such as signalling pathways or the function of genes that may be relevant to combat diseases in humans. Simple eukaryotic organisms like yeast, nematodes and flies have been exploited for the fast analysis of gene function and dysfunction in connection with diseases stemming from mutations (Russell *et al.*, 2017).

Saccharomyces cerevisiae (*S. cerevisiae*) is a single-celled budding yeast that has been used as the primary model organism in the discovery of molecular signalling pathways (Botstein and Fink, 2011). Due to its easy genetic manipulation, rapid growth and a vast amount of resources and molecular tools (Mohammadi *et al.*, 2015), *S. cerevisiae* has not only elucidated our understanding in human disorders, such as cancer (Pereira, Coutinho, *et al.*, 2012; Guaragnella *et al.*, 2014) and neurodegenerative disorders (Pereira, Bessa, *et al.*, 2012; Tenreiro *et al.*, 2013), but also in ageing research (Bonawitz *et al.*, 2007). In 1996, its genome was the first eukaryotic genome to be sequenced (Goffeau *et al.*, 1996) revealing strong conservation between humans and yeast in key functional pathways regulating cell cycle (Liu *et al.*, 2015) and metabolism (Petranovic *et al.*, 2010) e.g. mitogen-activated protein-kinase (MAPK) (Madrid *et al.*, 2016). Dysfunction or mis-regulation in any of these pathways are associated with many diseases in humans (Foury, 1997).

S. cerevisiae can also be used to express human proteins to unravel protein inhibitors and the roles of other proteins in multi-celled eukaryotes, including the human small GTPase protein Ras (Bourne, Sanders and McCormick, 1990; Laurent *et al.*, 2016).

1.2 Ras and the Ras superfamily

The small guanosine triphosphate hydrolases (GTPase) of the Ras superfamily function as binary switches within cells to convey extracellular stimuli to intracellular effectors.

Ras is one of the five branches that comprise the RAS superfamily of GTPases. Using evolutionary conserved orthologues in other organisms, such as *S. cerevisiae*, *C. elegans*, and *Drosophila melanogaster*, more than 150 members of the RAS superfamily in humans were identified ranging from 20 to 40 kDa in size.

Based on similarities in sequence and function, the five main branches of the RAS superfamily were grouped into Rho, Rab, Ran, Arf, and Ras (Bourne, Sanders and McCormick, 1990; Liu, Yan and Chan, 2017). Ras superfamily proteins show biochemical and functional similarities to the α subunit of heterotrimeric G proteins. However, while the main function, namely acting as binary molecular switches, remains the same, Ras GTPases are monomeric G proteins (Biou and Cherfils, 2004).

GTPases are tightly regulated modulators of various cellular processes which is enabled by several post-translational modifications, e.g. phosphorylation, and structural differences which in turn is dictated by their subcellular location, and hence their effectors and signalling pathways (Vetter, 2001; Biou and Cherfils, 2004).

The largest family in the Ras superfamily are Rab proteins (Ras -like proteins in brain) with 61 members (Pereira-Leal and Seabra, 2001; Seabra and Wasmeier, 2004). The main role of Rab GTPases is the control of intracellular vesicular transport and protein trafficking between organelles of the endocytic and secretory pathways. The localization to specific intracellular compartments relies on prenylation and divergent C-terminal sequences (Zerial and McBride, 2001).

The Arf (ADP-ribosylation factor) family is the second branch and also contributes to vesicular transport regulations. The GDP/GTP switch depends on specific Guanine exchange

factors (GEFs) and GTPase activating proteins (GAPs) (Nie, Hirsch and Randazzo, 2003; Memon, 2004).

The third branch is formed by Rho proteins (Ras homologous) consisting of 20 identified members. The most studied ones are RhoA, Rac1 and Cdc42. Rho proteins are crucial in actin organization, cell cycle progression, and gene expression as they vitally regulate extracellular-stimulus-mediated signalling pathways (Ridley, 2001; Etienne-Manneville and Hall, 2002).

Ran (Ras-like nuclear) proteins make up the fourth branch. While being the most abundant small GTPase in the cell, they are also best known for their role in nucleocytoplasmic transport of RNA and proteins (Weis, 2003). Interestingly, a spatial gradient of the GTP-bound form of Ran dictates Ran function, unlike other small GTPases (Li, Cao and Zheng, 2003).

1.2.1 The GTPase Ras

The small GTPases Ras form the fifth branch of the Ras superfamily and are the focus of this study. The human Ras subfamily consists of 35 proteins which are highly conserved within their G-Box domains and are mainly found at the plasma membrane where they activate complex signalling pathways (Willumsen *et al.*, 1984; Colicelli, 2004).

In *S. cerevisiae* Ras proteins regulate the response to nitrogen starvation, filamentous growth and sporulation (Kataoka *et al.*, 1984; Toda *et al.*, 1985) and are involved in the regulation of cell proliferation and differentiation in humans (Mulcahy, Smith and Stacey, 1985; Dobrowolski, Harter and Stacey, 1994). Three genes express mammalian Ras proteins, H-Ras, K-Ras, and N-Ras (Prior, Lewis and Mattos, 2012), whilst two Ras genes encode Ras1 (309 amino acid residues) and Ras2 (322 amino acid residues) in *S. cerevisiae*. The N-terminals of Ras1 and Ras2 share significant homology to the Ras proteins in mammals

(Powers *et al.*, 1984). The two Ras proteins in yeast are functionally the same, but they differ in expression giving them separable functions. Studies have demonstrated that Ras1 expression comes to an halt when cells are cultivated in glycerol or pyruvate-rich media which are both nonfermentable carbon sources (Breviario *et al.*, 1986). They also showed in Ras2 deletion strains that hyperactive Ras1 cannot only supress the deletion phenotype but also shows the same phenotype seen in constitutively activated Ras2 strain thus substantiating that the only difference between Ras1 and Ras2 lies in their level of expression (Marshall *et al.*, 1987). To display the high similarity between mammalian and yeast Ras proteins, yeast cells were depleted of Ras proteins but were rescued by expression of mammalian H-; and N-Ras (Boguski and McCormick, 1993).

1.2.2 Ras- a binary switch

As with all G proteins, Ras proteins can switch between an inactive GDP-bound state and an active GTP-bound state. This binary switch mechanism allows Ras proteins to function as intracellular signalling molecules converting extracellular stimuli into intracellular responses at specific effector sites in various complex intracellular signalling pathways (Wennerberg, Rossman and Der, 2005; Cox and Der, 2010).

In order to bind GTP or GDP and hence to activate or deactivate Ras proteins, respectively, all Ras proteins contain a conserved G-domain of about 20 kDa in size ultimately enabling a shared mechanism of action amongst all Ras proteins (Bourne, Sanders and McCormick, 1991; Boguski and McCormick, 1993; Wennerberg, Rossman and Der, 2005; Cox and Der, 2010).

Depending on the organism and the specific Ras protein, activation of Ras proteins induces different signalling cascades (Vetter, 2001; Cox and Der, 2010). To elicit downstream signalling pathways, effectors of Ras share a conserved RAS-binding-domain, or RAS-

association (RA) domain. The N-terminal domain contains a conserved set (1-5) of G box GDP/GTP-binding elements recognising phosphates and guanine nucleotides, forming the G-domain (Milburn *et al.*, 1990; Schlichting *et al.*, 1990; Scheffzek *et al.*, 1996). The switch regions switch I (aa 30-38) and switch II (aa 59-76) are vital motifs within the G-box as they change their conformation when switching between GDP and GTP-bound states (Vetter, 2001). When bound to GTP, switch I and switch II are held in the active conformation via hydrogen bonds formed between the y-phosphate and T35 and G60. These hydrogen bonds break down when GTP is hydrolysed resulting in the formation of the GDP-bound state (Boguski and McCormick, 1993). The main effect of the changes in switch I and switch II are different affinities for GDP-bound and GTP-bound Ras to regulatory proteins and effectors of Ras (Boguski and McCormick, 1993).

The binary switch mechanism i.e. the exchange of bound GDP to GTP (activation) and the hydrolysis of GTP to GDP (deactivation) is tightly regulated by Guanine Exchange Factors (GEFs) and GTPase Activating Proteins (GAPs) in all G-proteins **(Figure 1)**.

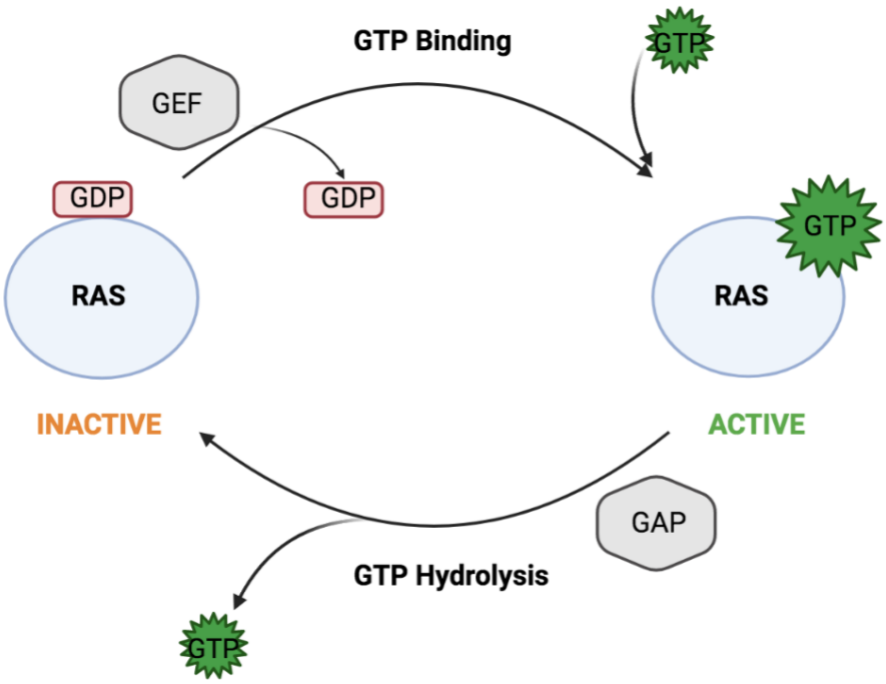

Figure 1.The binary switch mechanism of the small GTPase Ras.

GEF: Guanine exchange factor
GAP: GTPase activating protein
Inactive Ras is GDP-bound and gets activated through the help of GEFs. Active GTP-bound Ras converts extracellular stimuli into intracellular responses at specific effector sites. The hydrolysis of GTP is accelerated through GAPs thus deactivating Ras (Wennerberg, Rossman and Der, 2005; Cox and Der, 2010).

These regulatory proteins are necessary as reactions to exchange GDP to GTP and to hydrolyse GTP to GDP need acceleration (Broek *et al.*, 1987; Robinson *et al.*, 1987; Trahey and McCormick, 1987; Jones, Vignais and Broach, 1991). In the inactive GDP-bound states, Ras proteins show very slow off-rates for GDP ($t_{1/2}$ = 6 min, $k_{off} = 2 \times 10^{-3}\ s^{-1}$ at 20°) requiring GEFs to bind to Ras to change the switch regions and P loop (aa 10-17) ultimately resulting in the release and replacement of GDP as the affinity for GDP is no longer strong (Trahey and McCormick, 1987; Gibbs *et al.*, 1988). GAPs on the other hand control and accelerate the deactivation. However, Ras GAPs are highly diverse in their GAP-related domain (GRD) leading to specific functions in Ras regulation and thus signal transduction (Wennerberg, Rossman and Der, 2005; Cox and Der, 2010).

Other important regulator proteins for mammalian Ras are the Guanine nucleotide dissociation inhibitors (GDIs). Their main role lies in prolonging the inactive state by binding to GDP-bound GTPases and inhibiting the release of GDP (Rak, 2003). To date, GDIs have only been identified for the RHO and RAB subfamily (WU *et al.*, 1996; Olofsson, 1999).

1.3 Posttranslational modifications of Ras

The exchange of GDP to GTP is not the only mechanism that controls the activation and localisation of the four Ras proteins to the cytoplasmic side of the plasma membrane. Posttranslational modifications (PTMs) can also regulate Ras sub-cellular localisation affecting the interaction of Ras with a specific class of effectors and regulators thus dictating certain downstream signalling events (Wennerberg, Rossman and Der, 2005; Cox and Der, 2010).

An important motif in PTMs in Ras is the CAAX motif, whereby C is a cysteine, A is an aliphatic amino acid, and X is any amino acid. It is located at the C-terminal domain of Ras and is vital for membrane targeting (Hancock *et al.*, 1991). There are four PTMs that are absolutely necessary and represent the minimum signals needed for movement and interactions to and with the plasma membrane. During the first posttranslational modification, farnesylation, farnesyltransferase (FTase) targets the cysteine residue in CAAX to add a farnesyl isoprenoid. Studies have shown that farnesyltransferase activity depends at least on the genes DPR1/RAM1 and RAM2 encoding its α and β subunits (Casey *et al.*, 1989; He *et al.*, 1991). This modification allows loose and dynamic interaction with endomembranes, such as the ER and Golgi (Choy *et al.*, 1999). Following this, an endoprotease called Ras converting enzyme 1 (Rce1) proteolytically removes the AAX amino acids from the CAAX motif and leaves a prenyl cysteine at the C-terminus (Schmidt *et al.*, 1998). After the removal of the AXX motif carboxyl methylation via isoprenylcysteine

carboxymethyltransferase (ICMT) occurs. This is supposed to be pivotal in Ras signalling (Boivin, Bilodeau and Béliveau, 1996; Kramer *et al.*, 2003). However, just the CAAX processing is not sufficient to locate Ras proteins to the plasma membrane. The fourth sequential PTM is palmitoylation occurring upstream of the CAAX motif (Rocks, 2005; Rocks *et al.*, 2010).

For H-Ras, N-Ras, and K-Ras4A palmitoylation occurs at either two or one C-terminal cysteine residues (Cys^{181} and Cys^{184} in H-Ras or Cys^{181} in N-Ras). Ras hydrophobicity is thus increased determining its transport route via the exocytotic route, ultimately resulting in its assemblage at the plasma membrane (Roy *et al.*, 2005). However, unlike farnesylation palmitoylation is reversible allowing N-Ras and H-Ras dissociation from the plasma membrane and their reallocation to subcellular membranes like the golgi apparatus (Lynch *et al.*, 2015). Studies with palmitoylation-deficient N-Ras mutants and agonist-activated GTP-loaded N-Ras show that palmitoylation is important for Ras activation, and live-cell Ras-GTP imagining shows N-Ras activation only takes place at the plasma membrane (Song *et al.*, 2013). K-Ras is deficient of palmitoylation sites, thus its translocation route to the plasma membrane is yet to be elucidated. However, its translocation is reliant on a poly-lysine region located near the hypervariable region that is independent from the endomembrane trafficking (Choy *et al.*, 1999; Apolloni *et al.*, 2000; Schmick *et al.*, 2014). To confirm that Ras activation can occur at the ER and the golgi, the RBD of Raf-1 was fused with GFP which explicitly binds to active Ras proteins (Bivona *et al.*, 2003).

The enzymes responsible for the palmitoylation-depalmitoylation cycle regulating Ras trafficking in *S. cerevisiae* are the “Effectors of Ras Function” proteins Erf2 and Erf4 which were identified through genetic screens. Erf2 and Erf4 form the Ras protein acyltransferase (PAT) in yeast and Erf2 and DHHC9-GCP16 in mammalian cells (Mitchell *et al.*, 2012). In yeast, the main function of Erf4 is the regulation of the degradation of Erf2 through

ubiquitination, and the responsibility for the stability of the palmitate-Erf2 catalytic intermediate. Erf2 contains the DHHC PAT subunit. Studies show that Erf4 absence reduces palmitoyl transfer to Ras2 (Mitchell *et al.*, 2012) **(Fig. 2)**.

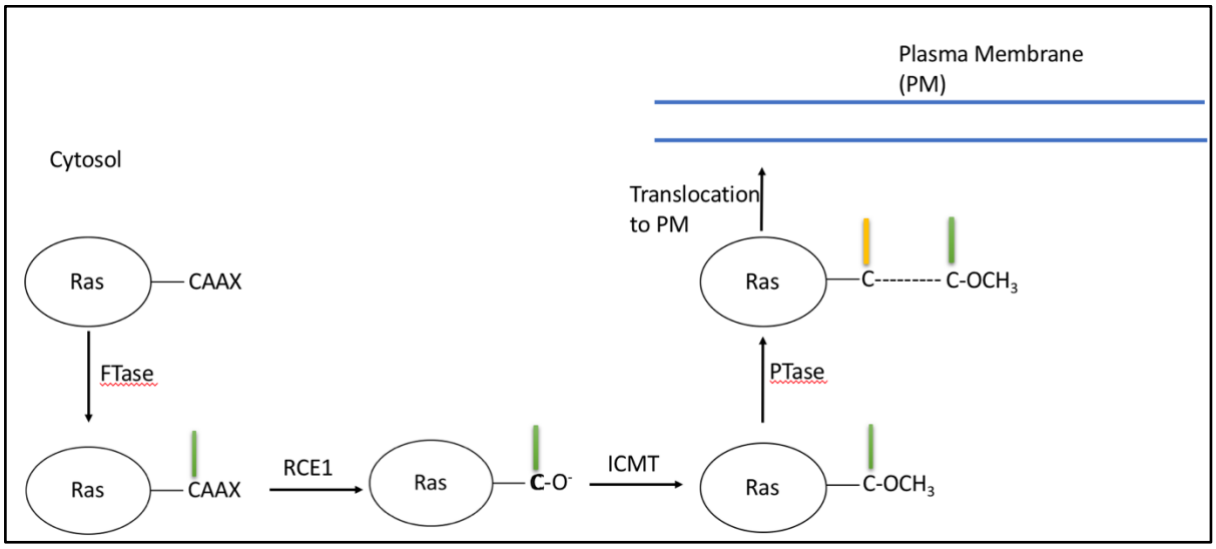

Figure 2. A simplified schematic showing the posttranslational modifications of Ras: CAAX processing.
During farnesylation, farnesyltransferase (FTase) targets the cysteine residue in CAAX to add a farnesyl isoprenoid (green rod). Following this modification, Rce1 proteolytically removes the AAX amino acids from the CAAX motif and leaves a prenyl cysteine at the C-terminus. After this, isoprenylcysteine carboxymethyltransferase (ICMT) catalyses the carboxyl methylation. The fourth sequential PTM is palmitoylation occurring upstream of the CAAX motif.

1.3.1 Ras protein phosphorylation

One of the most frequent and important PTMs in eukaryotes is phosphorylation. The chemical attachment of a phosphoryl group to an organic molecule catalysed by protein kinases controls and determines function, localisation, and activity of a variety of proteins. Dephosphorylation i.e. the removal of a phosphoryl group is in turn carried out by phosphatase proteins. Serine, threonine and tyrosine residues are typical sites of protein phosphorylation (Cohen, 2002; Vlastaridis *et al.*, 2017).

1.3.2 Ras protein phosphorylation in yeast

In *S. cerevisiae* protein phosphorylation is the most frequently occurring post translational event possessing more than 2300 phosphoproteins regulating cellular processes (Bodenmiller *et al.*, 2008). Around 160 protein kinases and phosphatases (Bodenmiller *et al.*, 2010) govern this complex process whereby an average of 70 targets are phosphorylated by a single kinase (Bodenmiller *et al.*, 2010; Sharifpoor *et al.*, 2011).

The yeast Ras proteins, Ras1 and Ras2 are solely phosphorylated on serine residues, and studies demonstrated that phosphorylated Ras2 exclusively occurs at the plasma membrane indicating an important role in localisation of Ras (Whistler and Rine, 1997). Putative serine phosphorylation sites in Ras2 include serine residues at positions 6, 214, 224, 225, 235, 238, and 262. However, the preferred phosphorylation site of Ras2 in Serine 214. When this serine residue is altered other sites close to serine 214 may be phosphorylated by protein kinases. Studies where Ras2 Serine 214 was replaced with alanine, which is non-phosphorylatable, showed reduced glycogen accumulation, increased cAMP levels and PKA-dependent activation of Ras2.GTP proposing a feedback regulation mechanism of the Ras/cAMP/PKA pathway to regulate phosphorylation (Cobitz *et al.*, 1989; Whistler and Rine, 1997).

1.3.3 Ras protein phosphorylation in humans

Not much is known about the phosphorylation processes of Ras2 in *S. cerevisiae* in terms of its intracellular localisation regulation, which is surprising as evidence suggests phosphorylation can regulate Ras localisation in humans. Studies (Bivona *et al.*, 2006) have shown that phosphorylated Serine181 of K-Ras via PKC induces rapid translocation of plasma membrane localised K-Ras to internal membranes, such as the outer membrane of the mitochondria and the endoplasmic reticulum. At the outer mitochondrial membrane

phosphorylated K-Ras can then interact with Bcl-xL thus implicating its role in cell death regulation (Bivona *et al.*, 2006; Sung *et al.*, 2013).

The first reports about phosphorylation events in human Ras demonstrated that phosphorylation of H-Ras occurs *in vitro* by the insulin receptor kinase in the presence of poly(L-lysine), whereas K-Ras could be phosphorylated in absence of poly(L-lysine). This difference was thought to be caused due to the basic hypervariable region of K-Ras substituting for basic proteins whereas the hypervariable region of H-RAS and N-RAS primarily consists of neutral amino acids requiring the addition of basic proteins (Fujita-Yamaguchi *et al.*, 1989). Others reported that abl kinase phosphorylates tyrosine137 of H-Ras altering its protein conformation and enhancing its effector binding (RAF1) by nearly 5-fold thus modulating Ras signalling via its effector (Ting *et al.*, 2015).

Recently, STK19 – a serine/threonine kinase – was found to activate N-Ras via phosphorylating Serine89, a highly conserved residue in the **α**3-helix. This phosphorylation event allows N-Ras to interact with its effectors B-Ras and PI3K**α** easily ultimately activating the PI3K and MAP kinase pathway. It was reported that the selective STK19 inhibitor, ZT-12-037 (1a), showed high therapeutic potential by preventing development and growth of N-Ras driven melanoma *in vitro* and in animals (Yin *et al.*, 2019).

1.4 Ras protein trafficking

Ras protein trafficking or localisation determines Ras function as - depending on its location- various interactions with different regulatory partners and downstream effectors are possible. The focus of scientific research is the function of Ras at the plasma membrane (Prior and Hancock, 2012). The site of Ras protein synthesis is the cytosol, therefore PTMs are pivotal for stable membrane interactions. One of those crucial PTMs for membrane interaction and protein trafficking is the CAAX processing- as previously described in “1.3 Posttranslational

Modifications of Ras". Here, hypervariable regions (HVR) of the Ras proteins are modified determining membrane interactions and differential localisation **(Fig. 3)** (Choy *et al.*, 1999; Apolloni *et al.*, 2000).

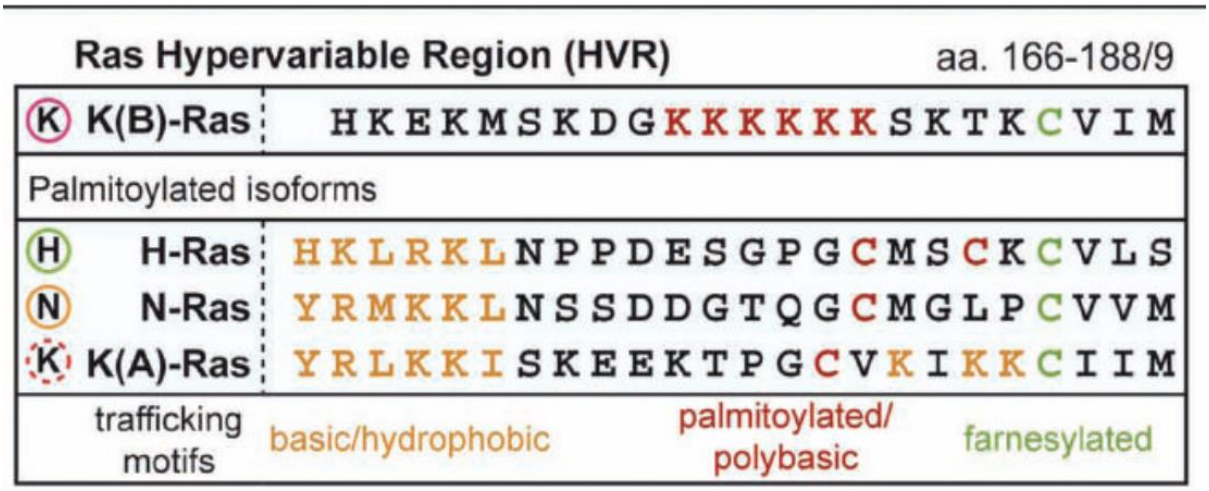

Image from (Henis, Hancock and Prior, 2009)
Figure 3. The C-terminal hypervariable regions (HVR) of the human Ras protein isoforms. PTM's of the HVR enable a vast variability of function between Ras isoforms e.g. through different membrane interactions and localisation (Henis, Hancock and Prior, 2009).

1.4.1 Ras protein trafficking in mammalian cells

The plasma membrane localisation of the mammalian K-Ras via the Golgi-dependent cytosolic route only requires the basic hexalysine patch along with the farnesyl group. The plasma membrane localisation of H-Ras via the Golgi and transport vesicles relies only on the farnesyl group and two palmitoyl groups on cysteines 181 and 184 (Choy *et al.*, 1999; Apolloni *et al.*, 2000). Surprisingly, additional hydrophobic/basic residues upstream in the HVR are needed to ensure stable membrane localisation of N-Ras (Laude and Prior, 2008). Studies have also shown that the de-palmitoylation process of N-Ras and H-Ras on the plasma membrane is possible thus enabling the returning to the Golgi (Goodwin *et al.*, 2005). The plasma membrane trafficking of K-Ras needs to be further elucidated. K-Ras lacks

palmitoylation sites **(Fig. 3)** and is independent from Golgi/endomembrane trafficking due to poly-lysine regions located near the HVR (Apolloni *et al.*, 2000; Abdelkarim *et al.*, 2019). Another organelle accessible for Ras proteins is the endosome- the intracellular sorting machinery. The trafficking pathway to the endosome for H-Ras and N-Ras occurs via the conventional clathrin-mediated endocytosis following palmitoylation (Prior and Hancock, 2012)**.** For K-Ras, the mediation of endosomal trafficking is still unclear. However, it is supposed that translocation is clathrin-mediated and occurs through a calcium/calmodulin mediated switch (Fivaz and Meyer, 2005; Lu *et al.*, 2009). Another destination of Ras is the mitochondria. Phosphorylation of Serine181 on K-Ras mediated through protein kinase C (PKC) enables the interaction with the plasma membrane which in turn facilitates the translocation to the cytosol and the accumulation on the mitochondria where apoptosis is eventually elicited (Bivona *et al.*, 2006).

1.4.2 Ras trafficking in yeast

In yeast, PTMs of Ras1 and Ras2 include the initial removal of a methionine at the N-terminus. Next, the C-terminal is modified e.g. through carboxyl methylation, farnesylation, and palmitic acid addition (Hancock *et al.*, 1989). As mentioned above in "1.3 Posttranslational Modifications of Ras", palmitoylation and localisation of Ras in *S. cerevisiae* occurs through PAT using palmitoyl-CoA (Mitchell *et al.*, 2012). Moreover, fluorescent tagging of yeast Ras and their partners Cyr1, GAPs like Ira and GEFs such as Cdc25 revealed their endomembrane localisation although adenylyl cyclase activation through Ras2 only occurs on the plasma membrane (Belotti *et al.*, 2012). It was also revealed that Ras2 is in contact with the ER via the Ras inhibitor 1 (Eri1) (Sobering *et al.*, 2003). Furthermore, Ras2 together with Ira proteins accumulate at mitochondrial membranes (Belotti *et al.*, 2012). This was further strengthened by studies investigating Ras

accumulation at the mitochondria in response to nutrient depletion in *whi2*, a phosphatase activator important in stress responses, lacking cells (Leadsham *et al.*, 2009).

However, many aspects of membrane trafficking other than to the plasma membrane have to be further elucidated in order to provide a better understanding of protein modification and its importance in protein localisation and hence function **(Fig. 4)**.

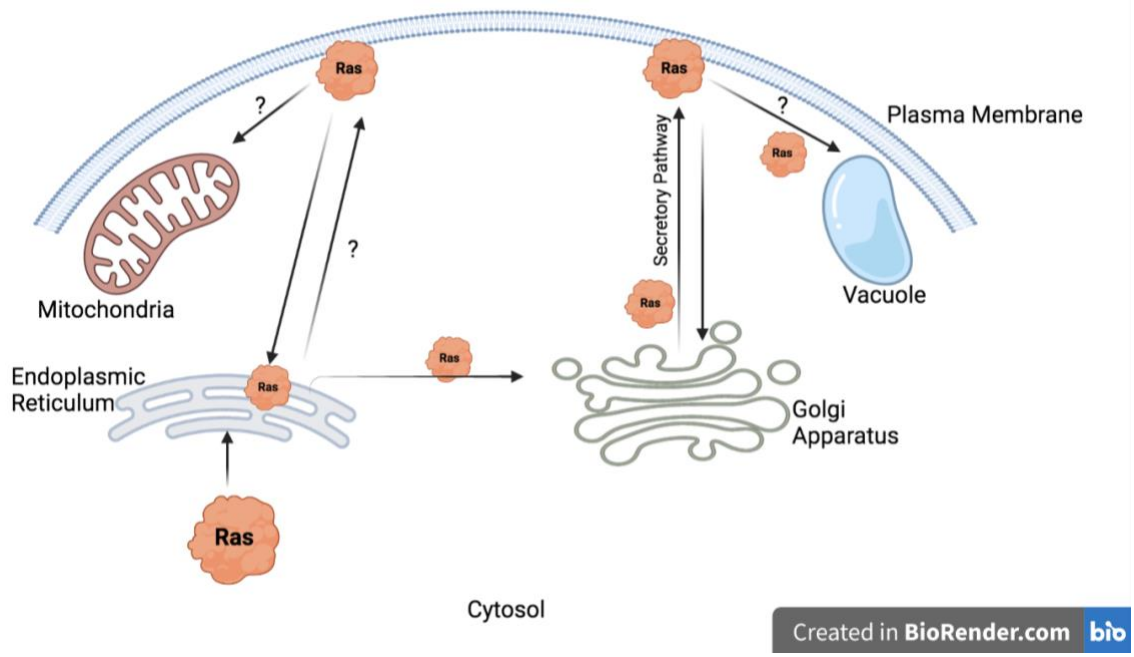

Figure 4. A graphic representation of subcellular Ras trafficking and localisation.
PTMs are pivotal in the localisation and trafficking of Ras protein. However, many aspects of membrane trafficking must be further investigated.

1.5 Ras in nutrient availability and acquisition in yeast cells

Nutrient availability and acquisition of key nutrients of not only sugars and amino acids, but also nitrogen compounds are pivotal for growth and proliferation, metabolism and stress resistance in yeast (Brauer *et al.*, 2008; Broach, 2012). Here, a network of multiple complex signalling pathways such as the Ras/cAMP/PKA, TOR1 complex, and the AMP-activated

kinase combine and thus affect gene expression and protein synthesis on a transcriptional, translational and posttranslational level dictating metabolism and cell fate (Broach, 2012). The Ras/cAMP/PKA pathway induces the majority of changes to the transcriptional profile of the cell in yeast following glucose addition. Here, activation of this pathway achieves almost (90 %) the transcriptional changes seen in glucose depressed cells when glucose is added back. *Vice versa*, the majority of the glucose induced responses are eliminated when inhibiting this pathway in combination with glucose addition (Zaman *et al.*, 2009). Seeing the importance of Ras in glucose induced signalling via the Ras/cAMP/PKA pathway, it can be suggested that other nutritional pathways are also controlled or modulated by Ras in yeast.

1.5.1 Ras in response to nutrient availability: The Ras/cAMP/PKA signalling pathway in yeast

The Ras/cAMP/PKA signalling pathway is important in the regulation of cell growth and proliferation, stress resistance, and metabolism in response to nutritional availability in *S. cerevisiae* (Tisi, Belotti and Martegani, 2014). The activation of the Ras/cAMP/PKA pathway can occur through sugar-sensing receptors (SSRs) called SNf3 and Rgt2. They can sense glucose through their extended C-termini which triggers the translocation of transcription factors (TFs) called Std1 and Mth1 to the cytoplasmic tail of the SSRs. Here, a casein kinase called Yck1 will phosphorylate the TFs. Following this, the TFs will be ubiquinated by Grr1 and eventually degraded by the proteasome. This leads to the expression of the glucose transporter HXT and metabolism genes; and on the other hand, to the suppression of the formation of inhibitory complexes Rgt2-Mth1/Std1. Glucose can now enter the cell through the transporters and glycolysis can occur converting glucose to pyruvate (Van Ende, Wijnants and Van Dijck, 2019). The by-product of this reaction, fructose 1,6 bisphosphate activates Cdc25 phosphatases resulting in the activation of Ras

proteins via GDP-GTP exchange. Activated Ras proteins will interact with adenylyl cyclase Cyr1 at the plasma membrane (Peeters *et al.*, 2017). Further stimulation by the GPCR Gpr1 through the binding of glucose leads to a GDP-GTP switch on Gpa2, which completely activates Cyr1 (Rolland *et al.*, 2000). Adenylyl cyclase consists of about 2,026 amino acids and includes four domains, namely an N-terminal, middle repetitive, catalytic and a C-terminal domain. The middle repetitive domain entails the LRR domain (674-1300 amino acids). This is a 23-residue amphipathic leucine-rich motif and the principle site of Ras interaction whereby its N-terminal domain (676-756) is determined as the Ras associating domain (RAD) (Toda *et al.*, 1985). Activated adenylyl cyclase will start using ATP to synthesize cAMP, ultimately activating the catalytic subunits of PKA, Tpk1/Tpk2/Tpk3 (Thevelein *et al.*, 2000; Van Ende, Wijnants and Van Dijck, 2019). Downstream TFs are targeted leading to filamentous growth (via Flo8), cell cycle progression and growth, stress responses and ageing control in *S. cerevisiae* (Cazzaniga *et al.*, 2008; Van Ende, Wijnants and Van Dijck, 2019). Inappropriate activation of PKA through mutations leads to cell cycle arrest in the G1 phase as well as glycogen accumulation and increased lifespan during starvation (Toda *et al.*, 1985).

In *S. cerevisiae*, not only feedback loops regulate the intracellular production of cAMP, but also two phosphodiesterases, Pde1 and Pde2, which catalyse the degradation of cAMP. Pde1 has low affinity and Pde2 has high affinity to cAMP (Sass *et al.*, 1986; Nikawa, Sass and Wigler, 1987).

The schematic given below describes the Ras/cAMP/PKA sugar signalling pathway in *S. cerevisiae* **(Fig. 5)**.

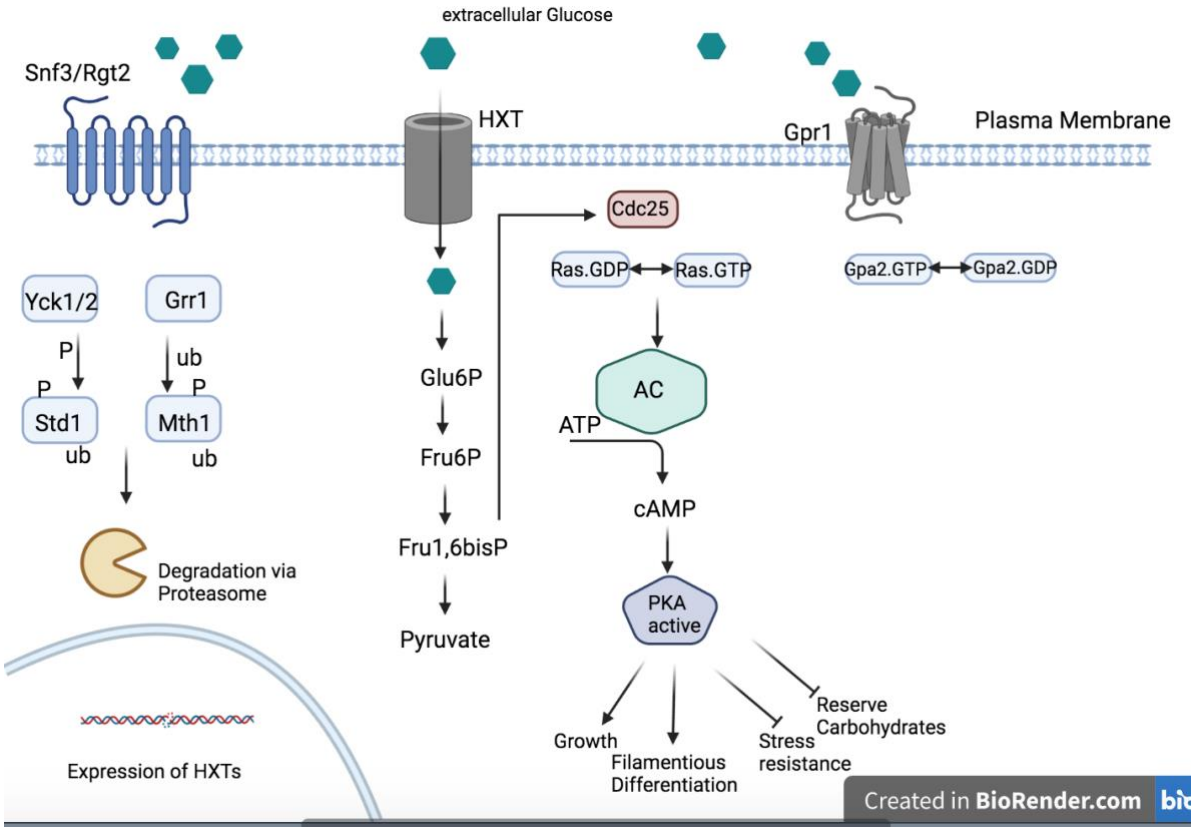

Figure 5. The Ras/cAMP/PKA sugar sensing pathway in S. cerevisiae.
The conversion of glucose to pyruvate creates the by-product fructose 1,6 bisphosphate which activates Cdc25 phosphatases. Ras proteins are then activated through a GDP-GTP exchange. Thus, Ras proteins can now interact with adenylyl cyclase Cyr1 at the plasma membrane which generates cAMP from ATP. The binding of cAMP to the regulatory subunits Bcy1 of the holoenzyme PKA causes their dissociation and a conformational change activating the catalytic subunits of PKA. PKA is now partially activated. Stimuli from the GPCRs are required to fully activate PKA. The activated PKA targets TFs like Flo8 in *S. cerevisiae* promoting growth and filamentous differentiation, and inhibiting stress resistance and reserving carbohydrates (Van Ende, Wijnants and Van Dijck, 2019).

1.5.2 Regulation of the Ras/cAMP/PKA pathway activity

As mentioned previously, in addition to Ras PKA can be activated by the seven-transmembrane GPCR Gpr1 and its G-protein Gpa1 which is a small GTP-binding protein homologous to the Ga subunit of heterotrimeric G proteins (Nakafuku *et al.*, 1988; Xue, Batlle and Hirsch, 1998; Kraakman *et al.*, 1999; Santangelo, 2006; Zaman *et al.*, 2008).

Upon glucose or sucrose binding the Gpr1-Gpa2 system is activated leading to an increase in cAMP production through AC thus activating PKA. Surprisingly, fructose to glucose analogues cannot activate Gpr1-Gpa2 (Kraakman *et al.*, 1999; Lemaire *et al.*, 2004).
The deletion of *GPA2* shows a phenotype with reduced PKA activity slowing the repression of genes, such as STRE-responsive genes (Colombo *et al.*, 1998; Kraakman *et al.*, 1999). Studies have also demonstrated, that the activation of Ras relies on sugar uptake but not on a GPCR system (Colombo *et al.*, 2004). It is still unclear how glucose activates Ras. A functioning sugar-sensing system is yet to be found (Rubio-Texeira *et al.*, 2010). However, is it supposed that the inhibition of GTPase activating proteins (GAPs) Ira1/2 protein is responsible for the glucose-induced increase in Ras2 activation, and not Guanine nucleotide exchange factors like Cdc25, thus making Ras a critical mediator in glucose-induced cAMP signalling (Goldberg, Segal and Levitzki, 1994).
Ras/cAMP/PKA signalling can also be regulated by the Guanine nucleotide exchange factors (GEFs), Cdc25 and Sds25, and the GTPase activating proteins (GAPs), Ira1 and Ira2 that regulate the binary switch mechanism i.e. the switch from the inactive GDP-bound state to the active GTP-bound state in Ras proteins (Robinson *et al.*, 1987; Tanaka, Matsumoto and Toh-E, 1989; K Tanaka *et al.*, 1990; Kazuma Tanaka *et al.*, 1990).
The 180 kDa polypeptide GEF Cdc25 has a highly conserved Ras-GEF catalytic domain (1,121-1,573 aa) (Jacquet *et al.*, 1994). Generally, it is bound to membranes, but its solubility may change when a hyperphosphorylation event within the 114-348 amino acid region occurs. This hinders its interaction with Ras. Hyperphosphorylation can take place through glucose addition, whereby it was reported that Cdc25 activity was inhibited (Gross, Goldberg and Levitzki, 1992; Jian *et al.*, 2010). Nutrient starvation can inhibit phosphorylation processes on Cdc25 and may be seen as a negative feedback loop in response to PKA activity (Gross, Goldberg and Levitzki, 1992; Jian *et al.*, 2010). However, while Cdc25 as a GEF is

well established, it is still not fully understood what precise role Cdc25 has in the Ras/cAMP signalling transduction in response to nutrients (Schomerus, Munder and Küntzel, 1990; Goldberg, Segal and Levitzki, 1994).

The GAPs, Ira1 and Ira2, are large proteins of a length of 3092 and 3079 amino acids, respectively. The GAP domain of these proteins is about 360 aa long and is located in the middle of the genes. The intrinsic GTPase activity of Ras is dependent on this domain (Kazuma Tanaka *et al.*, 1990). The supplementation of glucose triggers the inactivation of Ira2p and its ubiquitination which ultimately results in increases PKA activity as active GTP-bound Ras accumulates. The ubiquitination process regulating Ira2 is highly conserved in the Ras signalling pathway (Phan *et al.*, 2010).

1.5.3 Ras in nutrient acquisition: The Di/Tri-Peptide uptake mechanism in yeast

Another key cellular process to allow normal growth is nutrient acquisition. The underpinning process includes peptide transport.

The essential building blocks of proteins are provided by catabolised peptides composed of amino acid sequences. Peptides are not only essential for the synthesis of proteins. Some can also act as signalling molecules and nitrogen sources enabling alteration of cell behaviour: Leucine is an amino acid with a branched-chain that can regulate the activity of TORC1 (Stracka *et al.*, 2014; Kingsbury, Sen and Cardenas, 2015). TORC1 is the rapamycin-sensitive complex which regulates physiological responses of the cell concerning nitrogen sources and availability (De Virgilio and Loewith, 2006). TORC1 is a protein kinase comprised of Tor1 (or Tor2), Kog1 – homologous to the mammalian raptor -, Lst8 and Tco89. TORC1 activity is inhibited by rapamycin addition showing similar effects as in nitrogen depletion (Cardenas *et al.*, 1999; Bertram *et al.*, 2000; Shamji, Kuruvilla and Schreiber, 2000). However, the effects of nitrogen starvation are not fully phenocopied in

respect of retrograde transcription and nitrogen catabolite repression. It is therefore thought that another nitrogen signalling pathway must exist (Tate and Cooper, 2003; Tate *et al.*, 2009, 2010). In mammalian cells TORC1 is not only stimulated by leucine but also by an abundance of arginine and glutamine. Arginine is supposedly sensed through a lysosomal transporter called SLC38A9 which relays signals to mTORC1 in a Ras GTPases manner (Rebsamen *et al.*, 2015; Wang *et al.*, 2015). On the other hand, yeast and mammalian TORC1 receive glutamine levels independently of EGO/Rag GTPase (Stracka *et al.*, 2014).

In mammalian cells, protein synthesis is partially regulated through amino acids controlling mTOR and Gcn2 kinases having opposite effects on protein synthesis (Stracka *et al.*, 2014; Averous *et al.*, 2016). The activation of Gcn2 is based on its ability to sense an increase in uncharged tRNAs when essential amino acids are limited. Activated Gcn2 inhibits protein synthesis by phosphorylating the α-subunits of the eukaryotic initiation factor 2 alpha (eIF2α) (Berlanga, Santoyo and de Haro, 1999; Averous *et al.*, 2016).

Studying such underlying processes of amino acid and peptide sensing has been extensively conducted in yeast having highly conserved amino acid uptake mechanisms. There are two distinct peptide transport mechanisms in *S. cerevisiae*: a di/tri-peptide (PTR system) and a tetra/penta-peptide (OPT) transport system transporting amino acids, nitrates and peptides (Cai *et al.*, 2007).

The integral membrane protein Ptr2p is encoded by *PTR2* and consists of 601 amino acids and 12 membrane spanning domains translocating di/tri-peptides across the plasma membrane through proton-motive force (Perry *et al.*, 1994). Peptides containing hydrophobic amino acids are the preferred di/tri-peptide source. When the preferred nitrogen source is absent *PTR2* expression is induced (Island, Naider and Becker, 1987; Alagramam, Naider and Becker, 1995). *PTR2* transcription is regulated by its transcriptional repressor Cup9. Cellular levels of Cup9 are reduced when N-terminally basic or bulky hydrophobic di/tri-

peptides are imported thus increasing *PTR2* expression. Cup9 degradation is regulated by the E3 ubiquitin ligase Ubr1p which in turn is controlled by specific di/tri-peptides. Di/tri-peptides are thus functioning as both ligands and regulators (Varshavsky, 1996, 1997). Binding of N-terminally basic (Type 1: His, Lys, or Arg) or bulky (Type 2: Ille, Trp, Leu, Tyr, or Phe) di/tri-peptides to Ubr1p occurs at Type 1 or Type 2 Ubr1p substrate-binding sites through competition with larger protein substrates. This releases the auto inhibitory domain of Ubr1p exposing a substrate-binding domain in Ubr1p. The allosterically degradation of Cup9p is then mediated through the binding of this substrate-binding domain in Ubr1p to an internal degron in Cup9 (Du *et al.*, 2002). Di/tri-peptide uptake is regulated via a positive feedback loop where the more Cup9p is degraded, the more *PTR2* is expressed and thus the more di/tri-peptides are transported.

However, uptake of di/tri-peptides does not only occur through the Ptr2p transporter, but can also occur with low efficacy through the Dal5 transporter which predominantly imports nitrogen sources including allantoate and ureidosuccinate (Homann *et al.*, 2005).

The other peptide transport mechanism in *S. cerevisiae*, OPT, consisting of Opt1 and Opt2 transports peptides comprising four to five residues. Opt1 also functions as a high affinity transporter of the "noncanonical" tripeptide glutathione. In addition, Cup9p also downregulates the expression of *OPT2*, but not *OPT1* (Wiles *et al.*, 2006). Interestingly, Cup9p is also a regulator of the expression of *DAL5*. However, instead of acting as a repressor seen in *PTR2* and *OPT2*, Cup9p serves as an inducer of *DAL5* expression (Wiles *et al.*, 2006; Cai *et al.*, 2007).

1.5.4 Sulphur metabolic processes or Fe-S cluster machinery

The redox-active protein cofactors Iron-sulphur (Fe-S) clusters are not only extremely ancient, but also present in almost all organisms. Fe-S clusters can be found in the nucleus,

cytosol, and mitochondria and represent a crucial part in a variety of cellular functions, such as mitochondrial respiratory pathways, maintenance of genome stability, metabolic pathways, and gene regulation (Johnson *et al.*, 2005; Arnold, Grodick and Barton, 2016; Shi *et al.*, 2021). While mitochondria in yeast and animal cells assemble Fe-S clusters autonomously, other compartments of the cell rely on precursors or signals from the mitochondria to assemble Fe-S clusters (Stehling and Lill, 2013). In eukaryotes, Fe-S clusters are located in the mitochondria (ISC) and in the cytosolic Fe-S cluster assembly machinery (CIA) (Lill *et al.*, 1999; Lill, 2009).

Currently in yeast there are 18 proteins known to form the mitochondrial Fe-S cluster (ISC). Those proteins are all function in trafficking and the biogenesis of clusters within the mitochondria (Braymer and Lill, 2017). Usually four steps are required for the process: The first stage involved the *de novo* [2Fe-2S] cluster synthesis, those are then trafficked and inserted into mitochondrial apo-proteins, or exported out of the mitochondria into the cytosol by an as yet unidentified component (X-S). In the third stage [2Fe-2S] clusters are converted into [4Fe-4S] clusters and eventually trafficked and inserted into mitochondrial [4Fe-4S] apo-proteins, e.g. lipoate synthase, and succinate dehydrogenase during the fourth stage (Braymer and Lill, 2017).

Absolutely crucial for supporting cytosolic and nuclear Fe-S cluster proteins in eukaryotes is the cytosolic Fe-S cluster machinery (CIA). Up to this date, 11 proteins are involved in the synthesis, trafficking, and insertion of clusters in the cytosol and nucleus in yeast (Tsaousis *et al.*, 2014; Braymer and Lill, 2017; Tonini *et al.*, 2018). The CIA comprises a nucleotide-dependent cycle using the Cfd1-Nbp35 as a scaffold. Here, diflavin reductase Tah18 and Dre2 -the Fe-S protein- provide electron transfer from NADPH. Nar1 another Fe-S protein and the CIA targeting complex Cia1-Cia2-Mms19 will then transfer and insert transiently

bound [4Fe-4S] clusters of Cfd1-Nbp35 into apo-proteins (Sharma *et al.*, 2010; Stehling *et al.*, 2012, 2013; Russell *et al.*, 2017).

1.6 Ras and the cell cycle and quiescence in *S. cerevisiae*

The eukaryotic cell cycle includes four stages: the G1 (gap1), S (replication of DNA), G2 (gap2) and M (mitosis or cell division). The gap phases, G1 and G2, are the important phases where a series of checks are conducted before another stage can be entered. However, under unfavourable conditions, cells may rest in a so-called quiescence phase or G0 phase (*G1 phase called START primarily regulates cell cycle progression*, 2014). In the yeast *S. cerevisiae*, a stage in the late G1 phase called START primarily regulates cell cycle progression. Here, environmental and internal signals, such as nutritional and metabolic machinery status as well as pro-survival signals are evaluated and determines either the entry of a new cell cycle or an alternative pathway e.g. sporulation (Hartwell, 1974; Smets *et al.*, 2010). The Ras/cAMP/PKA signalling pathway controls multiple intracellular processes, one of which is the cell cycle. Its progression is regulated at the transitions from G1 to S and G2 to M (Drebot *et al.*, 1990; Anghileri *et al.*, 1999; Schneper *et al.*, 2004). The presence of growth factors and pro-survival signals like growth factors are imperative for Ras activation in humans, and the presence of glucose are required to activate yeast Ras (Busti *et al.*, 2010). The activation of Ras may alter specific cyclin (Clns) expression. These are important for the formation of cyclin-dependent kinases (Cdks)/Clns complexes which trigger the transition of a cell into the S phase (Baroni, Monti and Alberghina, 1994; Tokiwa *et al.*, 1994). PKA can also phosphorylate a negative G1 cyclin regulator called Whi3 causing the transition into S-phase (Mizunuma *et al.*, 2013). A significant decrease in cell size has been observed in mutants with decreased cAMP signalling or a weak constitutive PKA activity, such as the cdc25 temperature-sensitive mutant showing a defect in Ras activation, and the

tpk1^{w}tpk2tpk3 *bcy1* mutant, respectively (Cameron *et al.*, 1988; Baroni *et al.*, 1989; Tokiwa *et al.*, 1994). An increased cell size was observed in response to the over-activation of the Ras/cAMP/PKA pathway shown by hyperactive Ras2^{V19} mutants in which either the regulatory subunit of PKA, PDE1 and PDE2, or the GTPase Ira2 are deleted (Mitsuzawa, 1994; Jorgensen, 2002). While cAMP delays the transition from the G1 phase to the S phase in smaller cells, it has no effect in larger cells. Its effect is mainly caused by CLN1 and CLN2 transcription repression. Cln3 remains unaffected by cAMP counteracting the other cyclin inhibition and facilitating their growth-dependent expression (Baroni *et al.*, 1992; Baroni, Monti and Alberghina, 1994; Tokiwa *et al.*, 1994).

The Ras/cAMP/PKA signalling pathway is also involved in regulating the non-proliferating quiescence phase, or G0, in which cells are locked for a large proportion of their life. In this phase protein synthesis is decreased, thermo-resistance established, and storage molecules are gathered. The non-proliferating stage and the ability to re-enter the proliferation phase must be carefully controlled to prevent the establishment of disease (Gray *et al.*, 2004). Nutrient deprivation is one factor leading to the entry of cells into the quiescence phase in *S. cerevisiae*. The interaction of the PKA and Tor pathway (TORC1)- both being positive regulators of cell growth- contribute to the cell's transition into the G0 phase. Reduced PKA activity ceases growth and promotes quiescence transition (Thevelein and de Winde, 1999; Smets *et al.*, 2010).

1.7 Ras signalling in humans

In humans, Ras conveys extracellular stimuli in form of pro-survival signals to intracellular compartments through tyrosine kinase receptors (TKRs). Ligands bind to the receptors causing their dimerization. A conformational change is induced activating the catalytical tyrosine kinase domain. This in turn allows autophosphorylation of the intracellular carboxyl-

terminal domain which ultimately leads to the activation of the tyrosine kinase domain (Martinelli *et al.*, 2009; Normanno *et al.*, 2009). After the phosphorylation of the TKR, GEFs can be recruited and thus activation of Ras occurs ultimately enabling downstream signalling (Schulze, Deng and Mann, 2005). The 20 different effectors that can be activated by active Ras include the rapidly-accelerate fibrosarcoma kinases (RAF), phosphatidylinositol-3-kinase (PI3K), RAL guanine nucleotide-dissociation stimulator (RALGDS), RIN1, T-lymphoma invasion and metastasis-inducing 1 (Tiam1), Af6, Nore1, PLCS and PKC (Downward, 2003; Herrmann, 2003).

An important pathway exerting pro-proliferation signals is the Ras/Raf/MEK/ERK pathway. Here, Ras is activated through TKRs, GPCRs and/or integrins by forming large signalling complexes enabling the recruitment of Ras prior to promoting the GDP-GTP exchange. An important GEF here is called son of sevenless (SOS). Activated Ras then recruits the mitogen activated protein kinase kinase kinase (MAPKKK) Raf (c-Raf, a-Raf, b-Raf) to the plasma membrane and activates RAF. Activated RAF kinases in turn activate MAPK/ERK kinases through phosphorylation. 80 different substrates located in the cytoplasm and the nucleus can now be phosphorylated by the activated ERK (Yung *et al.*, 1997; KOLCH, 2000).

The activation of the phosphatidylinositol-3-kianse PI3K pathway leads to the activation of the mammalian target of rapamycin (mTOR): Activation of PI3K causes the phosphorylation of Pip2 inducing the generation of phosphatidylinositol-3, 4-triphosphate (Pip3). Pip3 then activates the phosphatidylinositol dependent kinase 1 (PDK1) which leads to the activation of AKT at the plasma membrane (Scheid and Woodgett, 2001). Activated AKT can now activate its effector mTOR, a serine/threonine kinase. Depending on the proteins mTOR interacts with two distinct complexes can be formed- mTORC1 and mTORC2. While mTORC1 promotes energy metabolism, cell cycle progression and cell proliferation through

the regulation of the transcription of specific genes involved in these cellular processes, mTORC2 mainly acts as an AKT kinase resulting in cell survival and proliferation, increased telomerase activity, and inhibition of apoptosis. Apoptosis is inhibited by the ability of phosphorylated AKT to prevent cytochrome c release from the mitochondria, thus downregulating pro-apoptotic factors and pro-caspase 9. Furthermore, phosphorylated AKT activates nitric oxide synthase thus regulating angiogenesis modulators (Yan *et al.*, 1998; Scheid and Woodgett, 2001; Wang, 2014).

1.8 Ras in human cancer

The small GTPases Ras have an important role in cell growth and proliferation. Thus, mutations leading to constantly activated Ras proteins may lead to diseases in humans, like cancer (Relógio *et al.*, 2014). The name "Ras" comes from a collection of genes of rat-derived murine sarcoma retroviruses involved in tumorigenesis in rats and are called the "rat sarcoma virus" (Rasheed, Gardner and Huebner, 1978; Barbacid, 1987). Mammalian Ras proteins are proto-oncogenes expressed by three genes called HRAS, KRAS, and NRAS encoding Ras proteins H-Ras, K-Ras, and N-Ras, respectively. Single mutations usually at codons 12, 13, or 61 result in the constitutive activation of Ras as GTP binding is facilitated ultimately leading to hyperproliferation of cells (Prior, Lewis and Mattos, 2012; Stolze *et al.*, 2015). The first discovery of the involvement of mutated RAS proteins in human cancer was established in 1984. Here, the mutational activation of K-Ras was studied in lung cancer (Rodenhuis *et al.*, 1987). In subsequent years it became clear that mutated K-Ras proteins cause cancers in the colon (Forrester *et al.*, 1987), lung (Rodenhuis *et al.*, 1987), and the pancreas (Almoguera *et al.*, 1988).

About 30% of all human cancers include a mutated Ras protein. 15% of oral cancers involve H-Ras mutations (Munirajan *et al.*, 1998; Murugan *et al.*, 2009). 23% of all human cancers

involve K-Ras mutations, hence mutated K-Ras proteins are the most mutated oncogenes in human cancers especially in cancers affecting the pancreas. 7.51% of N-Ras mutations contribute to human cancers whereby the highest incidence of N-Ras mutations is in malignant melanomas or haematopoietic and lymphoid tissue cancers (Kodaz, 2017; Murugan, Grieco and Tsuchida, 2019).

About one million deaths per year worldwide are due to mutations in KRAS whereby 85% are missense mutations. Mutations replacing glycine at codons 12 or 13 with any amino acid except proline block the arginine finger of GAPs from interacting with the GTPase site where it would promote GTP-hydrolysis (Scheffzek, 1997). A146 mutations present in 4% of colorectal cancers decrease nucleotide affinity facilitating the rapid dissociation of GDP and the non-specific i.e. not via GEFs and upstream signals aberrant accumulation of GTP-bound Ras (Edkins and O'Meara, 2006). Ras GTPases in cancer cells have more than seven specific effectors including RAF kinases (serine/threonine-specific protein kinases) (best studied), Phosphatidylinositol 3-kinase (PI3K), phospholipase Cε (PLCε), RAS and Rab interactor 1 (RIN1), T cell lymphoma invasion and metastasis-inducing protein (TIAM), etc. controlling cellular processes like growth and survival, cell proliferation and differentiation, and rearrangements of the cytoskeleton (Murugan, Grieco and Tsuchida, 2019). Interestingly, the Ras-related proteins Rit1 and Rit2 are only 44% identical to Ras proteins, however, they share almost the same effector binding site and activate RAF kinases, PI3Kalpha and PI3Ky. F82V and T83P mutations in Rit1 and Rit2 inhibiting GTP hydrolysis are seen in lung adenocarcinoma (Rodriguez-Viciana, Sabatier and McCormick, 2004).

However, the classic view of how *RAS* oncogenes cause cancer, namely that tumour cells contain one normal and one mutant allele, needs further consideration of recent observations where secondary alterations of mutant *RAS*, such as copy number, increase oncogenic signalling providing substantial evidence of the existence of a selective pressure for copy

number increase (Burgess *et al.*, 2017). Studies have shown that in murine skin carcinogenesis the oncogenic *Hras* copy number is increased early on (Bremner and Balmain, 1990; Chen *et al.*, 2009), and mouse non-small-cell lung cancer (NSCLC) models identified an amplification of $Kras^{G12D}$ copy number and a loss in copy number of wild type *Kras* in primary tumours. This increase in copy number of $Kras^{G12D}$ led to metabolic re-programming, increased activation of MAPK pathway signalling, and was associated with an advanced histologic grade (Junttila *et al.*, 2010; Kerr *et al.*, 2016). *RAS* gene amplification in combination with or without loss of the corresponding normal *RAS* allele is seen in several mouse cancer models, and multiple cancer cell lines show elevated mutant *KRAS/NRAS* expression (Bremner and Balmain, 1990; Modrek *et al.*, 2009; Soh *et al.*, 2009; Junttila *et al.*, 2010; Li *et al.*, 2011). A pre-clinical trial using human colorectal cancer cell lines with increased frequency of *KRAS* mutant alleles showed more sensitivity to MAP kinase inhibition. In heterozygous mutant HCT116 cells replacement of the normal wild type *KRAS* with a mutant *KRAS* allele provided increased sensitivity of these cells to treatment (Burgess *et al.*, 2017). These studies give substantial evidence that an increase in *KRAS* copy number are frequent in cancer regulating MEK dependency and competitive fitness (Burgess *et al.*, 2017).

1.9 Therapeutic approaches to target Ras-mutation driven cancer

Therapeutic treatment in Ras-driven cancers is still immensely difficult despite more than three decades of intensive research. Ras proteins are thus termed “undruggable” (Cox *et al.*, 2014; Stephen *et al.*, 2014). However, our understanding of some cellular and biochemical elements of the Ras signalling pathway has increased over the last decade (Gysin *et al.*, 2011; Stephen *et al.*, 2014). There are three main approaches in targeting oncogenic Ras mutations: Targeting upstream signalling, targeting Ras directly, and targeting Ras effectors. Upstream

targeting, however, shows little to no effect since Ras proteins are located downstream of upstream signalling targets. However, there is evidence that Ras-mutants in cancer cells are to some extent dependent on wild-type Ras which elicits downstream signalling in response to activated RTK. This suggests that blocking upstream signalling in combination with downstream effector inhibition may prevent feedback activation of RTKs, thus helping treatment in cancers caused by Ras (Young, Lou and McCormick, 2013). Paramount in Ras-dependent cancer growth are Ras effectors like RAF serine/threonine kinases (ARAF, BRAF and CRAF). Studies in non-small cell lung carcinoma (NSCLC) and pancreatic ductal adenocarcinoma show that RAF kinases have a pivotal role in driving Ras-mediated cancer (Blasco *et al.*, 2011; Collisson *et al.*, 2012). However, clinical trials of the first RAF kinase inhibitor, sorafenib, have shown no effect on KRAS-driven cancers (Williams, Cohen and Stewart, 2011). Due to this unforeseen outcome, MEK inhibitors received increased attention. Though, inhibiting MEK can trigger increased RTK or ERK activity eliminating the effects of MEK inhibition (Lito *et al.*, 2012). Another approach to target Ras effectors is via the RBDs. The small-molecule inhibitor, rigosertib, interacts with the RBDs of RAF kinases, mimicking Ras and thus preventing Ras from binding to RAF (Athuluri-Divakar *et al.*, 2016). No therapeutic agent to treat K-Ras mutations directly has been approved in clinical trials yet, which led to the conclusion that the GTP binding pocket on Ras is "undruggable". Recently, two new pockets have been identified on the surface of Ras which may be targeted by small molecules. One of these pockets is located between the switch I and II regions of KRAS which was found to bind to small molecules (Maurer *et al.*, 2012; Quevedo *et al.*, 2018; Cruz-Migoni *et al.*, 2019). The other pocket is localised above the switch II loop in GDP-$KRAS^{G12C}$ which is also found to bind to covalently linked small molecules (Ostrem and Shokat, 2016). In addition, a nanomolar inhibitor, BI-2852, was discovered using structure-based drug design. BI-2852 binds to the pocket located between the switch I and II regions

showing an antiproliferative effect in KRAS mutant cells. This nanomolar inhibitor works differently to the covalent $KRAS^{G12C}$ inhibitors (Ostrem *et al.*, 2013). Recent studies using crystallography identified a new shallow pocket beneath the switch II region of Ras near the mutated cysteine residue in G12C mutants found in 12% of Ras induced cancers. Thiol-reactive compounds seem to be able to bind to this pocket and "lock" switch II in a GDP/inactive conformation hence stopping the Ras signalling pathway (Ostrem *et al.*, 2013). Furthermore, small molecule pan-Ras ligands, such as compound 3144, can bind to Ras proteins. Studies in xenograft mouse cancer models showed that compound 3144 has anti-tumour activity (Welsch *et al.*, 2017). Other approaches target the enzymes e.g. farnesyltransferase required for the posttranslational modifications of Ras modifying the CAAX motif to initiate membrane interaction (Head and Johnston, 2004).

1.10 Aims of this study

As mentioned in the beginning, the majority of our understanding of the posttranslational processes needed for the translocation of Ras to the plasma membrane comes from studies using the model organism *S. cerevisiae* investigating the roles of Ras proteins (Clark, McGrath and Levinson, 1985). Findings ,such as the first Ras effectors and GEFs, adenylate cyclase and Cdc25, respectively (Papageorge *et al.*, 1984; Toda *et al.*, 1985), as well as the finding that acetylation was not the first translational modification of Ras (Fujiyama, Matsumoto and Tamanoi, 1987), were identified in *S. cerevisiae.* Analogous proteins and conserved signalling pathways in humans have been able to be identified due to such breakthroughs (Toda *et al.*, 1985). Significant evidence exists that phosphorylation events of Ras influence Ras localisation in humans (Bivona *et al.*, 2006; Qiu *et al.*, 2021). Surprisingly, this has not been studied in *S. cerevisiae*.

In the laboratory of Dr Campbell Gourlay, previous bioinformatics investigations using the PhosphoPep (v2.0) database provided information about potential phosphatase and kinase enzymes affecting Ras2p phosphorylation. Furthermore, various serine residues could be identified which may be subject to phosphorylation on Ras2p. Focus fell upon the serine residue at position 225 of Ras2p and its modification S225A and S225E. In previous studies changes in Ras2 localisation and activity within the cells were studied using S225A/E modifications. The results suggested that modifications of S225 of Ras2p lead to a mis location of active Ras to the nuclear envelop of cells resulting in considerable growth defects mediated through aberrant Ras/cAMP/PKA signalling. In this respect, decreased viability was observed which is suggested to display quiescence in cells. Furthermore, the deletion of the *PTR2* repressor Cup9 rescues these growth defects.

In addition, sequence alignment analysis between yeast Ras2 and human NRas discovered that the Serine residue at position 225 is conserved in human NRas at position 173.

As the above phenotypes were generated by plasmid expression, in the present study we sought to further investigate the impact of Ras2p Serine 225 modifications in regards to Ras2p trafficking inside the cell and nutrient acquisition through the peptide transport mechanism PTR in a more stable system. We sought to approach this using a genome integration system applying the Gateway Cloning Method investigating:

The aims of this project are therefore to:

- Integrate and express the mutant *RAS2* alleles into the genome of wild type *S. cerevisiae* and in a *Δras2* background
- Investigate the effect of mutant *RAS2* alleles on Growth and viability in wild type and *Δras2* background
- Investigate the impact of Ras2p Serine 225 modifications in regards to nutrient acquisition through the peptide transport mechanism PTR

- Express mutant *RAS2* alleles in the *Δcup9* background
- High resolution respirometry to measure respiration in wild type cells overexpressing *RAS2*^{S225A} and effect of *Δcup9* on possible S225A related respiratory defects
- Gene Ontology to find link between cell cycle, nutrient acquisition and Ras mutations
- Further investigations in effect of mutant *RAS2* alleles and nutrient acquisition

2 Materials and methods

2.1 Growth conditions and media for the culture of *Saccharomyces cerevisiae* and *Escherichia coli*

All media was sterilised using a Prestige Medical bench-top autoclave at 121 °C, 15 Ib/sQ.in for 11 min. All *Escherichia coli* liquid cultures were incubated at 37 °C with constant rotation at 180 rpm. All liquid cultures of *Saccharomyces cerevisiae* were incubated at 30 °C with constant rotation at 180 rpm. 2 % w/v granulated agar (Oxoid technical agar No. 3) was added prior to autoclaving for solid medium and glucose- if required- was added after autoclaving.

2.1.1 LB growth media for *E. coli*

The LB media contained 1 % Yeast Extract (BD), 2 % Sodium Chloride (Fisher), 2 % Bactotryptone (BD), and if required 2 % agar (Oxoid). The appropriate antibiotics (Ampicillin, Kanamycin; Sigma-Aldrich) were added for the selection of successfully transformed *E. coli* containing the plasmid of interest. To select for *E. coli* colonies containing plasmids with the *AmpR* gene, Ampicillin (Sigma-Aldrich) was supplemented to the growth medium to a final concentration of 100 μg/ml (stock solution 100 mg/ml in sterile deionised water) after autoclaving. Kanamycin (Sigma-Aldrich) was added to the growth medium to a final concentration of 50 μg/ml (stock solution 10 mg/ml in sterile deionised water) after autoclaving to select for successfully transformed *E. coli* colonies containing the gene for kanamycin resistance.

2.1.2 Yeast extract, peptone, dextrose (YPD) growth media

The YPD growth media contained 2 % w/v glucose (Fisher), 1 % w/v yeast extract (BD) and 2 % w/v Bactopeptone (BD).

2.1.3 Synthetic complete (SC) drop-out medium

Ingredients for this medium included 2 % w/v glucose (Fisher), 0.77 % Yeast Nitrogen Base without amino acids (Kaiser, Formedium), yeast synthetic complete drop-out media supplement (Formedium). Ammonium sulphate is the source of nitrogen for the yeast cells grown in this media.

Once yeast was transformed with plasmid DNA containing the selective marker (uracil, leucine), Yeast Synthetic Complete Drop-Out Media Supplement (Formedium) lacking the appropriate nutrient was used to select successfully transformed yeast.

2.2 *Saccharomyces cerevisiae* strains used in this study

Table 1. The Saccharomyces cerevisiae strains used in this study

Strain	**Genotype**	**strain ID**
BY4741 (S288C ancestry)	MATa *his3Δ1 leu2Δ0 met15Δ0 ura3Δ0*	CGY424
BY4741 *Δras2*	MATa *his3Δ1 leu2Δ0 Met15Δ0 ura3Δ0 Δras2::KANMX*	CGY926
BY4741 *Δcup9*	MATa his3Δ1 leu2Δ0 met15Δ0 ura3Δ0 Δcup9::KANMX	CGY1342
BY4741 Ras2^{S315P}	MATa *his3Δ1 leu2Δ0 met15Δ0 ura3Δ0 pADH-Ras2::ura3*	This study

BY4741 Ras2$^{S225A\ S315P}$	MATa *his3Δ1 leu2Δ0 met15Δ0 ura3Δ0 pADH-Ras2^{S225A}::ura3*	This study
BY4741 Ras2$^{S225E\ S315P}$	MATa his3Δ1 leu2Δ0 met15Δ0 ura3Δ0 pADH-Ras2^{S225E}::ura3	This study
BY4741 pAG306	MATa *his3Δ1 leu2Δ0 met15Δ0 ura3Δ0 pADH-pAG306::ura3*	This study
BY4741 *Δras2* Ras2^{S315P}	MATa *his3Δ1 leu2Δ0 Met15Δ0 ura3Δ0 Δras2Ras2::ura3*	This study
BY4741 *Δras2* Ras2$^{S225A\ S315P}$	MATa *his3Δ1 leu2Δ0 Met15Δ0 ura3Δ0 Δras2Ras2^{S225A}::ura3*	This study
BY4741 *Δras2* Ras2$^{S225E\ S315P}$	MATa *his3Δ1 leu2Δ0 Met15Δ0 ura3Δ0 Δras2Ras2^{S225E}::ura3*	This study
BY4741 *Δras2* pAG306	MATa *his3Δ1 leu2Δ0 Met15Δ0 ura3Δ0 Δras2::ura3*	This study
***Δcup9* Ras2**	MATa his3Δ1 leu2Δ0 met15Δ0 ura3Δ0 Δ*cup9Ras2*::ura3	This study

***Δcup9* Ras2$^{S225A\ S315P}$**	MATa his3Δ1 leu2Δ0 met15Δ0 ura3Δ0 Δc*up9* *Ras2^{S225A}*::ura3	This study
***Δcup9* Ras2$^{S225E\ S315P}$**	MATa his3Δ1 leu2Δ0 met15Δ0 ura3Δ0 Δc*up9* *Ras2^{S225E}*::ura3	This study
***Δcup9* pAG306**	MATa his3Δ1 leu2Δ0 met15Δ0 ura3Δ0 Δc*up9*::ura3	This study

2.3 *Escherichia coli* strains used in this study

DH5α: The genotype of the competent *E. coli* cells used in this study is F- endA1 glnV44 thi-1 recA1 relA1 gyrA96 deoR nupG Φ80dlacZΔM15 Δ(lacZYA-argF) U169, hsdR17(rK-mK+), λ–.

DB3.1: Competent *E. coli* cells were used in this study, the genotype of these cells is: F-gyrA462 endA1 glnV44 Δ(sr1-recA) mcrB mrr hsdS20(rB-, mB-) ara14 galK2 lacY1 proA2 rpsL20(Smr) xyl5 Δleu mtl1.

2.4 Plasmids used in this study

Table 2. Plasmids used in this study

Plasmid	Description	Selective Marker	Source
pDONR221	Gateway Entry Vector	N/A	Addgene

	(Bacterial Resistance Kan.)		
pAG306-ccdB	Gateway Destination Vector (Bacterial Resistance Amp.)	URA3	Addgene
pAG306 empty vector	Gateway Destination Vector (Bacterial Resistance Amp.)	URA3	Addgene
pCG583	*RAS2* in Gateway Destination Vector pAG306-ccdB Amp^R	URA3	This study
pCG586	$RAS2^{S225E}$ in Gateway Destination Vector pAG306-ccdB Amp^R	URA3	This study
pCG587	$RAS2^{S225A}$ in Gateway Destination Vector pAG306-ccdB Amp^R	URA3	This study
pCG349 – RBDx3-GFP-Ras2 (active RAS2)		LEU2	This study
***pCG583**	*RAS2* in pCG558 Amp^R	URA3	This study
***pCG586**	$RAS2^{S225E}$ in pCG558 Amp^R		

	(Episomal Vector/Expression Vector (non-integrating system))		
***pCG587**	*RAS2*^{S225A} in pCG558 Amp^{R} (Episomal Vector/Expression Vector (non-integrating system))	URA3	This study

*Overexpression plasmids

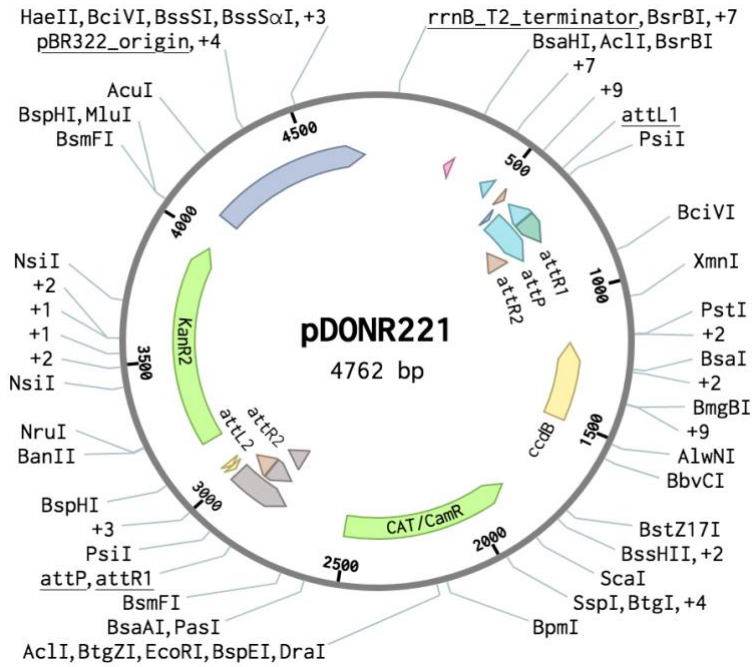
HaeII, BciVI, BssSI, BssSαI, +3
pBR322_origin, +4
AcuI
BspHI, MluI
BsmFI
rrnB_T2_terminator, BsrBI, +7
BsaHI, AclI, BsrBI
+7
+9
attL1
PsiI
BciVI
XmnI
PstI
+2
BsaI
+2
BmgBI
+9
AlwNI
BbvCI
BstZ17I
BssHII, +2
ScaI
SspI, BtgI, +4
BpmI
AclI, BtgZI, EcoRI, BspEI, DraI
BsaAI, PasI
BsmFI
attP, attR1
PsiI
+3
BspHI
NruI
BanII
attL2
attR2
NsiI
+2
+1
+1
+2
NsiI
attR1
attP
attR2
ccdB
CAT/CamR
KanR2
pDONR221
4762 bp
500
1000
1500
2000
2500
3000
3500
4000
4500

A)

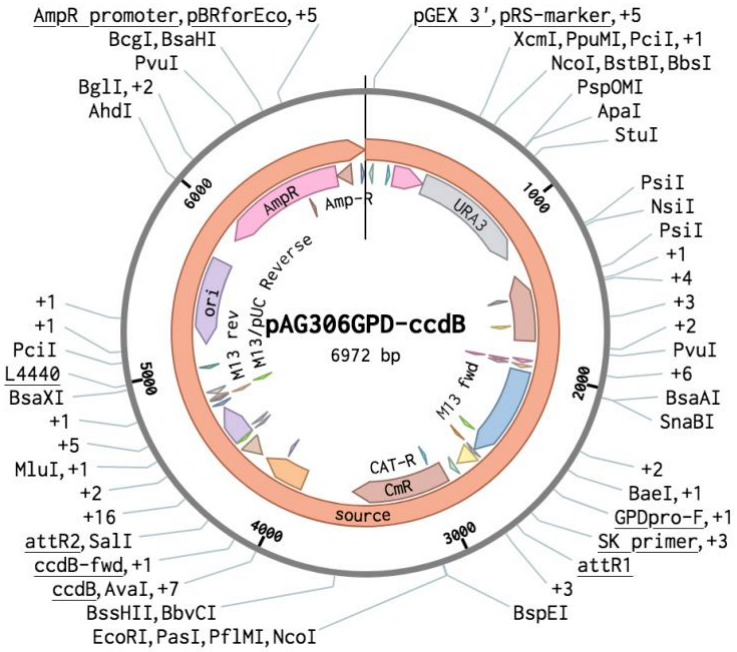
AmpR promoter, pBRforEco, +5
BcgI, BsaHI
PvuI
BglI, +2
AhdI
pGEX 3', pRS-marker, +5
XcmI, PpuMI, PciI, +1
NcoI, BstBI, BbsI
PspOMI
ApaI
StuI
PsiI
NsiI
PsiI
+1
+4
+3
+2
PvuI
+6
BsaAI
SnaBI
+2
BaeI, +1
GPDpro-F, +1
SK primer, +3
attR1
+3
BspEI
BssHII, BbvCI
EcoRI, PasI, PflMI, NcoI
ccdB, AvaI, +7
ccdB-fwd, +1
attR2, SalI
+16
+2
MluI, +1
+5
+1
BsaXI
L4440
PciI
+1
+1
AmpR
Amp-R
URA3
ori
M13 rev
M13/pUC Reverse
M13 fwd
CAT-R
CmR
source
pAG306GPD-ccdB
6972 bp
1000
2000
3000
4000
5000
6000

B)

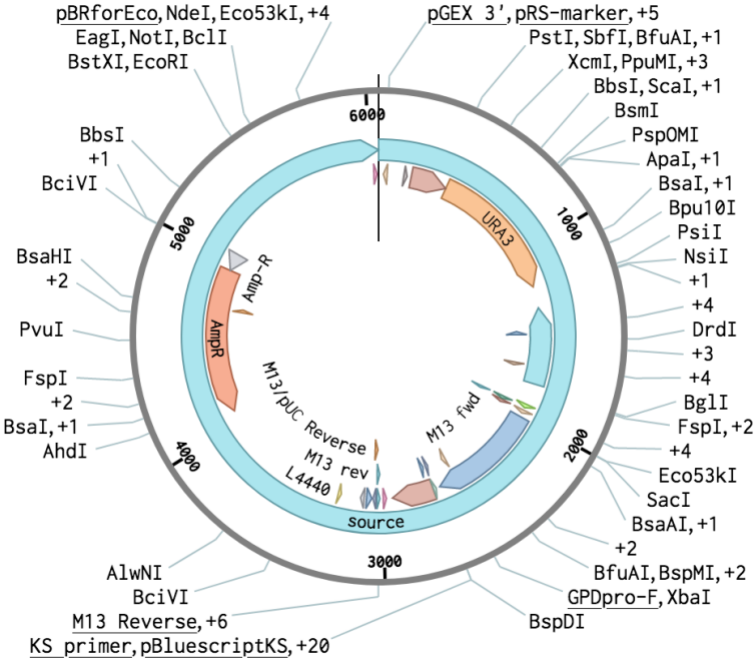

C)

Figure 6. Maps of the plasmids used in the Gateway Cloning Reaction.
A) pDONR221 Gateway Entry Vector
B) pAG306-ccdB Gateway Destination Vector
C) pAG306 control Gateway Destination Vector

2.5 Transformation of plasmid DNA into *S. cerevisiae* and *E. coli*

2.5.1 Transformation of *S. cerevisiae* using the lithium acetate method

A fresh colony of yeast was picked using a sterile inoculation loop and inoculated into 5 ml of appropriate medium and grown overnight at 30 °C with shaking at 180 rpm. The yeast strain was inoculated into 20 ml of YPD media to an OD of 0.1 and incubated at 30 °C with shaking at 180 rpm for 4-5 hours. 1 ml of the culture was transferred to a 1.5 ml microcentrifuge tube and harvested in a bench-top centrifuge at 4000rpm for 5 minutes at room temperature. The supernatant was discarded, and the pellet resuspended in 400 µl of sterile water. 100 µl of this solution was transferred into a sterile Eppendorf tube and centrifuged at 10,000g for 30 seconds. The supernatant was removed and the following mixture was added to the pellet: 240 µl of 50% polyethylene glycol 3300 (PEG; Sigma), 36

µl of 10x (1M) LiAoc solution, 10 µl of 10 mg/ml single stranded DNA (boiled herring sperm DNA), 64 µl water and 10 µl of plasmid DNA. Once all the solutions were added the pellet was resuspended by vortexing and the tubes were placed into a 42 °C water bath for 40 minutes. After the 40 minutes heat shock the cells were centrifuged at 10,000g for 30 seconds, the supernatant was removed and the pellet was resuspended in 150 µl of sterile water. The cell suspension was spread onto agar plates with the appropriate selective media and incubated at 30 °C for at least two days to allow colony growth.

2.5.2 Transformation of *E. coli* with plasmid DNA

A 50 µl aliquot of competent cell (refer to Materials and Methods Section 2.5 for preparation protocol) suspension was thawed on ice. To the solution of competent cells, a volume of plasmid DNA at a concentration of at least 50 ng/ml was added and mixed gently. The mixture was incubated on ice for 30 minutes and then incubated at 42 °C for 45 seconds. The tubes were put back on ice for 2 minutes. 500 µl of appropriate medium (LB growth medium with appropriate antibiotics) was added to the cells and they were grown at 37 °C with shaking at 180 rpm for 45 minutes. The tubes containing the transformed bacteria were centrifuged at 5000g for 3 minutes. Around 350 µl of the supernatant was removed and the pellet was resuspended. The suspension was then spread onto LB agar plates containing the appropriate antibiotic to select for transformants and incubated at 37 °C overnight. Plates were checked for colony growth the next morning.

2.6 *E. coli* competent cell preparation

E. coli cells (DH5α) were grown overnight in 10 ml of LB broth at 37 °C with constant shaking at 180 rpm in a flask with aeration. 8 µl of the overnight culture was sub-cultured

and diluted in 28 ml of LB media to an OD_{600} of 0.5. A volume of 3.75 ml of sterile warm 100 % glycerol was added to the 28 ml flask. The cells were then chilled on ice for 10 minutes. The cells were pelleted at 4 °C for 10 minutes at 1789g. The supernatant was removed carefully and the cells resuspend in 3.75 ml of ice-cold 0.1 M $MgCl_2$ and 15 % glycerol (v/v). The cells were again pelleted at 4 °C for 8 minutes at 1614g. The supernatant was removed and the cells resuspend in 6.25 ml ice-cold T-salts containing 0.075 M $CaCl_2$, 0.006 M $MgCl_2$, and 15 % glycerol (v/v). The suspension was incubated on ice for 20 min with occasional mixing. The cells were then centrifuged at 4 °C for 6 min at 1449g and gently resuspended in 1.25 ml T-salts. The competent cells were then aliquot into pre-cooled tubes and stored immediately at -80 °C for at least overnight before use.

2.7 Molecular biology methods

2.7.1 Plasmid DNA purification from *Escherichia coli* (mini prep)

A fresh colony of *E. coli* containing the plasmid of interest was picked using a sterile inoculation loop. The colony was inoculated into 5 ml of LB media supplemented with the appropriate antibiotic and placed overnight at 37 °C with constant rotation at 180 rpm for growth. The cells were harvested in a benchtop centrifuge at 8000 rpm for 3 minutes at room temperature. The supernatant was removed and the plasmid DNA of interest was extracted from the cell pellet using a Qiagen QIAprep Spin Miniprep Kit according to the manufactures' instructions.

2.7.2 Yeast colony PCR

A small sample of a yeast colony was taken using a sterile pipette tip and mixed into 40 µl of 0.02 M NaOH. The sample was heated for 10 min at 95 °C and then iced for 10 min. The cells were then centrifuged at 2000g for 5 min. 1 µl of the supernatant/DNA was used for the PCR reaction and mixed with PCR reagents (**Table 3**). The mixture was made up to a final volume of 25 µl with sterile water. The samples were run on an 0.4 g agarose gel in 50 ml TAE (= 0.8 %).

Table 3. The reagent mixture for the PCR reaction used for the yeast DNA extraction.

PCR reagents
10X PCR Buffer, -Mg 2.5 µl
50 mM MgCl2 0.75 µl
10 mM dNTP Mix 0.5 µl
10 µM forward primer AmpR 1.25 µl
10 µM reverse prime 503 Chr1rev2 1.25 µl
Template DNA 1 µl
Taq DNA Polymerase (5 U/µl) 0.1 µl

2.7.3 Restriction enzyme digest of DNA

Using restriction endonucleases from New England Biolabs (Not1), enzymatic scission of DNA at specific sequence points was carried out. The manufacturer's protocol was used and the buffer was supplied by the manufacturer. The reagents listed below (**Table 4**) were added together to create a 20 µl reaction mix. The incubation time for the digests was at least 1 hour

(sometimes 4h) at 37 °C. 10 µl of the samples was loaded onto an agarose gel in order to analyse the digested products.

Table 4. Basic reaction mixture used for the restriction enzyme digest used in this study.

Reagent	**Volume**	**Concentrations**
Sterile water	14.8 µl	
Plasmid DNA of interest	2 µl	2 µg/µl
BSA	0.2 µl	10 µg/µl
Buffer D	2 µl	10X
NOT1 (restriction enzyme)	1 µl	5 u/µl

2.7.4 Agarose gel electrophoresis

To analyse DNA fragments and plasmids, agarose gel electrophoresis was carried out. The agarose gels were generally composed of 0.8 % (w/v) agarose (Melford, MB12000) in TAE buffer (**recipe Table 5**).

Table 5. Recipe for 1x TAE Buffer.

Ingredient	amount
Tris base	4.84 g
Glacial acetic acid	1.14 ml
0.5 M EDTA, pH 8.0	2 ml
Milli-Q water	To 1 L final volume

0.4 g of agarose was dissolved in 50 ml 1x TAE by microwaving for 1 min until the solution became clear. The solution was left to cool for 5 min to around 60 °C before 3 µl of ethidium bromide (10 mg/ml) was added to a final concentration of 0.5 µg/ml. The solution was poured into a gel cassette, and a comb was inserted. The gel was left to set for 30-60 min. The solidified gel was placed into an electrophoresis tank and 1x TAE buffer was poured over the gel to cover its surface by 2-3 mm. The comb was then removed. 10 µl of the Invitrogen Fisher 1 kb + gene ruler DNA ladder was transferred into the first well. 1 µl of 10x blue juice loading dye was mixed with the DNA samples in a 1 in 6 manner. 10 µl of sample was loaded into the wells. A voltage of 120 V was applied to the tank for 25 min until the DNA bands had migrated the desired distance.

2.7.5 Invitrogen Gateway cloning reaction

To generate the plasmids used in this study, the Invitrogen Gateway© cloning method was used. This cloning method uses the site-specific recombination of the *lambda bacteriophage*. The Gateway cloning system allows the recombination between the two types of recombination sites that were designed and the two ends of a source sequence and a host vector. This cloning system consists of two completely reversible recombination reactions, namely the BP reaction to create entry clones and the LR reaction to generate expression clones using the corresponding catalytic enzymes BP clonase II and LR clonase II, respectively. In the BP reaction the recombination sites attB and attP are recombined, whereas the LR reaction recombines attL and attR sites. The transformation of the recombined sites occurs through swapping the opposites halves into the opposite set e.g. attL and attR become attB and attP and conversely attB and attP become attL and attR. The names for those engineered vectors are called Entry Clone, Expression Clone, Donor Vector, and Destination Vector.

2.7.6 BP cloning reaction

The Invitrogen Gateway BP cloning reaction was performed to generate the entry vectors used in this study. Prior to the BP reaction, plasmids containing the RAS2, $RAS2^{S225E}$, and $RAS2^{S225A}$ nucleotide sequences were extracted and purified using the Qiagen Spin Miniprep Kit and sequenced by Eurofin. 1 µl of the purified episomal expression vector (50 ng/ml) was mixed with 1 µl of the pDONR221 entry vector (75 ng/ml) together with 2 µl of 1x TE buffer (pH 8.0). The reagents were mixed well while the BP clonase II enzyme was thawed on ice for around 2 minutes and then vortex for 2 seconds. 1 µl of the BP clonase II was then transferred into the reaction mixture and incubated at room temperature for 1 hour. 0.5 µl of Proteinase K solution (2 mg/ml) was added to the solution in order to end the reaction. After briefly vortexing the reaction mixture, the tubes were incubated at 37 °C for 10 minutes. The samples were then stored at -20 °C or transformed into bacteria. The pDONR221 entry clone used contained Kanamycin resistance genes. The samples were sent to GATC Eurofin for sanger sequencing with M13F or T7 promotor primers.

2.7.7 LR cloning reaction

To generate the expression clones used in this study, the Invitrogen Gateway LR cloning reaction was used. This reaction allows the recombination of the destination vector with the entry vector containing the gene of interest. Prior to the LR reaction, bacteria containing the destination vector pAG306 ccdB and pAG306 empty were grown and the plasmid was extracted and purified using the Qiagen Spin Miniprep Kit. The plasmids were checked using agarose gel electrophoresis. 2 µl of the entry clone (50-150 ng/ µl) was mixed with 2 µl of the destination vector (150 ng/ µl) together with 6 µl of 1x TE buffer (pH 8.0). The LR clonase II

enzyme mix was thawed on ice for 2 minutes and vortexed for 2 seconds. To each sample 2 µl of LR clonase II was added and well mixed by vortexing. The reaction was incubated at 25 °C for an hour. 1 µl of Proteinase K solution (2 mg/ml) was added to each sample to terminate the reaction. The samples were vortexed briefly and incubated at 37 °C for 10 minutes before they were stored at -20 °C or transformed into bacteria. The destination vector pAG306 ccdB contained an ampicillin resistance gene. The samples were sent GATC Eurofin for sanger sequencing with the GDPro-F primers.

2.7.8 DNA sequencing

80-100 ng/µl of purified plasmid DNA samples (refer to section 2.6.1 Plasmid DNA purification from *E. coli*) with the associated primers (5 µM) were sent for sequencing to Eurofin. The electronically received data from the sequencing reaction was analysed using snapGene and Blast.

2.8 Biochemical methods

2.8.1 Whole cell protein extraction for SDS page

Overnight cultures of yeast were set up in 5 ml of SD-ura media and OD_{600} readings of 1:10 dilutions were taken the next day. The amount of culture to add to 3 ml of appropriate medium was calculated and the samples were incubated at 30 °C for 24 h in the shaking incubator at 180 rpm. The following day $1x10^8$ cells were harvested via centrifugation at 10,000 rpm for 1 min. Lysis buffer (1 ml of 1 M NaOH; 1 ml of 0.5 M EDTA pH8; 2 ml of 10% SDS; 200 µl ß-mercaptoethanol) was prepared and made up to 10 ml with sterile water before the harvested cells were resuspended in 200 µl of the lysis buffer. The samples were heated for 10 min at 90 °C using a heat block. 5 µl of 4 M Acetic acid was then added to each

sample before vortexing for 30 seconds. A second 10 min incubation at 90 °C followed before 50 µl of loading buffer (50 % glycerol, 0.25 M Tris-HCl pH 6.8, 0.05% bromophenol blue) was added to each sample. The samples were then centrifuged at 10,000 rpm for 1 min in a bench microcentrifuge to clear the lysate before loading onto a polyacrylamide gel.

2.8.2 Polyacrylamide gel electrophoresis

Polyacrylamide gels were prepared as described in **Table 6** whereby each gel was composed of a 7.5-12 % acrylamide resolving gel forming the lower part and a 5 % acrylamide stacking gel forming the upper part. 0.75 mm glass cassettes (Bio-Rad) were used to cast the gels and plastic sealant was used to ensure the glass cassettes stuck together with no leakage gaps. The two glass cassettes were clamped together and water was poured in to confirm no leakage occurred. The cassette was left to dry for a few minutes before the resolving gel layer was poured into it. Isopropanol was added on top of the layer to protect the gel from air and to provide an even top layer surface after solidification of the gel. The resolving gel was allowed to set for 30 min. After solidification occurred, the isopropanol was discarded and the stacking gel was poured into the cassette. An appropriately sized comb was carefully inserted to ensure no bubbles were formed underneath the wells. The stacking gel was allowed to set for 60 min.

Table 6. A table showing the SDS-Page reagents

Resolving gel	**Stacking Gel**	**SDS running buffer**
2 ml of 1.5 M tris pH 8.8 0.4 % SDS	4 ml of 1 M Tris pH 6.8 0.4 % SDS	0.3 % (w/v) Tris-HCL
3 ml of 40% acrylamide (29:1)	1.34 ml of 40% acrylamide (29:1)	1.44 % (w/v) glycine

3 ml sterile water	4.5 ml of sterile water	0.15 % (w/v) SDS
5 µl of TEMED (0.07 %)	8 µl of TEMED (0.07 %)	
35 µl of 10% Ammonium persulphate (APS)	85 µl of 10% APS	

Once the stacking gel was set, the comb and the sealant were carefully removed before the cassette was placed into a gel tank and sealed against the central column. The gel tank was carefully filled with 1x SDS running buffer ensuring no bubbles were formed. A page Ruler^{TM} Plus Prestained Protein ladder was loaded into the first well of each gel. The protein samples containing loading buffer were then loaded into subsequent wells. A voltage of 90 V was applied until the samples migrated out of the wells for about 20 min before the voltage was increased to 135 V for around 2 hours until the protein front migrated to the end of the acrylamide gel to ensure proper separation. The voltage was then stopped before the protein front run off the gel. The cassettes were removed from the gel tank and the gels were used for western blotting described in 2.8.3-4

2.8.3 Semi-dry transfer of proteins to PVDF membranes

After the protein separation via molecular mass using SDS-PAGE, four 8x9 cm pieces of Whatman blotting paper (Thermo Fisher) were cut and soaked in transfer buffer for about 20 min. The PVDF membrane was activated by wetting in methanol for a few secs. before placing the membrane into transfer buffer for 20 min together with the blotting paper. An anode plate of a trans-Blot Semi-Dry Transfer cell (BioRad) was used to place two pieces of blotting paper, followed by the PVDF membrane, the polyacrylamide gel, and the remaining two blotting papers. A roller was used to roll out any excess air between the layers. However, it was not used directly on the PVDF membrane and the gel. The cathode plate was placed

back into the trans-Blot Semi-Dry Transfer cell and connected to a power pack where 25 V was applied for 30 mins. Once the semi-dry transfer was completed, the PVDF membrane was removed and used for the immunoblotting procedure described below.

2.8.4 Immunoblotting

The PVDF membrane was placed in 10 ml of blocking solution (5 % w/v dried skimmed milk (Oxoid) and PBS (Phosphate Buffered Saline)) for 45 mins with rotation at room temperature. The membrane was then placed into a fresh falcon tube filled with blocking solution and the appropriate concentration of the primary antibody (refer to 2.8.7). The falcon tube was placed onto a shaker at room temperature over night for best results. The following day, the membrane was removed from the falcon tube, placed into a fresh tube, and washed with PBS/T (Phosphate Buffered Saline and 0.2 % Tween 20 (Sigma)) for 15 mins via shaking. Another two washes of 5 mins each followed before the membrane was placed into a new falcon tube containing blocking solution with the horse-radish peroxidase conjugates secondary antibody. The tube was incubated at shaking for 45 mins at room temperature. The membrane was again removed from the tube and placed into a new tube for washing it for 15 mins with PBS/T followed by three more washes of 5 mins each. The membrane was finally placed in a new tube containing PBS, and the blots visualised using the ECL detection (Enhanced Chemiluminescence).

2.8.5 ECL detection (enhanced chemiluminescence)

The PBS solution was discarded and the PVDF membrane was placed into a clean container before a 1:1 ratio of the ECL solutions (**Table 7**) was added for 1 min with constant shaking. The ECL solution was discarded after the 1 min incubation and the membrane was placed into the SynGene gel doc where the blot was visualised. To analyse the blots the GeneSys

Software (Version 1.6.5.0) was used and a Synoptics 6MP camera was used to capture the images. The programme Fiji (ImageJ) version (2.1.0/1.53c) was used to calculate the Ras2p band intensity relative to the Pgk1p loading control. The Ras2p band was normalised to the control by calculating the integrated intensity of the Ras2p band which was then divided by the integrated intensity of the loading control band of Pgk1p.

Table 7. ECL Solutions

Name of ECL Solution	**Recipe**
ECL 1	1 ml luminol 250 mM 0.44 ml p-coumaric acid 90 mM (Sigma No C9008) 10 ml 1 M Tris.HCL pH 8.5 Make up to 100 ml with water
ECL 2	64 µl 30% hydrogen peroxide 10 ml 1 M Trs.HCL pH 8.5 Make up to 100 ml with water

2.8.6 Stripping of PVDF membrane

To confirm that an even loading of protein to the gel occurred, a loading control was required following the ECL detection. The membrane was placed into a fresh falcon tube containing stripping buffer (Thermo Scientific) for 30 mins to remove previously bound antibodies in order to allow antibodies used for the detection of the loading control to bind. The membrane was removed from the falcon tube and briefly washed with PBS/T twice. The membrane was then placed into 10 ml of blocking solution (5 % w/v dried skimmed milk (Oxoid) and PBS

(Phosphate Buffered Saline)) for 45 mins at constant shaking at room temperature. After completing the blocking incubation, the membrane was probed with a fresh primary antibody.

2.8.7 Antibodies used in the study

For the analysis of western blots antibodies listed below were used.

Primary antibody used for Ras2p detection: Goat anti-Ras2 polyclonal IgG at a dilution of 1/1000 (Santa Cruz Biotechnology, Inc. Bergheimer Str. 89-2, 69115 Heidelberg, Germany)

Secondary antibody for Ras2p detection: Anti-sheep IgG HRP (Sigma, catalogue number A3415) and was used at a dilution of 1/10 000.

Primary antibody used for Pgk1p/loading control detection: Rabbit anti-Pgk1p (Supplied by Professor Mick Tuite, University of Kent) at a 1:1000 dilution.

Secondary antibody used for Pgk1p detection: Anti-rabbit IgG HRP (Sigma A6154) at a 1:10 000 dilution.

2.9 Cell biology techniques

2.9.1 Absorbance assays for growth rate analysis of *S. cerevisiae* cells

A fresh colony of yeast was picked with a sterile inoculation loop and inoculated into 5 ml of appropriate medium over night for growth at 30 °C with constant shaking at 180 rpm. The optical density of the overnight culture was measured using an Eppendorf Biophotometer plus at an OD_{600}. The yeast cultures were diluted to an OD_{600} of 0.1 in 1000 µl of appropriate medium with or without supplements (**Table 8**) into a sterile 24-well plate (Greiner). The 24-well plate was placed into a BMG LABTECH FLUOstar OPTIMA or a BMG LABTECH

SPECTROstar Nano plate reader for 24 hours where the growth was measured (**Table 9**). The protocol setting used can be found in the table below. To analyse the generated data by the plate reader the data analysis software BMG LABTECH MARS was used. The data was then exported to Microsoft Excel to further analysing it. In this thesis each growth curve represents the sum of three biological repeats, each of which included three technical repeats.

Table 8. A list of supplements added to SD-URA media.

Supplement	**Concentration**	**Solubility**
Methionine (Sigma Aldrich)	100%, 50%, 25%, 0%	water
S-Adenosyl Methionine (Sigma Aldrich)	0.5 mM	H_2O at 100 mg/ml = 196.9 mM
S-AdenosylHomocysteine (Sigma Aldrich)	0.5 mM	HCl at 20 mg/ml = 52 mM
L-Homocysteine (Sigma Aldrich)	0.5 mM	H_2O at 14 mg/ml 103.6 mM

Table 9. The protocol setting used to measure growth rate

Cycle Time	1800 seconds
Flashes per Well	3
Excitation	600 nm
Shaking Frequency	400 nm
Shaking Mode	Double Orbital
Additional Shaking Time	30 seconds before each cycle
Temperature	30 °C
Positioning Delay	0.5 seconds

2.9.2 Cell counting using a haemocytometer

A haemocytometer was used to count the cells. The cultures grown in the 24-well plate for 24 hours were diluted 1:100 in sterile water. 10 µl of this solution was added onto the haemocytometer right after vortexing for 10 secs. The cells were counted under a light microscope using the 100x magnification. Buds were not included in the cell count unless the bud size was greater than one third the size of the mother cell. The West-North-rule was used to prevent counting cells twice. A minimum of 100 cells were counted.

2.9.3 Viability assay

A sterile inoculation loop was used to pick a fresh colony of yeast which was then inoculated into 5 ml of appropriate medium and grown overnight at 30 °C with constant shaking at 180 rpm. The exact same steps were followed as in 2.9.1. Once the 24 hours growth in the plate reader was completed, a 1:100 dilution was made and vortexed thoroughly. The number of cells in a culture was counted under a microscope using a haemocytometer. Here, 10 µl of the 1:100 dilution was plated onto the microscope slide and at least 100 cells were counted in one square of the haemocytometer. A 1:10 000 dilution was made from the 1:100 dilution and it was calculated how much of this dilution has to be added in order to plate 300 cells of each sample onto the appropriate agar plates. For 100 % viability, 300 colony forming units (CFU) should grow. The plates were incubated at 30 °C for 48 hours prior counting. The percentage viability was determined by the dividing the number of observed CFU's by the number of expected CFU's and multiplied by 100.

2.9.4 Ferrozine sensitivity assay

A fresh colony of yeast was picked using a sterile inoculation loop. The colony was then inoculated into 5 ml of appropriate medium and placed into the shaking incubator at 30 °C at 200 rpm for growth overnight. The next morning measurements of the optical density were taken using an Eppendorf Biophotometer plus. The Overnight cultures were diluted to an OD_{600} 0.1 in 1 ml of the appropriate medium. The cells were then diluted to 1 x 10^7 cells/ml. A dilution of 1000-fold over three serial dilutions was applied. Each 100-fold dilution was plated onto three agar plates with a ferrozine concentration of 0.25 mM. Prior, a 1 mM working stock of ferrozine was made. From this, a concentration of 0.25 mM of ferrozine was added to the 40 ml agar media. Plates were left until they were dry and placed into a 30 °C incubator for 48 hours. After 48 hours, visual analysis was conducted using the SynGene gel doc and the GeneSys Software (Version 1.6.5.0). A Synoptics 6MP camera was used to capture the images.

2.10 Fluorescence microscopy of yeast cells

2.10.1 Fluorescence microscopy

An Olympus 1X81 inverted microscope was used to visualise fluorescent cells. A Cool LED pE4000 illumination system provided the light, and an Andor's Zyla 4.2 PLUS sCMOS camera was used to capture all images. The acquisition software Micro-Manager version 1.4.22 was used to obtain the images. An Olympus 100 x objective lens (NA = 1.4) was used to visualise cells from a sample. The GFP channel with excitation/emission wavelengths of 488/512 nm was used to observe Cells with GFP-tagged Ras2 proteins. A halogen light source was used to capture DIC images. Each experiment was repeated in biological

triplicate. The software ImageJ FIJI was used for the analysis and processing of the microscopy images.

2.10.2 Sample preparation

A fresh colony of yeast was picked with a sterile inoculation loop. The colony was inoculated into 5 ml of appropriate SD media and grown overnight at 30 °C with shaking at 180 rpm. The OD_{600} of this culture was measured using an Eppendorf Biophotometer plus. To analyse yeast cells in logarithmic phase of cell growth, cells were sub-cultured and grown to OD_{600} 0.4-0.7 in YPD media. 2 µl of the culture was pipetted onto a microscope slide and covered using a 20 mm by 20 mm cover slip. A single drop of Olympus Immoil-F30CC immersion oil was applied to the surface of the 100x (1.4 NA) objective lens prior to the examination under the microscope.

2.11 High resolution respirometry

To examine the consumption of oxygen from mitochondria in cell suspensions, the Orobus O2K Oxygraph High Resolution Respirometer was used. For the analysis and acquisition of data generated, the Datlab 4 software was used. The two chambers of the respirometer held 2 ml of cells suspended in media without glucose and were kept at 30 °C. The respirometer was calibrated using Phosphate Buffered Saline (PBS). A liquid culture was grown overnight and diluted to a calculated OD_{600} of 0.1 the next day. After 24 h the cells were counted using a haemocytometer to ensure an equal volume of cells was present in each chamber. To do this, a 1/50 dilution was carried out and an entire haemocytometer grid of cells was counted in order to calculate the number of yeast cells contained din 1 ml of culture. The samples were

diluted to a cell density of 10^6 cells/ml into 3 ml of appropriate media. 2.5 ml of each diluted culture was then pipetted into one of the two chambers. The chamber stoppers were placed into position and any residual liquid culture was removed. In order to obtain an accurate oxygen flux/cell reading, the precise cell concentration was entered into the Datlab4 software.

To analyse the mitochondria of the cells, drugs were introduced into the chamber using specific syringes. Those drugs target different specific parts of the electron transport chain. The following drugs were administered into each sample: 0.2 mM Triethiltyn bromide (TET; 50 mM stock solution in DMSO) (Sigma-Aldrich), 0.012 mM carbonylcyanidep-trifluoromethoxyphenylhydrazone (FCCP; 12 mM stock in ethanol) (Fluka), and 0.002 mM Antimycin A (AntA; 2 mM stock solution in ethanol) (Sigma-Aldrich). A 5 min interval between the additions of each drug was left to facilitate the detection of a full drug response.

3. Results

3.1 Confirmation of *RAS2* mutant alleles by DNA sequencing

We wished to examine if phosphorylation of the Serine residue at position 225 plays a role in active Ras2p localisation as well as growth and viability. In advance of this study site-directed mutagenesis had been carried out in order to substitute Serine^{225} with either Alanine or Glutamate in the wild type *RAS2* gene. Here, Alanine should produce a non-phosphorylatable residue whereas the mutation to Glutamate mimics phosphorylation. Prior to beginning analysis, I sent a gateway donor vector (PDONR221) containing *RAS2*^{S225A} and *RAS2*^{S225E} for DNA sequencing. The translation of the DNA sequences obtained are shown (**Fig. 7, 8**). A gateway LR clonase reaction (Materials and Methods, Section 2.7.7) was carried out to obtain expression vectors from the donor vector. We noticed a secondary mutation on a Serine residue at position 315 substituting Serine to Proline. The *RAS2* gene used for mutagenesis was obtained pre-cloned within an entry vector after an LR reaction, called DNASU plasmid repository (http://dnasu.org/DNASU/GetCloneDetail.do?cloneid=23931). Using this the S225 A/E mutations using site-directed mutagenesis were made by Eman Badr. We know from Piper-brown, 2019, that the *RAS2* gene from DNASU behaved exactly like a *RAS2* wild type allele in several assays (localisation, activity) very different to the S225A and E strains, so we are confident in the data with regards to 225A and E having important effects over and above the background mutation.

```
Query: CLJ914_16479143_16479143 Query ID: lcl|Query_21668 Length: 1075

>Ras family GTPase RAS2 [Saccharomyces cerevisiae S288C]
Sequence ID: NP_014301.1 Length: 322
>RecName: Full=Ras-like protein 2; Flags: Precursor [Saccharomyces cerevisiae S288C]
Sequence ID: P01120.4 Length: 322
Range 1: 1 to 319

Score:574 bits(1479), Expect:0.0,
Method:Compositional matrix adjust.,
Identities:317/319(99%), Positives:318/319(99%), Gaps:0/319(0%)

Query  117   MPLNKSNIREYKLvvvggggvgKSALTIQLTQSHFVDEYDPTIEDSYRKQVVIDDEVSIL  296
             MPLNKSNIREYKLVVVGGGGVGKSALTIQLTQSHFVDEYDPTIEDSYRKQVVIDDEVSIL
Sbjct  1     MPLNKSNIREYKLVVVGGGGVGKSALTIQLTQSHFVDEYDPTIEDSYRKQVVIDDEVSIL  60

Query  297   DILDTAGQEEYSAMREQYMRNGEGFLLVYSITSKSSLDELMTYYQQILRVKDTDYVPIVV  476
             DILDTAGQEEYSAMREQYMRNGEGFLLVYSITSKSSLDELMTYYQQILRVKDTDYVPIVV
Sbjct  61    DILDTAGQEEYSAMREQYMRNGEGFLLVYSITSKSSLDELMTYYQQILRVKDTDYVPIVV  120

Query  477   VGNKSDLENEKQVSYQDGLNMAKQMNAPFLETSAKQAINVEEAFYTLARLVRDEGGKYNK  656
             VGNKSDLENEKQVSYQDGLNMAKQMNAPFLETSAKQAINVEEAFYTLARLVRDEGGKYNK
Sbjct  121   VGNKSDLENEKQVSYQDGLNMAKQMNAPFLETSAKQAINVEEAFYTLARLVRDEGGKYNK  180

Query  657   TLTENDNSKQTSQDTKGSGANSVPRNSGGHRKMSNAANGKNVNSATTVVNARNASIESKT  836
             TLTENDNSKQTSQDTKGSGANSVPRNSGGHRKMSNAANGKNVNS+TTVVNARNASIESKT
Sbjct  181   TLTENDNSKQTSQDTKGSGANSVPRNSGGHRKMSNAANGKNVNSSTTVVNARNASIESKT  240

Query  837   GLAGNQATNGKTQTDRTNIDnstgqagqanaqsantvnnrvnnnSKAGQVSNAKQARKQQ  1016
             GLAGNQATNGKTQTDRTNIDNSTGQAGQANAQSANTVNNRVNNNSKAGQVSNAKQARKQQ
Sbjct  241   GLAGNQATNGKTQTDRTNIDNSTGQAGQANAQSANTVNNRVNNNSKAGQVSNAKQARKQQ  300

Query  1017  AAPGGNTSEASKSGPGGCC  1073
             AAPGGNTSEASKSG GGCC
Sbjct  301   AAPGGNTSEASKSGSGGCC  319
```

Figure 7. The translated sequence showing the substitution of Serine225 to Alanine and a secondary mutation at position 315 substituting Serine to Proline.
Query: protein sequence submitted
Subject: matching gene bank sequence

Length = 323

Score = 578 bits (1491), Expect = 0.0

Identities = 320/322 (99%), Positives = 320/322 (99%)

```
Query: 15  MPLNKSNIREYKLvvvggggvgKSALTIQLTQSHFVDEYDPTIEDSYRKQVVIDDEVSIL 74
           MPLNKSNIREYKLVVVGGGGVGKSALTIQLTQSHFVDEYDPTIEDSYRKQVVIDDEVSIL
Sbjct: 1   MPLNKSNIREYKLVVVGGGGVGKSALTIQLTQSHFVDEYDPTIEDSYRKQVVIDDEVSIL 60

Query: 75  DILDTAGQEEYSAMREQYMRNGEGFLLVYSITSKSSLDELMTYYQQILRVKDTDYVPIVV 134
           DILDTAGQEEYSAMREQYMRNGEGFLLVYSITSKSSLDELMTYYQQILRVKDTDYVPIVV
Sbjct: 61  DILDTAGQEEYSAMREQYMRNGEGFLLVYSITSKSSLDELMTYYQQILRVKDTDYVPIVV 120

Query: 135 VGNKSDLENEKQVSYQDGLNMAKQMNAPFLETSAKQAINVEEAFYTLARLVRDEGGKYNK 194
           VGNKSDLENEKQVSYQDGLNMAKQMNAPFLETSAKQAINVEEAFYTLARLVRDEGGKYNK
Sbjct: 121 VGNKSDLENEKQVSYQDGLNMAKQMNAPFLETSAKQAINVEEAFYTLARLVRDEGGKYNK 180

Query: 195 TLTENDNSKQTSQDTKGSGANSVPRNSGGHRKMSNAANGKNVNSETTVVNARNASIESKT 254
           TLTENDNSKQTSQDTKGSGANSVPRNSGGHRKMSNAANGKNVNS TTVVNARNASIESKT
Sbjct: 181 TLTENDNSKQTSQDTKGSGANSVPRNSGGHRKMSNAANGKNVNSSTTVVNARNASIESKT 240

Query: 255 GLAGNQATNGKTQTDRTNIDnstgqagqanaqsantvnnrvnnnSKAGQVSNAKQARKQQ 314
           GLAGNQATNGKTQTDRTNIDNSTGQAGQANAQSANTVNNRVNNNSKAGQVSNAKQARKQQ
Sbjct: 241 GLAGNQATNGKTQTDRTNIDNSTGQAGQANAQSANTVNNRVNNNSKAGQVSNAKQARKQQ 300

Query: 315 AAPGGNTSEASKSGPGGCCIIS 336
           AAPGGNTSEASKSG GGCCIIS
Sbjct: 301 AAPGGNTSEASKSGSGGCCIIS 322
```

Figure 8. The translated sequence showing the substitution of Serine225 to Glutamate and a secondary mutation at position 315 substituting Serine to Proline.
Query: protein sequence submitted
Subject: matching gene bank sequence

3.2 Expression of RAS2, RAS2^{S225A} and RAS2^{S225E} alleles in *S. cerevisiae*

The alleles *ras2*, *ras2*^{S225A}, and *ras2*^{S225E} were expressed in *S. cerevisiae* using two different vector sets: overexpression vectors that contained a 2μ origin of replication and thus multiple copies, and via genome integration vectors that, when inserted, generated a single copy. The following analyses therefore focused on cells carrying both single and multiple copies of the *ras2*, *ras2*^{S225A}, and *ras2*^{S225E} alleles.

Western blot analysis was used to determine the levels of wild type and mutant Ras2p (Materials and Methods, Section 2.8) during stationary phase 24 hours after inoculation. Uniform protein loading was confirmed by assessing levels of 3-PhosphoGlycerate Kinase (Pgk1p) in each strain. Fiji (ImageJ) was used for the calculation of the Ras2p band intensity relative to the Pgk1p loading control. The integrated intensity of the Ras2p band was calculated first and then divided by the integrated intensity of the control band Pgk1p thereby normalising it to the control strain. The levels of wild type and mutant Ras2p were analysed in both the wild type background and a *Δras2* background.

An increase in the levels of wild type and mutant Ras2p was observed in the wild type background of both 2μ and integration expression strains when compared to the wild type control (**Fig. 9 and 11)**. Furthermore, quantification revealed that in 2μ and integration systems an increase in Ras2p^{S225A} and Ras2p^{S225E} was seen when compared to the Ras2 overexpression (**Fig. 10 and 12)**.

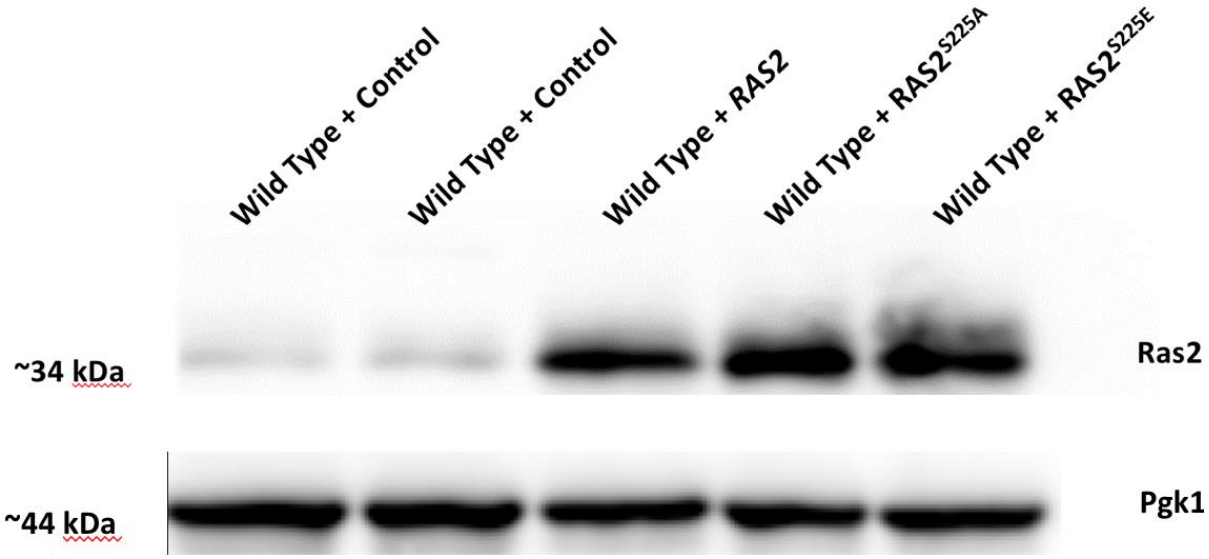

Figure 9. A Western blot showing the detection of Ras2p in cells overexpressing *RAS2*, *RAS2*^{S225A}, *RAS2*^{S225E} or control cells in the 2µ system.
The cells were cultured in SD-URA media and sampled during stationary phase of growth 24 hours after inoculation. Uniform protein loading was ensured by probing levels of Pgk1 after probing for Ras2p. This experiment is a representative data set of three repeats. This Western blot was generated by Elliot Piper-Brown, a member of the Gourlay lab.

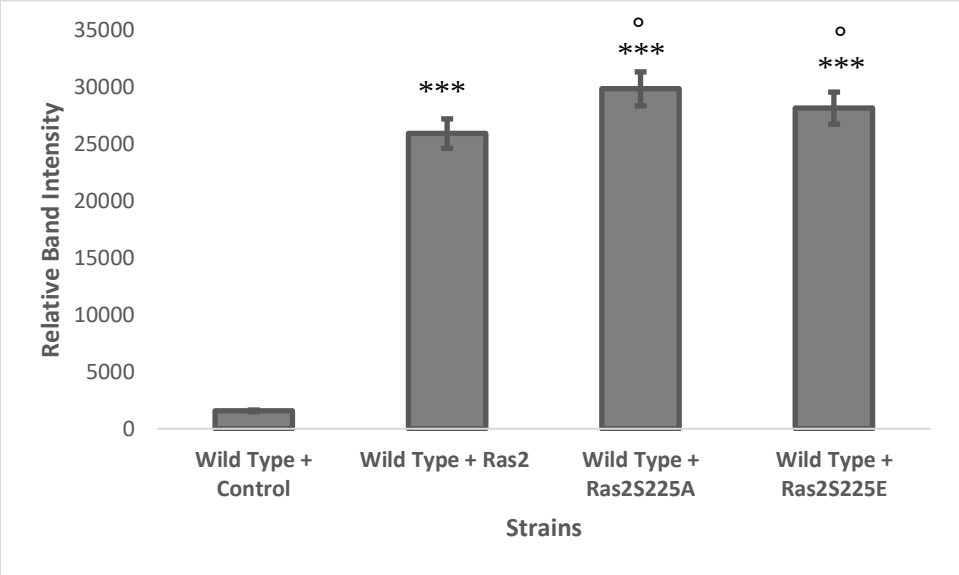

Figure 10. A bar chart representing the change in Ras2p band intensity relative to the Pgk1p loading control of wild type cells overexpressing *RAS2*, *RAS2*^{S225A}, *RAS2*^{S225E} or control cells in the 2µ system.
The cells were grown in SD-URA media and sampled during stationary phase of growth 24 hours after inoculation. The data shown represents and average of three biological repeats. The error bars display the standard deviation. A One-way ANOVA using a Tukey multiple comparison test was used to determine statistical significance. (*) flags levels of significance compared to the control and (°) flags levels of significance compared to WT + Ras2.

*/° = adjusted p-value ≤ 0.05 and ***/°°° = adjusted p value ≤ 0.001.

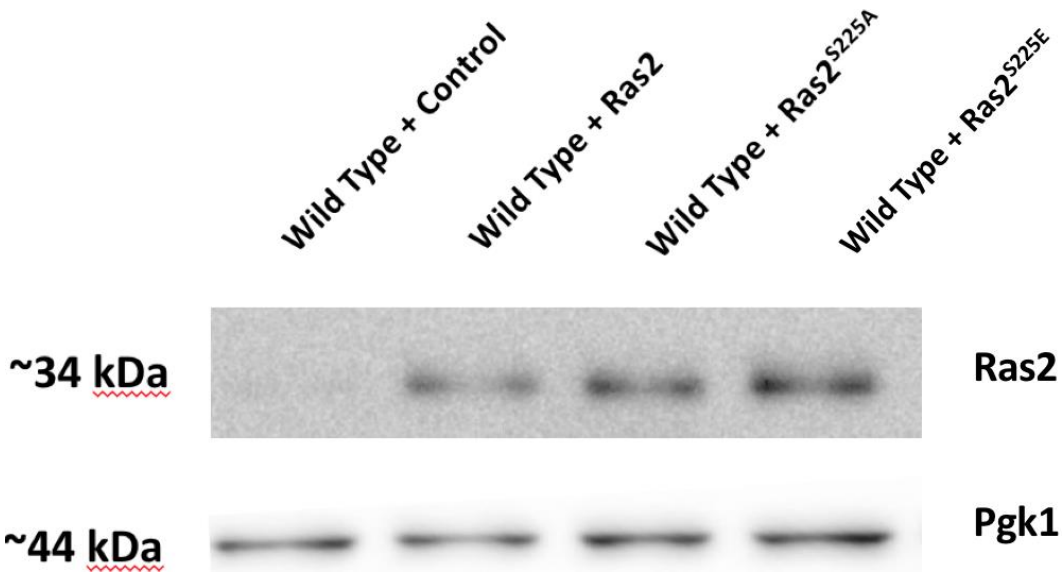

Figure 11. A Western blot showing the detection of Ras2p in cells overexpressing *RAS2*, *RAS2*^{S225A}, *RAS2*^{S225E} control cells using genome integrating plasmids.
The cells were cultured in SD-URA media and sampled during stationary phase of growth 24 hours after inoculation. Uniform protein loading was ensured by probing levels of Pgk1 after probing for Ras2p. This experiment is a representative data set of three repeats.

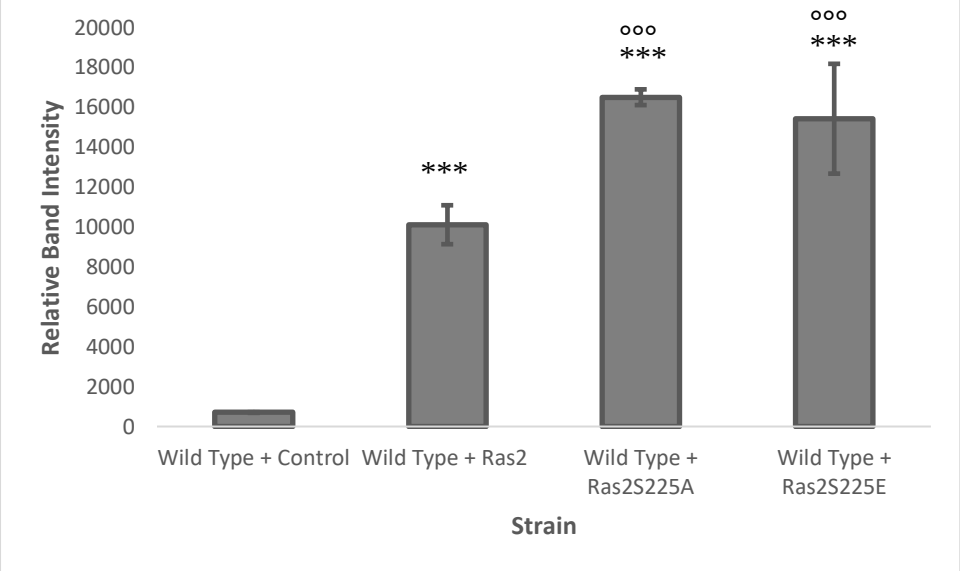

Figure 12. A bar chart representing the change in Ras2p band intensity relative to the Pgk1p loading control of wild type cells overexpressing *RAS2, RAS2^{S225A}, RAS2^{S225E}* or control cells using genome integrating plasmids.
The cells were grown in SD-URA media and sampled during stationary phase of growth 24 hours after inoculation. The data shown represents and average of three biological repeats. The error bars display the standard deviation. A One-way ANOVA using a Tukey multiple comparison test was used to determine statistical significance. (*) flags levels of significance compared to the control and (°) flags levels of significance compared to WT + Ras2.
*/° = adjusted p-value ≤ 0.05 and ***/°°° = adjusted p value ≤ 0.001.

RAS2, RAS2^{S225A} RAS2^{S225E} or an empty plasmid were expressed in a *Δras2* background to investigate the effects of the *RAS2* mutants on the levels of Ras2p produced in the absence of endogenous Ras2p. The *Δras2* strain expressing the empty plasmid backbone control showed no Ras2p signal confirming the deletion of *RAS2* in this background (**Fig. 13-16).** No significant differences in levels (relative intensity) of Ras2p were observed in cells overexpressing *RAS2^{S225A} RAS2^{S225E}* compared to the *RAS2* overexpression strains in the 2μ system *Δras2* background (**Fig. 14**).

In the genome integration system *Δras2* background no significant difference in Ras2p levels was observed in cells overexpressing *RAS2, RAS2^{S225A} RAS2^{S225E}* (**Fig. 16**).

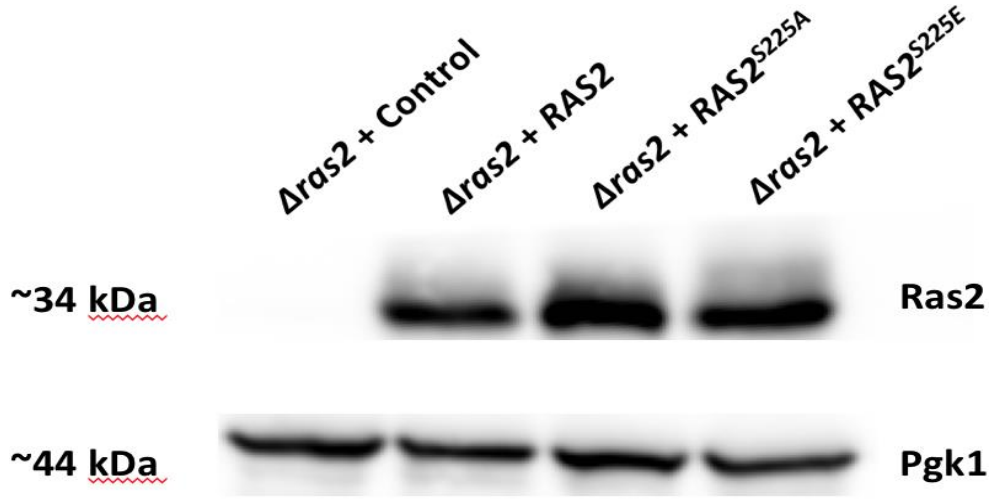

Figure 13. A Western blot displaying the detection of Ras2p in a *Δras2* background overexpressing *RAS2, RAS2^{S225A}, RAS2^{S225E}* or control cells using the 2µ system.
The cells were cultured in SD-URA media and sampled during stationary phase of growth 24 hours after inoculation. Uniform protein loading was ensured by probing levels of Pgk1 after probing for Ras2p. This experiment is a representative data set of three repeats. This Western blot was generated by Elliot Piper-Brown, a member of the Gourlay lab.

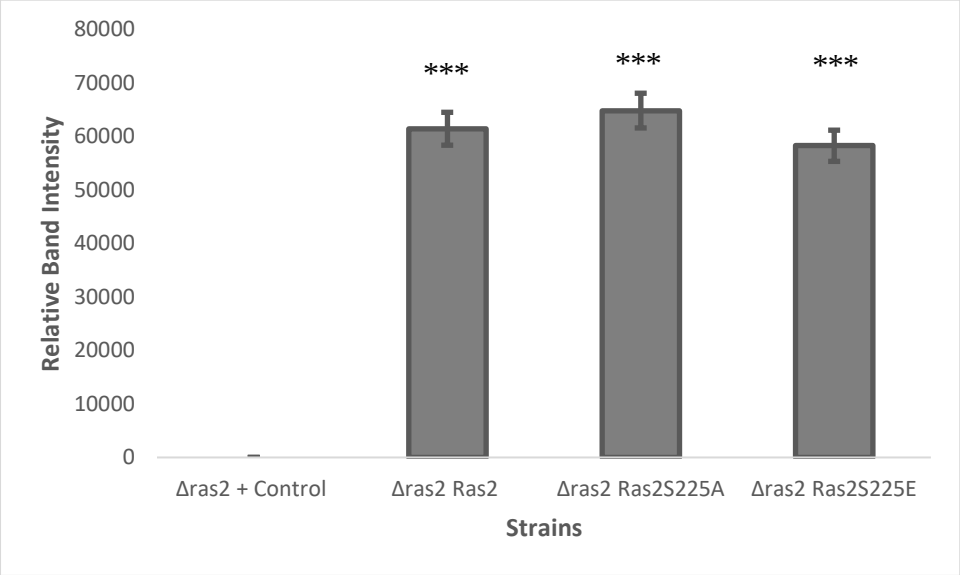

Figure 14. A bar chart representing the change in Ras2p band intensity relative to the Pgk1p loading control of *Δras2* cells overexpressing *RAS2, RAS2^{S225A}, RAS2^{S225E}* or control cells using the 2µ system.
The cells were grown in SD-URA media and sampled during stationary phase of growth 24 hours after inoculation. The data shown represents and average of three biological repeats. The error bars display the standard deviation. A One-way ANOVA using a Tukey multiple comparison test was used to determine statistical significance. (*) flags levels of significance compared to the control and (°) flags levels of significance compared to *Δras2* + Ras2.
*/° = adjusted p-value ≤ 0.05 and ***/°°° = adjusted p value ≤ 0.001.

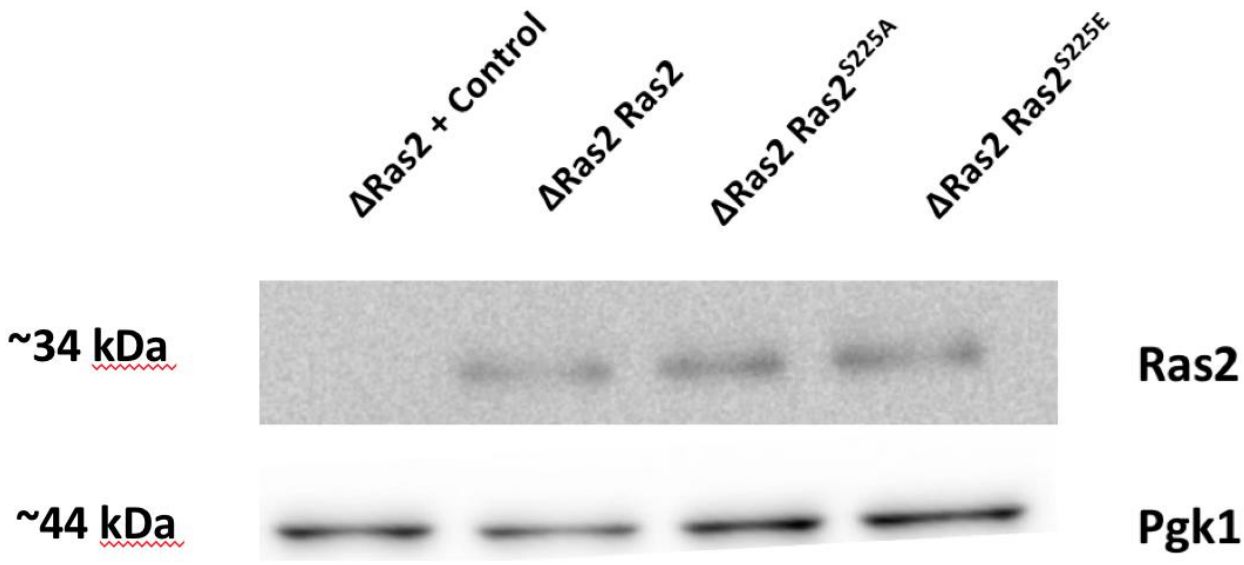

Figure 15. A Western blot displaying the detection of Ras2p in a Δras2 background overexpressing *RAS2, RAS2^{S225A}, RAS2^{S225E}* or control cells using genome integrating plasmids.
The cells were cultured in SD-URA media and sampled during stationary phase of growth 24 hours after inoculation. Uniform protein loading was ensured by probing levels of Pgk1 after probing for Ras2p. This experiment is a representative data set of three repeats.

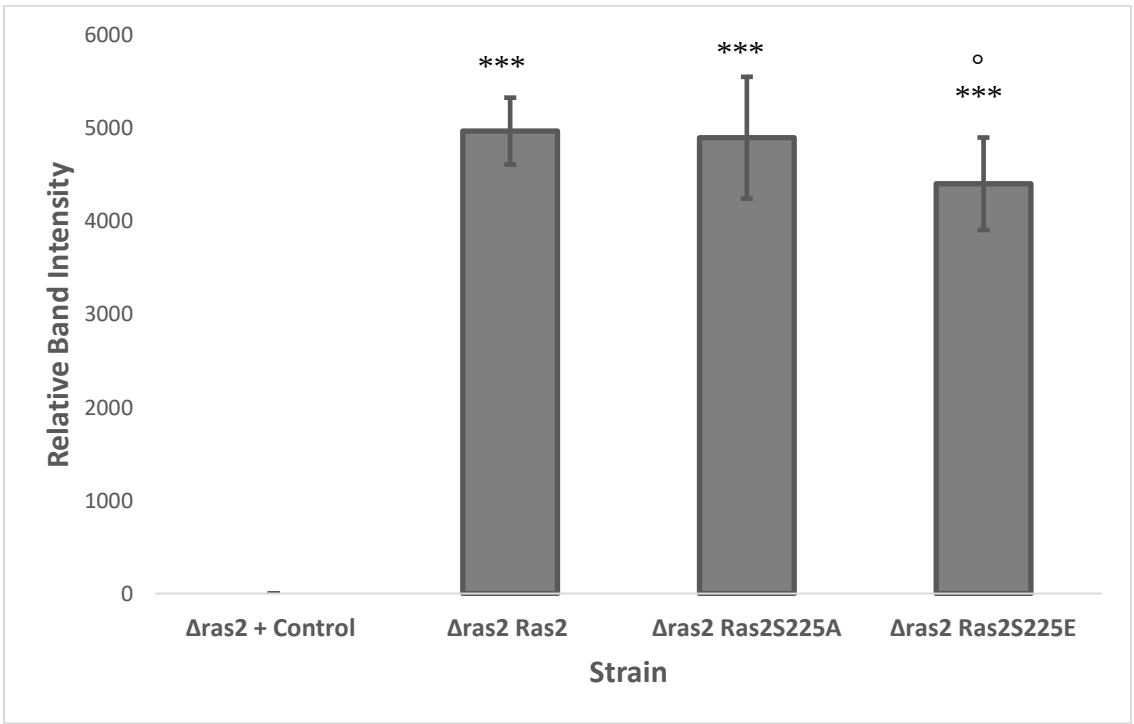

Figure 16. A bar chart representing the change in Ras2p band intensity relative to the Pgk1p loading control of *Δras2* cells overexpressing *RAS2, RAS2^{S225A}, RAS2^{S225E}* or control cells using genome integrating plasmids.

The cells were grown in SD-URA media and sampled during stationary phase of growth 24 hours after inoculation. The data shown represents and average of three biological repeats. The error bars display the standard deviation. A One-way ANOVA using a Tukey multiple comparison test was used to determine statistical significance. (*) flags levels of significance compared to the control and (°) flags levels of significance compared to *Δras2* + Ras2.
*/° = adjusted p-value ≤ 0.05 and ***/°°° = adjusted p value ≤ 0.001.

Comparing the change in Ras2p band intensity relative to the Pgk1p loading control, the values of the overall relative band intensities of the 2μ system was almost doubled compared to the genome integration system in the wild type background e.g. Wild Type + $RAS2^{S225A}$ ~30.000 (**Fig. 10**) vs. Wild Type + $RAS2^{S225A}$ ~16.500 (**Fig. 12**). This was also observed in the *Δras2* background comparing the *Δras2* + RAS2 overexpression strains (**Fig. 14, 16)**. This is in line with the expected increase in copy number of the 2μ system.

3.3 Microscopic analysis of wild type cells expressing Ras2p, $Ras2p^{S225A}$ or $Ras2p^{S225E}$ co-expressed with as active Ras probe

Active GTP bound Ras can be visualised within cells using a fusion of GFP to the Raf1 binding domain (RBD). Ras activity was investigated using the GFP-RBD probe in cells overexpressing Ras2p, $Ras2p^{S225A}$ or $Ras2p^{S225E}$ from a 2μ plasmid. Localisation of active Ras proteins was examined during the logarithmic and stationary phase in a wild type background. The fluorescence microscopy images presented were generated by Elliot Piper-Brown (Piper-brown, 2019), however we wished to quantify the phenotypes identified within this data set.

During the logarithmic phase of growth, the wild type strains expressing Ras2 showed accumulation of active Ras at the plasma membrane and within the nucleus (**Fig. 17**). In contrast, those expressing $Ras2p^{S225A}$ or $Ras2p^{S225E}$ were rather found at the nuclear envelope and the endoplasmic reticulum (**Fig. 17/18**). This was different to the wild type strains

expressing Ras2p or the empty plasmid control which were found to accumulate at the plasma membrane or nucleus (**Fig. 17/18**). Interestingly, the RBD-GFP probe signal in all strains was found at a certain percentage at internal membranes and intracellular foci (**Fig. 17/18**).

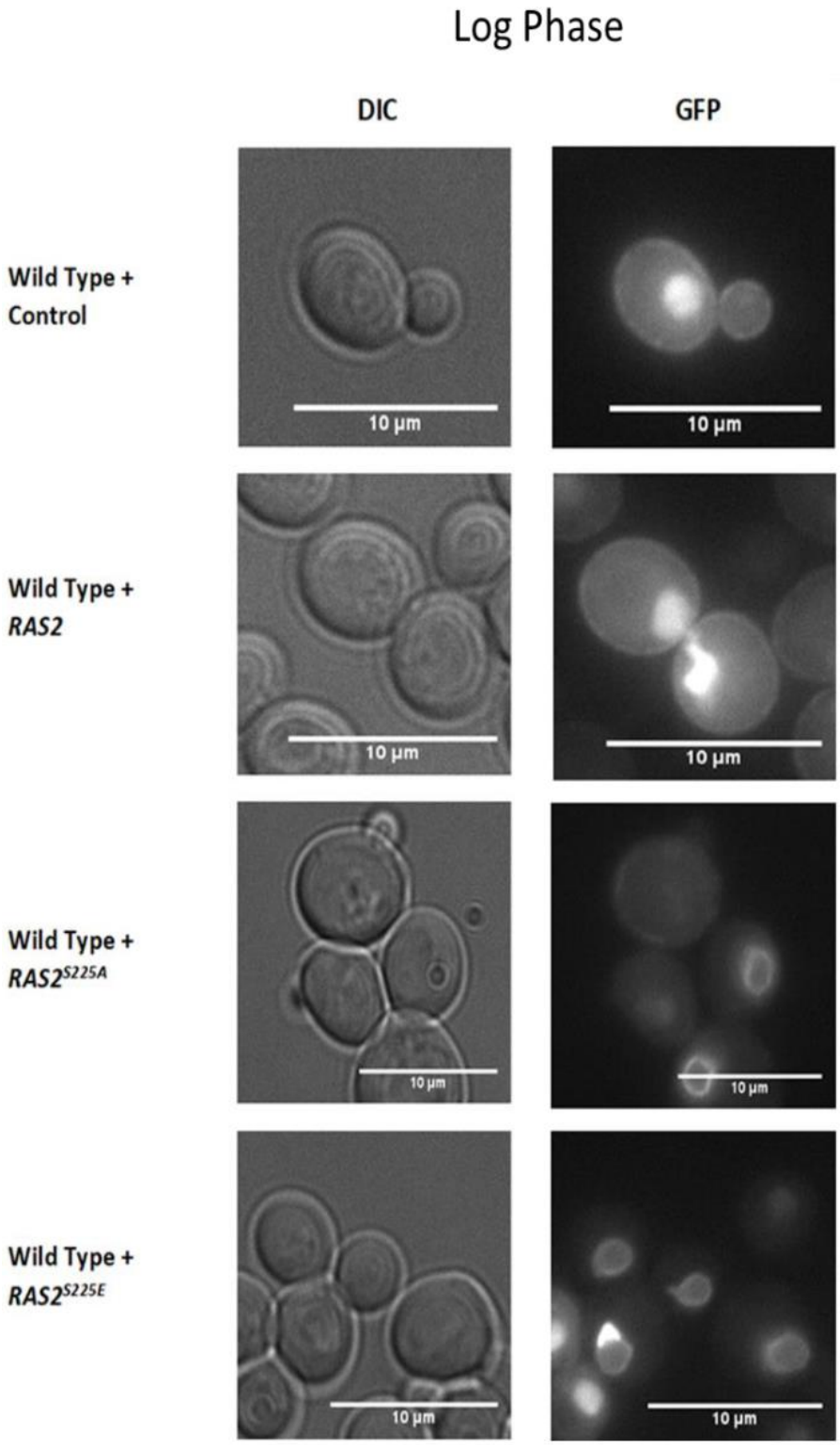

Figure 17. Fluorescence microscopy images of wild type strains overexpressing *RAS2*, *RAS2*^{S225A}, *RAS2*^{S225E} or an empty plasmid control using a GFP-RBD probe during logarithmic phase of growth. Images by Elliot Piper-Brown.
Fluorescence signal displays the presence of active Ras within the cells (RBD-GFP localisation). Cells were cultured in SD-URA/-LEU growth media. This experiment was repeated three times and a representative data set is shown. The scale bar is 10 μm.

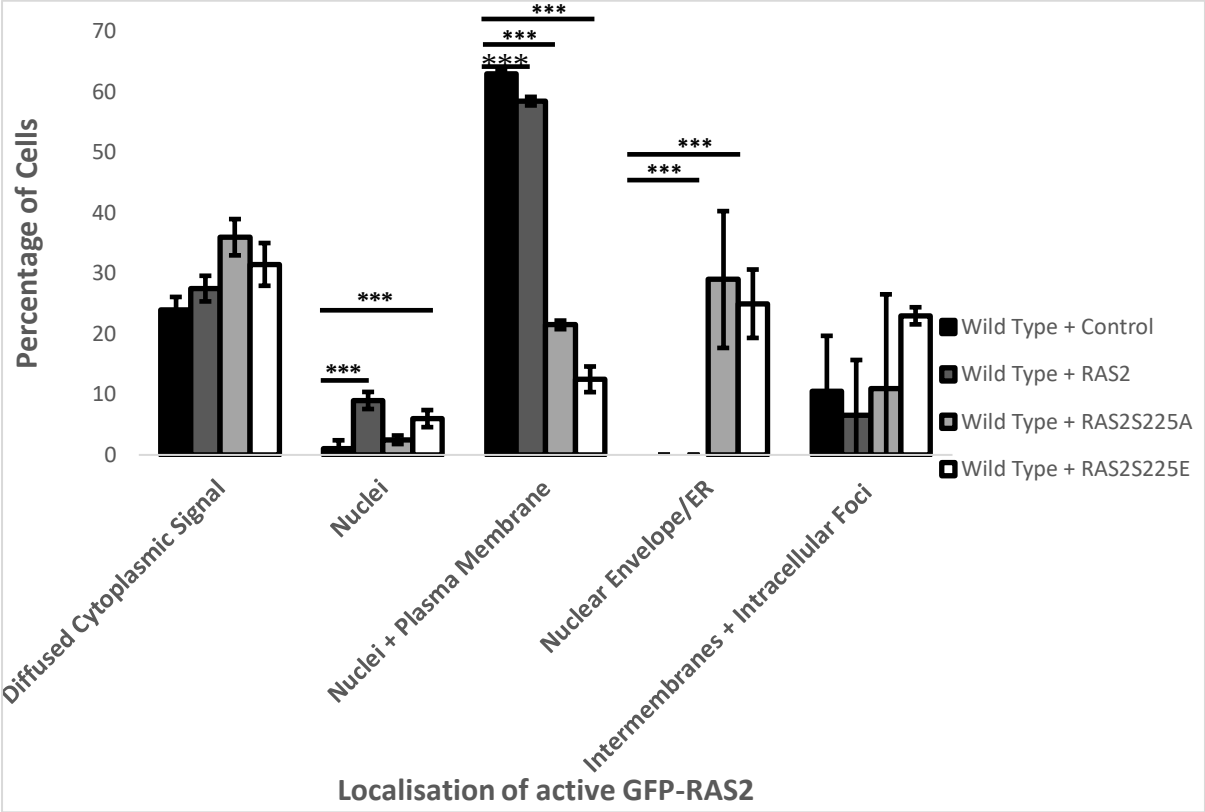

Figure 18. A Graphical representation of the localisation of active RAS2 in wild type cells overexpressing *RAS2*, *RAS2*^{S225A}, *RAS2*^{S225E} or an empty plasmid control during logarithmic phase of cell growth.
Cells were cultured in SD-URA/-LEU growth media.
100 cells for each strain were counted of samples taken on three separate days with a total 300 cells being counted. The number of cells represent the phenotypes seen and are represented and calculated as a percentage of the total number of cells counted. The data displays an average of three biological repeats. The error bars indicate the standard deviation. A One-way ANOVA using a Tukey multiple comparison test was used to determine statistical significance. (*) flags levels of significance compared to the control. NS = non-significant, * = adjusted p-value ≤ 0.05 and *** = adjusted p value ≤ 0.001.

During stationary phase of growth, the majority of the wild type strains expressing Ras2p was seen as a diffused cytoplasmic signal with some intracellular foci within the vacuole consistent with the shut-down of Ras activity. Wild type cells expressing Ras2p were found in the nucleus (**Fig. 20**) which was only little observed in the other strains and much higher

during stationary phase compared to the logarithmic phase (**Fig. 18**). Again, wild type cells expressing Ras2p^{S225A} or Ras2p^{S225E} showed a strong RBD-GFP signal at the nuclear envelope strongly manifesting into intracellular foci (**Fig. 19/20**). Interestingly, the S225E mutant also showed RBD-GFP signal as a diffused cytoplasmic signal with intracellular foci (**Fig. 19/20**).

In general, there was a strong manifestation of intracellular foci in all strains during the stationary phase (**Fig. 20**) which was not seen during the logarithmic phase (**Fig. 18**).

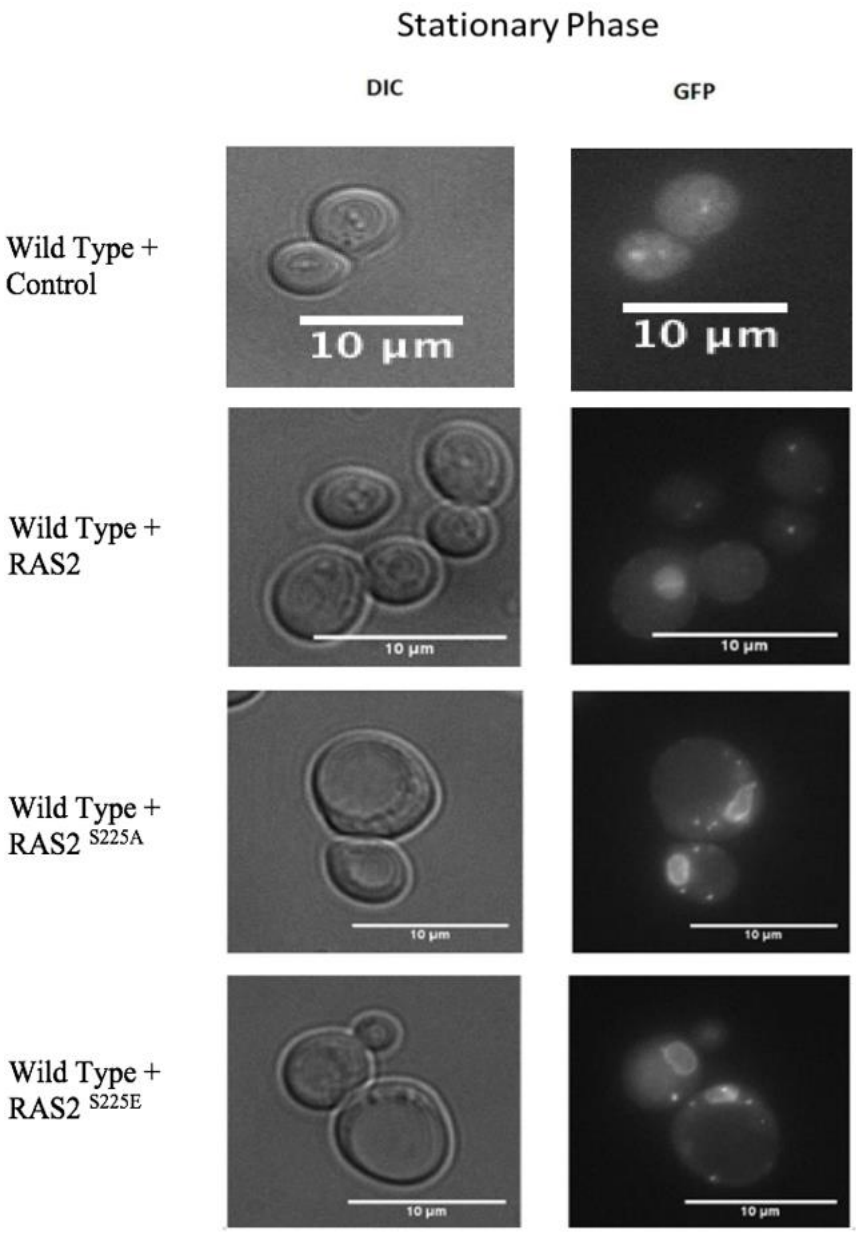

Figure 19. Fluorescence microscopy images of wild type strains overexpressing *RAS2*, *RAS2*^{S225A}, *RAS2*^{S225E} or an empty plasmid control using a GFP-RBD probe during stationary phase of growth. Images by Elliot Piper-Brown.

Fluorescence signal displays the presence of active Ras within the cells. Cells were cultured in SD-URA/-LEU growth media. This experiment was repeated three times and a representative data set is shown. The scale bar is 10 µm.

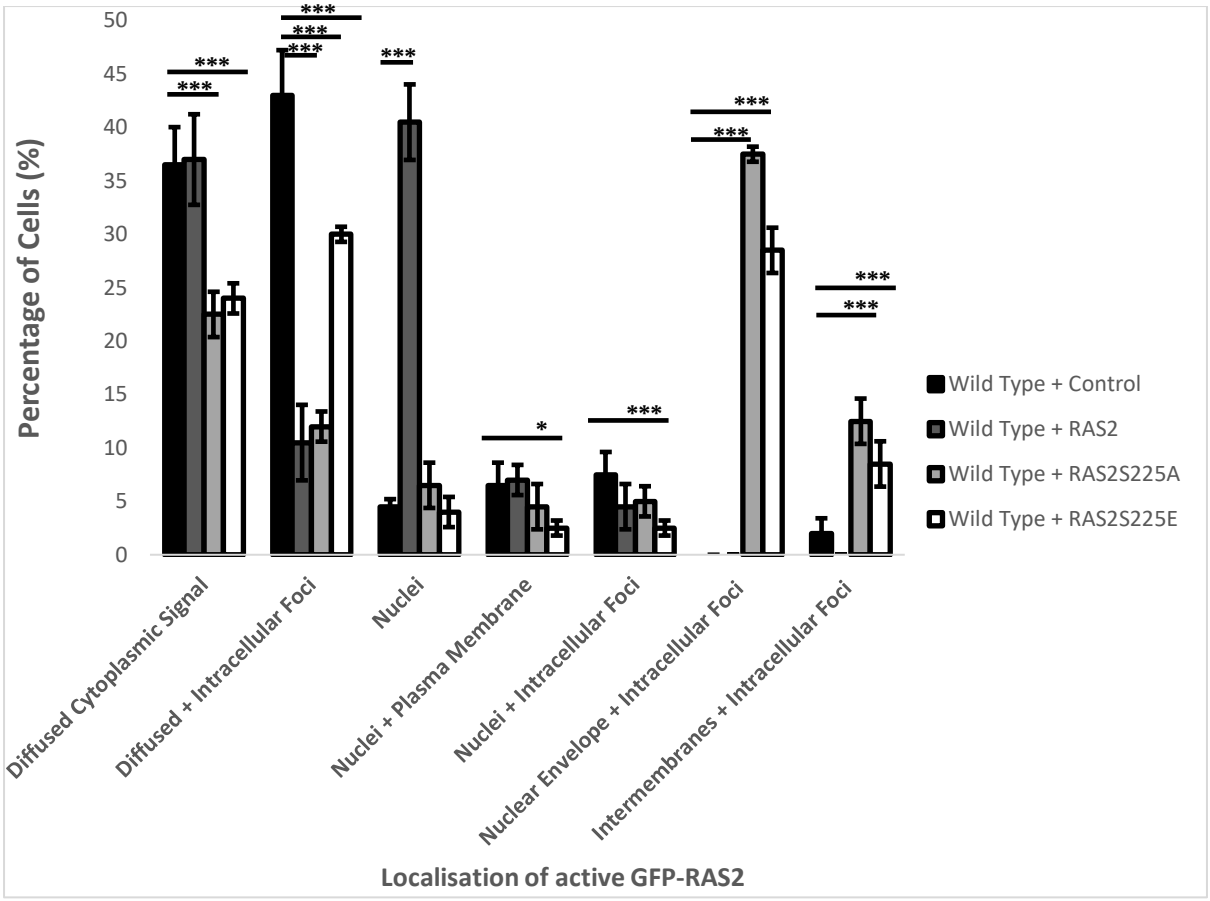

Figure 20. A Graphical representation of the localisation of active *RAS2* in wild type cells overexpressing *RAS2, RAS2^{S225A}* or *RAS2^{S225E}* or an empty plasmid control during stationary phase of cell growth.
Cells were cultured in SD-URA/-LEU growth media.
100 cells for each strain were counted of samples taken on three separate days with a total 300 cells being counted. The number of cells represent the phenotypes seen and are represented and calculated as a percentage of the total number of cells counted. The data displays an average of three biological repeats. The error bars indicate the standard deviation. A One-way ANOVA using a Tukey multiple comparison test was used to determine statistical significance. (*) flags levels of significance compared to the control. NS = non-significant, * = adjusted p-value ≤ 0.05 and *** = adjusted p value ≤ 0.001.

3.4 Growth analysis of yeast cells overexpressing *RAS2, RAS2^{S225A}* or *RAS2^{S225E}*

Growth of yeast strains overexpressing *ras2, ras2^{S225A}, ras2^{S225E}* mutant alleles or an empty plasmid control were examined in a wild type or *Δras2* background. There are four distinct phases characterising the growth of *S. cerevisiae* liquid cultures, called lag, logarithmic (exponential), post-diauxic and stationary phase (**Fig. 21**). Those growth phases mirror nutrient availability and the adaptation during changes in nutrient levels or stresses. During the lag phase minimal growth or time spent in the G_O phase of the cell cycle is observed as

cells are adapting to their new environment or media addition. The logarithmic phase represents actively proliferating cells growing exponentially. Here, *S. cerevisiae* uses glucose as their preferable energy source fermenting it. Oxidative phosphorylation is supressed. This is the Crabtree effect (Jin *et al.*, 2016). The diauxic phase marks a period of glucose de-repression, utilisation of ethanol generated during fermentation, and an upregulation of mitochondrial biogenesis to sustain oxidative phosphorylation. The stationary phase represents limited growth due to cell cycle exit. A functional mitochondrial electron transport chain is crucial for this (Herskowitz, 1988).

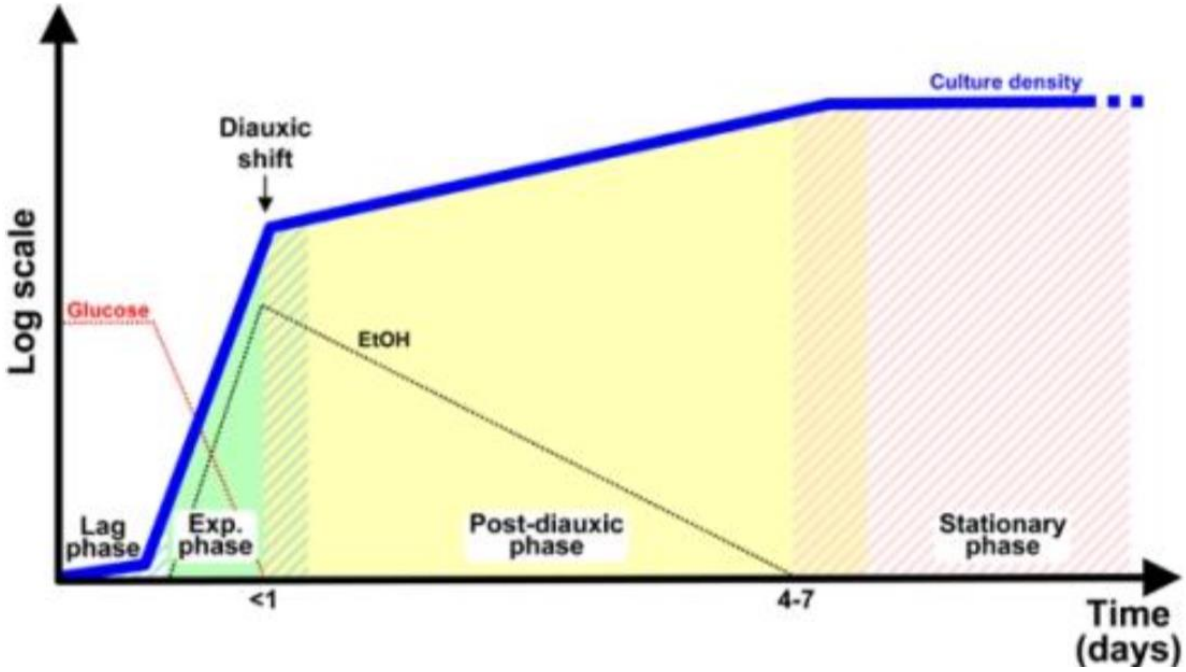

Figure 21. A schematic showing the growth phases of *S. cerevisiae* cultivated in rich medium containing glucose.
Optical density (OD) measurements of yeast are taken at 600 nm. During lag phase minimal growth is observed as cells are adapting to their new environment. The logarithmic (log) phase or exponential growth represents fermentation of glucose. Here, mitochondrial respiratory is suppressed due to the presence of glucose (glucose repression). During this phase of growth energy is obtained through fermentative glycolysis generating ethanol. When glucose levels become scarce cells must shift their metabolism to respiratory growth and aerobic utilisation of ethanol which is called the diauxic shift. The post-diauxic phase represents the complete shift to respiratory growth and the utilisation of oxidative phosphorylation. During stationary phase minimal growth is visible as nutrients are depleted and the cell density is high (Herskowitz, 1988; Jin *et al.*, 2016). **Image adapted from** (Busti *et al.*, 2010)

3.4.1 2µ system: Growth analysis of yeast cells overexpressing *RAS2*, *RAS2*^{S225A} or *RAS2*^{S225E}

A growth assay was performed (Materials and Methods, Section 2.8.1) to investigate the growth of yeast strains overexpressing *RAS2*, *RAS2*^{S225A}, *RAS2*^{S225E} or an empty plasmid control. The growth of *ras2* mutant alleles was analysed in both a wild type and a *Δras2* background to determine whether the overexpression of *RAS2*^{S225A} *or RAS2*^{S225E} affects cells when endogenous Ras2p was present.

Furthermore, to clarify the role of both the mutation and the level of expression, data using the 2µ system from (Piper-brown, 2019) was reproduced.

A lower final OD was observed in strains overexpressing *RAS2*^{S225A} or *RAS2*^{S225E} in a wild type background (**Fig. 22**). Furthermore, the post-diauxic phase of cell growth was entered earlier, and a slightly elongated lag phase was seen compared to the control strain (**Fig. 22**). These data suggest that overexpression of *RAS2*^{S225A} or *RAS2*^{S225E} have a dominant negative effect on growth.

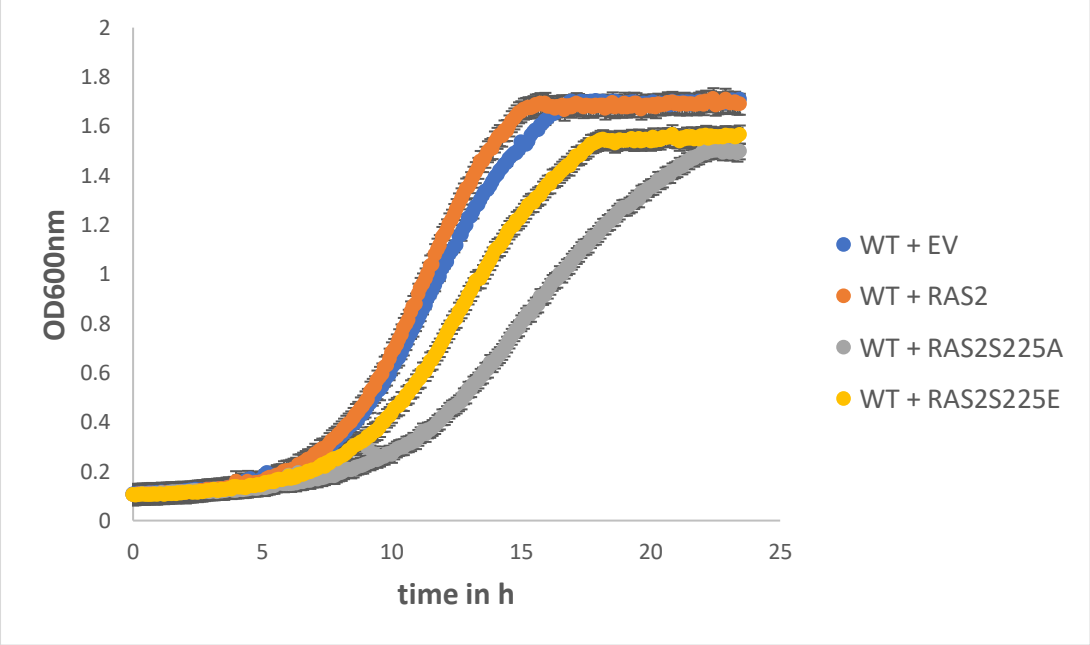

Figure 22. Growth analysis of *S. cerevisiae* wild type cells overexpressing *RAS2*, *RAS2*^{S225A} or *RAS2*^{S225E} or an empty plasmid (EV) control.

The growth analysis was conducted in SD-URA media (Material and Methods, Section 2.8.1) and represents an average of three biological repeats. The error bars display the standard deviation.

To examine the growth phenotype of the mutant alleles in the absence of endogenous Ras2p, *RAS2*, *RAS2*^{S225A} and *RAS2*^{S225E} were overexpressed in the *Δras2* background. A lower final OD, early transition into the post-diauxic phase, and an extended lag phase was ascertained when compared to the control strain (**Fig. 23**; generated by Elliot Piper-Brown).

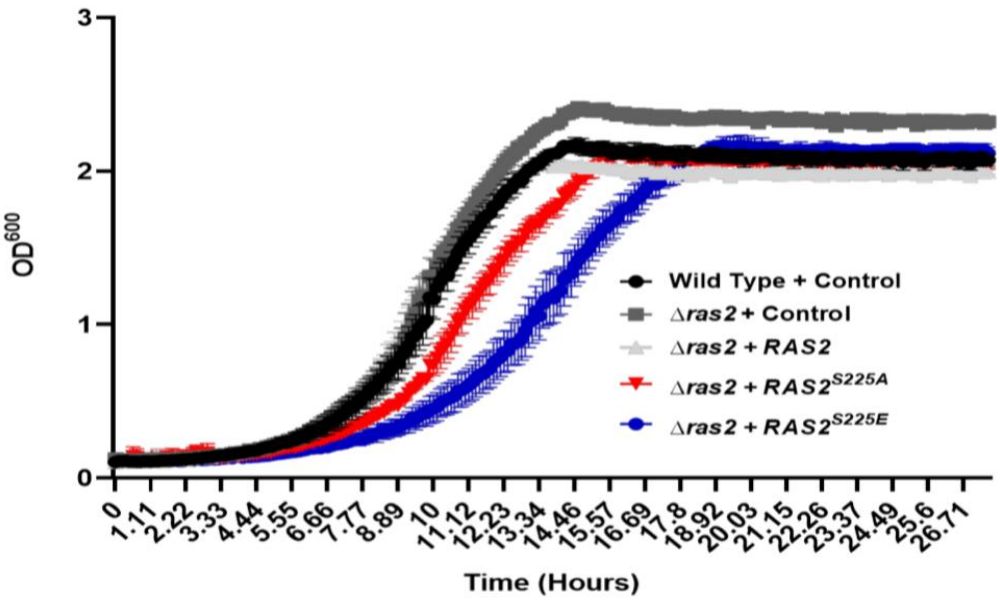

Figure 23. Growth analysis of *S. cerevisiae Δras2* strain overexpressing *RAS2*, *RAS2*^{S225A}, *RAS2*^{S225E} or an empty plasmid control.
The growth analysis was conducted in SD-URA media (Material and Methods, Section 2.8.1) and represents an average of three biological repeats. The error bars display the standard deviation. This data set was generated by Elliot Piper-Brown.

3.4.2 Genome integration system: Growth analysis of yeast cells overexpressing *RAS2*, *RAS2*^{S225A} or *RAS2*^{S225E}

To determine if the same growth defect detected in the growth curves using the overexpression system could be observed using just one copy of the mutant alleles to overexpress *RAS2*, *RAS2*^{S225A} *and RAS2*^{S225E}, a genome integration system was used. A growth assay was performed (Materials and Methods, Section 2.8.1) to investigate the growth

of yeast strains overexpressing *RAS2*, *RAS2*^{S225A}, *RAS2*^{S225E} or an empty plasmid control. The growth of *ras2* mutant alleles was analysed in both a wild type and a *Δras2* background to determine whether the overexpression of *RAS2*^{S225A} or *RAS2*^{S225E} affected cells when endogenous Ras2p was present.

A slightly lower final OD was noticed in the wild type strains overexpressing *RAS2*, *RAS2*^{S225A} or *RAS2*^{S225E} compared to the wild type control strain (**Fig. 24**). However, no significant lower final OD or other growth defect e.g. extended lag phase, lower log phase was observed.

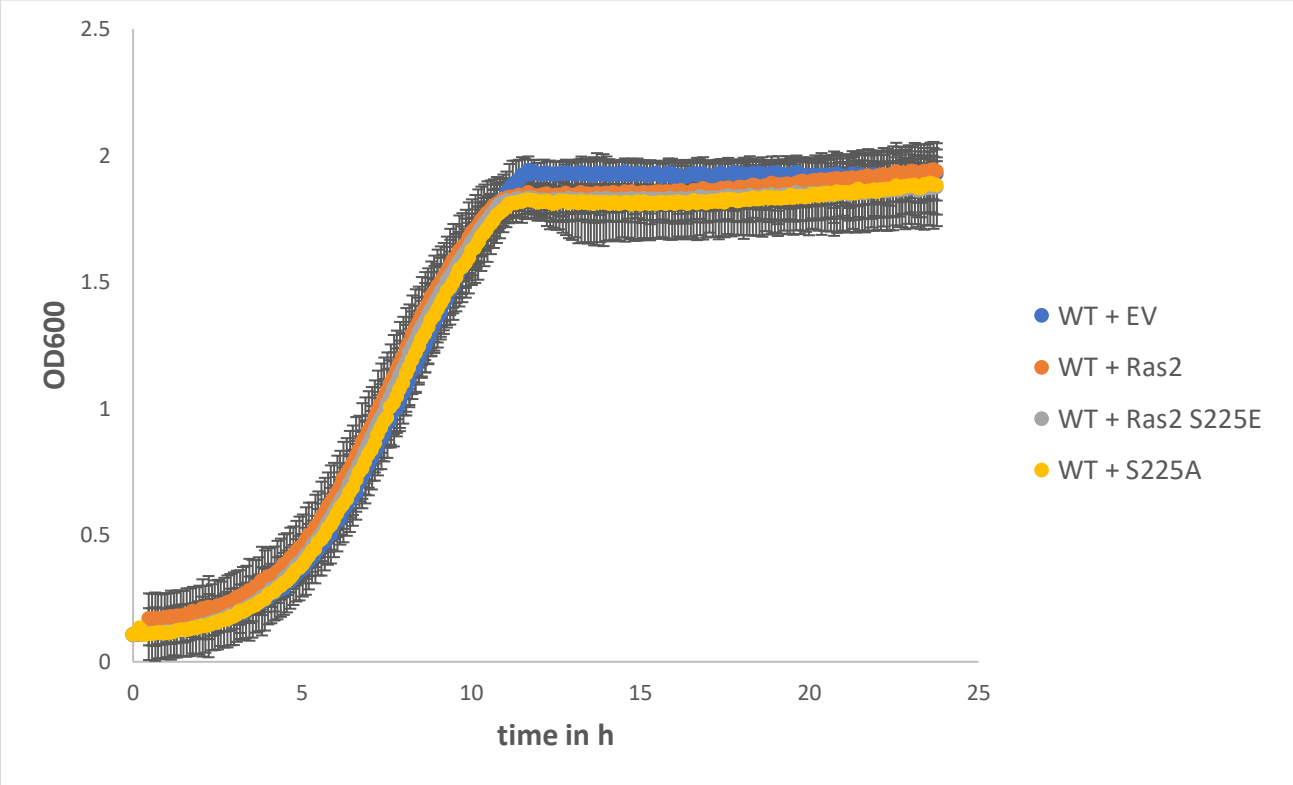

Figure 24. Growth analysis of *S. cerevisiae* wild type cells overexpressing *RAS2*, *RAS2*^{S225A}, *RAS2*^{S225E} or an empty plasmid control.
The growth analysis was conducted in SD-URA media (Material and Methods, Section 2.8.1) and represents an average of three biological repeats. The error bars display the standard deviation.

To examine the growth phenotype of the mutant alleles in the absence of endogenous Ras2p, *RAS2*, *RAS2*^{S225A} and *RAS2*^{S225E} are overexpressed in the *Δras2* background. Here, a lower final OD of strains expressing *RAS2*, *RAS2*^{S225A} or *RAS2*^{S225E} is observed compared to the *Δras2* control strains. Only a slight decrease in the final OD of strains expressing *RAS2*, *RAS2*^{S225A} or *RAS2*^{S225E} in the *Δras2* background is seen compared to the control strain in the wild type background. It was noted that the *Δras2* control strain had a slower exponential phase compared to the strains expressing *RAS2*, *RAS2*^{S225A} or *RAS2*^{S225E} in the *Δras2* background and the wild type control (**Fig. 25**).

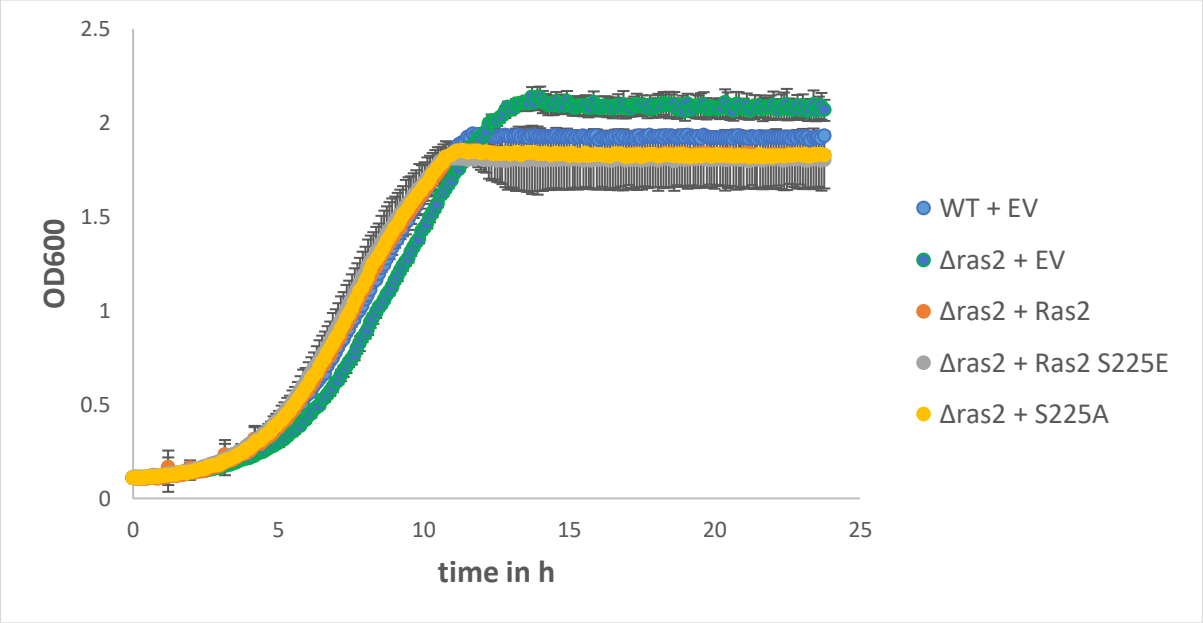

Figure 25. Growth analysis of *S. cerevisiae Δras2* strain overexpressing *RAS2*, *RAS2*^{S225A}, *RAS2*^{S225E} or an empty plasmid (EV) control.
The growth analysis was conducted in SD-URA media (Material and Methods, Section 2.8.1) and represents an average of three biological repeats. The error bars display the standard deviation.

3.5.1 2µ system: Colony forming unit (CFU) analysis of yeast cells overexpressing *RAS2*, *RAS2*^{S225A} or *RAS2*^{S225E}

A viability assay was carried out, as described in Materials and Methods, Section 2.8.3, to determine if the overexpression of either *RAS2*^{S225A} or *RAS2*^{S225E} had an effect on viability or cell functioning in both wild type and *Δras2* background.

To clarify and contrast the role of both the mutation and the level of expression on viability, data using the 2µ system from (Piper-brown, 2019) was presented below.

The control strains in both wild type and *Δras2* background had approximately 40 % viability when grown on SD-URA plates (**Fig. 26**). Therefore, the loss of Ras2 lead to no significant change in viability. The low colony forming efficiency of the wild (**Fig. 26/27**) might be due to a combination of cell toxicity exerted by the empty vector plasmid and a limiting component in the media used in this study. This effect was observed in studies when 2µ circles were present at high copy number (Falcón and Aris, 2003). However, the exact cause is yet to be identified. An increase in cell viability when compared to the control strains was observed in the overexpression strains of *RAS2* in both wild type and *Δras2* background (**Fig. 26**). A two-fold reduction in colony forming efficiency was found in the overexpression strains of *RAS2*^{S225A} or *RAS2*^{S225E} in both wild type and *Δras2* background when compared to the wild type and *Δras2* background control strains (**Fig. 26**).

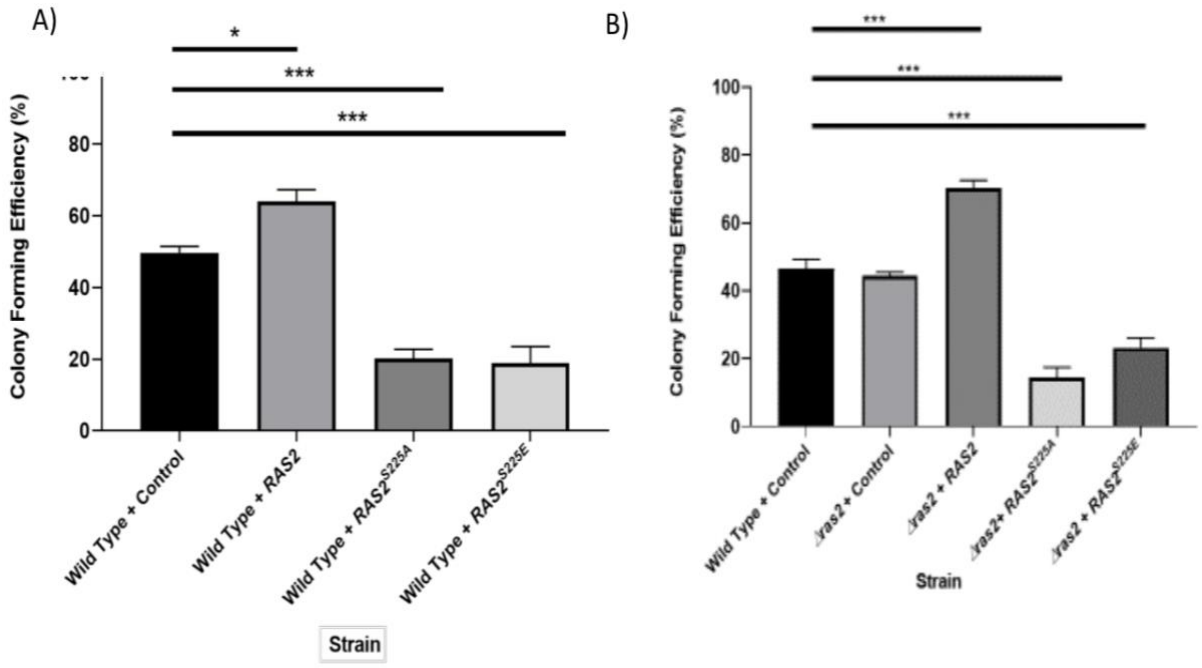

Figure 26. A colony forming efficiency assay of *S. cerevisiae* wild type or *Δras2* cells overexpressing *RAS2, RAS2*^{S225A}, *RAS2*^{S225E} or control cells grown in SD –URA media.
Data generated by Elliot Piper-Brown.
A) A colony forming efficiency assay of *S. cerevisiae* wild type cells overexpressing *RAS2, RAS2S225A, RAS2S225E* or an empty plasmid control grown in SD –URA media. A colony forming efficiency analysis was carried out as described in Materials and Methods (Section 2.9.3). A One-way ANOVA using a Dunnetts multiple comparison test was used to determine statistical significance. Non-significant = NS, * = adjusted p-value ≤ 0.05 and *** = adjusted p value ≤ 0.001. B) A colony forming efficiency assay of *S. cerevisiae Δras2* cells overexpressing *RAS2, RAS2S225A, RAS2S225E* or an empty plasmid control, grown in SD –URA. The colony forming efficiency analysis was carried out as described in Materials and Methods (Section 2.9.3). A One-way ANOVA using a Tukey multiple comparison test was used to determine statistical significance. Non-significant = NS, * = adjusted p-value ≤ 0.05 and *** = adjusted p value ≤ 0.001 (Piper-brown, 2019).

3.5.2 Genome integration system: Colony forming unit (CFU) analysis of yeast cells overexpressing *RAS2, RAS2*^{S225A} or *RAS2*^{S225E}

A viability assay was carried out, as described in Materials and Methods, Section 2.8.3, to determine if the overexpression of either *RAS2*^{S225A} or *RAS2*^{S225E} had an effect on viability or cell functioning in both wild type and *Δras2* background using a genome integrating system. Here, the viability assay was conducted on both the rich YPD media and the selective SD-URA media.

There was no significant difference between all of the strains observed in neither the wild type nor the *Δras2* background (**Fig. 27**).

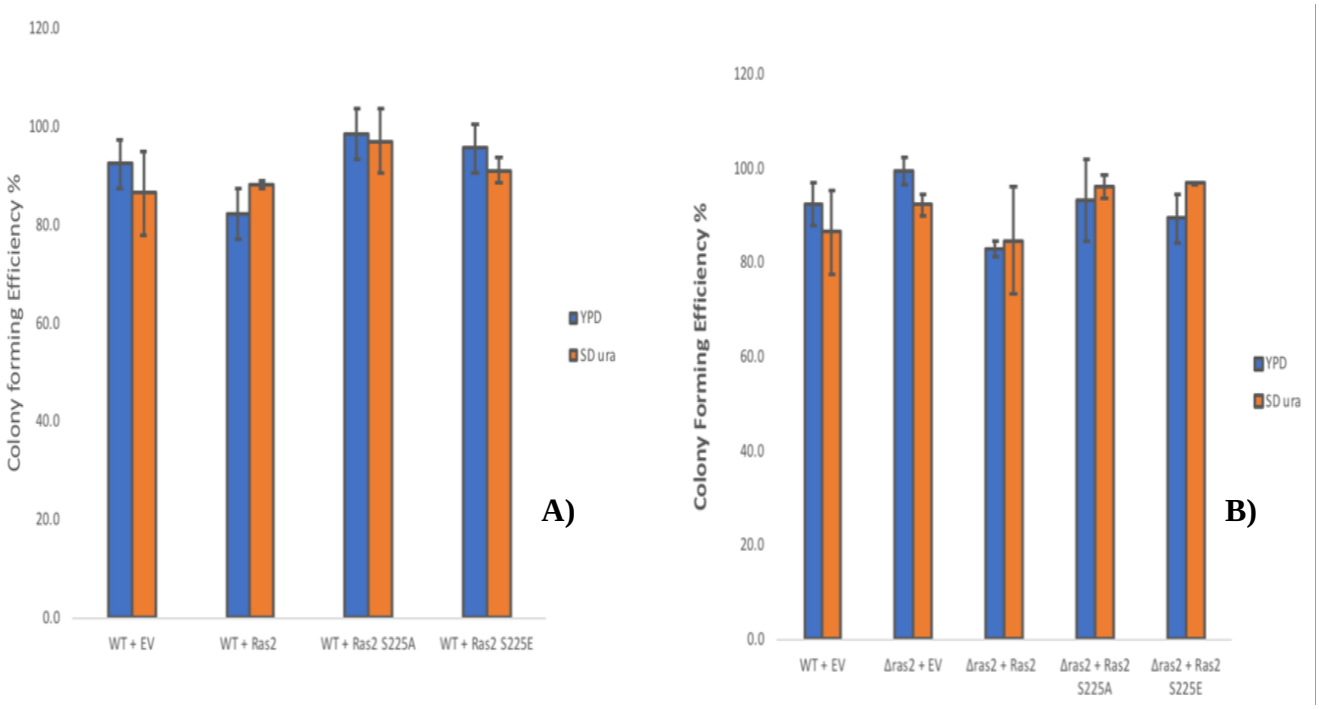

Figure 27. A colony forming efficiency assay of *S. cerevisiae* wild type (A) or *Δras2* (B) cells overexpressing *RAS2*, *RAS2*^{S225A}, *RAS2*^{S225E} or an empty plasmid control grown in SD –URA media and YPD media.
A colony forming efficiency assay of *S. cerevisiae Δras2* cells overexpressing *RAS2, RAS2S225A, RAS2S225E* or an empty plasmid control, grown in SD –URA. The colony forming efficiency analysis was carried out as described in Materials and Methods (Section **2.9.3**). A One-way ANOVA using a Tukey multiple comparison test was used to determine statistical significance. Non-significant = NS, * = adjusted p-value ≤ 0.05 and *** = adjusted p value ≤ 0.001. In both assays each comparison was non-significant.

3.6.1 2µ system: Growth analysis of yeast cells overexpressing *RAS2*, *RAS2*^{S225A} or *RAS2*^{S225E} in a *Δcup9* background

Based on previous work carried out by Elliot Piper-Brown we know that deletion of the *CUP9* gene which supresses expression of the Ptr2 di-peptide transporter rescues the growth defects associated with *RAS2*^{S225A} or *RAS2*^{S225E} overexpression from a 2µ plasmid (**Fig. 28**).

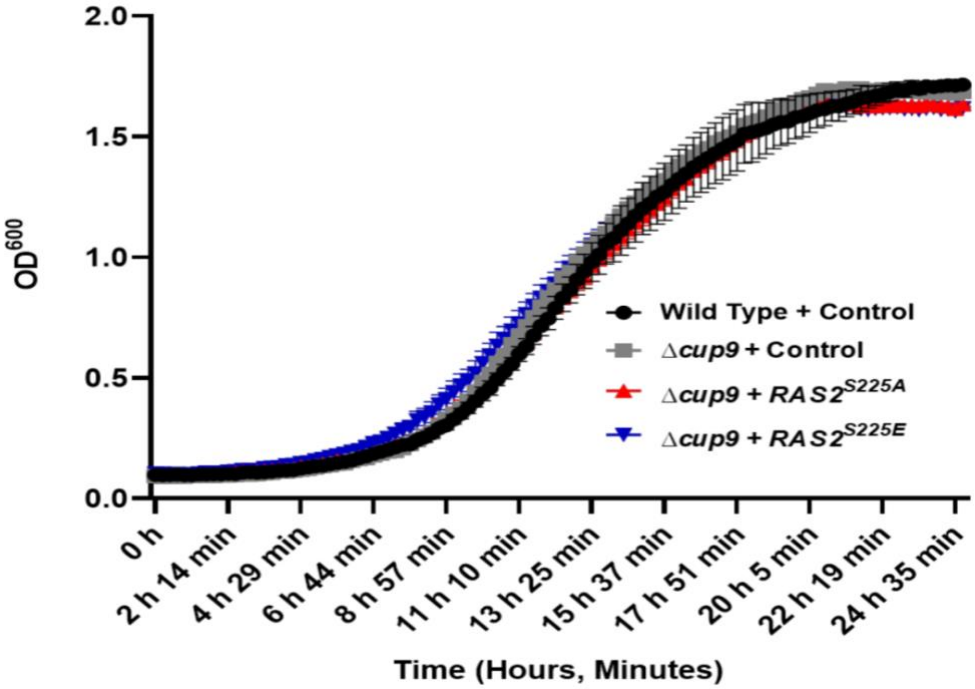

Figure 28. A growth curve of *S. cerevisiae* wild type and *Δcup9* strains overexpressing *RAS2*^{S225A}, *RAS2*^{S225E} or an empty plasmid control.
The growth analysis was conducted for 24 hours in SD-URA media as described in Materials and Methods, Section 2.8.1. An average of three biological repeats are represented and the error bard in the graph show the standard deviation. This data set was generated by Elliot Piper-Brown.

3.6.2 Mitochondrial function in wild type cells overexpressing the mutant allele *RAS2*^{S225A}

As seen in our results in **Fig. 22** and **Fig. 26 A**, overexpression of either *RAS2*^{S225A} or *RAS2*^{S225E} in wild type cells can cause loss of viability and growth defects. We wished to determine whether loss of viability, which we know represents entry in a state of quiescence (Piper-brown, 2019), was accompanied by a change in respiration. In addition, we wished to determine if loss of cup9 restored respiration in cells expressing *RAS2*^{S225A}. To examine this, high resolution respirometry was carried out to measure respiration within wild type cells overexpressing *RAS2*^{S225A}. Here, the consumption of oxygen in wild type cells overexpressing *RAS2*^{S225A} or an empty plasmid control was measured in order to analyse respiration using a high-resolution respirometer. The oxygen consumption was measured as O_2 flow per cell. To

analyse individual components of the mitochondrial respiratory chain different drugs targeting specific components were added: Triethiltyn bromide (TET), Carbonylcyanide p-trifluoromethoxyphenylhydrazone (FCCP), and Antimycin A (AntA). A typical respirometry profile generated from the Oroboros oxygraphy-2k is shown below (**Fig. 29**).

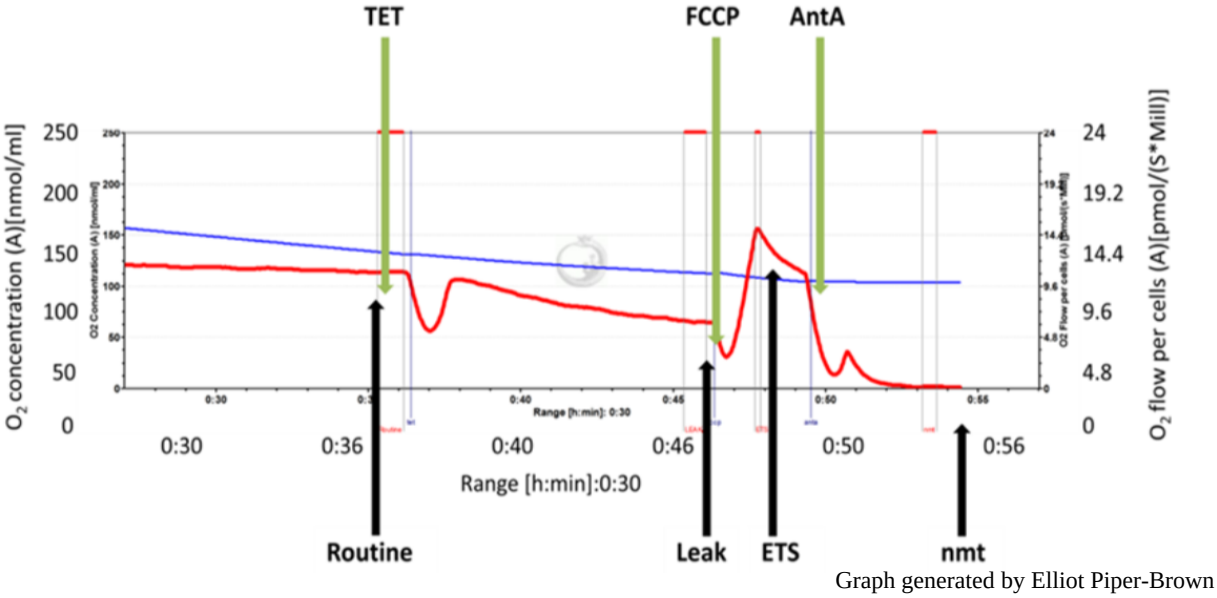

Graph generated by Elliot Piper-Brown

Figure 29. A respirometry profile produced by the Oroboros oxygraphy-2k.
The oxygen flux per cell (pmol/s*Mill) is shown as the red line whereas the blue line represents the oxygen concentration. A normal respirometry profile can be divided into four parts indicated by the black arrows: the "Routine" indicating the steady state oxygen flux, the "Leak" or induced mitochondrial resting state, "ETS" the maximal capacity of the electron transport system, and the "nmt" the non-mitochondrial oxygen flux. Specific drugs (green arrows) can be added to the chambers in order to analyse individual components of the respiratory chain: TET induces leak respiration, FCCP inhibits ATP synthase allowing maximal electron transport through the ETS, and AntA inhibits all respiratory.

The drug TET was used to measure the "Leak" respiration. TET inhibits the ATP synthase complex V which pumps protons across the mitochondrial inner-membrane space or IMS into the mitochondrial matrix in order to generate energy in the form of ATP. Inhibiting ATP synthase causes protons to accumulate within the IMS ultimately preventing electrons to move through the electron transport chain. Leak respiration is so called as this is protons moving freely across the IMM independently of the proton pump ATP synthase which is

inhibited by TET upon addition. An increased leak respiration of a strain when compared to the control strain indicates an increased respiration independent of ATP synthase proton pumping activity and ATP synthesis.

Inhibiting ATP synthase and hence stopping electron movement also increases the membrane potential: the mitochondrial membrane potential is crucial in regulating electron passage. If the membrane potential is too high electron are hindered to pass along the electron transport chain or ETC as this is dependent on proton pumping into the IMS. However, proton pumping into the IMS is more difficile when the membrane potential is too high. When the addition of TET does not drop respiration, it can be concluded that oxygen consumption and electron movement occur independently of ATP synthase and therefore stops ATP synthesis as this requires proton movement through the pump. This is called uncoupled respiration.

FCCP is a proton ionophore generating pores in the IMM making it permeable allowing the free flow of protons across it. The membrane potential is thus disrupted enabling the maximal potential of the ETC. FCCP is thus used to measure the maximal capacity of the electron transport system (ETS). One can therefore conclude that the higher the ETS is, the higher is the capacity of the ETC.

Antimycin A (AntA) is used to identify any non-mitochondrial (nmt) respiration. AntA inhibits cytochrome C reductase (complex III) by preventing electron transfer through binding to the Qi site. The Qi site is the site where Complex III is oxidised, thus re-oxidation by oxygen is prevented when this site is inhibited. Therefore, Oxygen consumption after the addition of AntA must be of nmt origin.

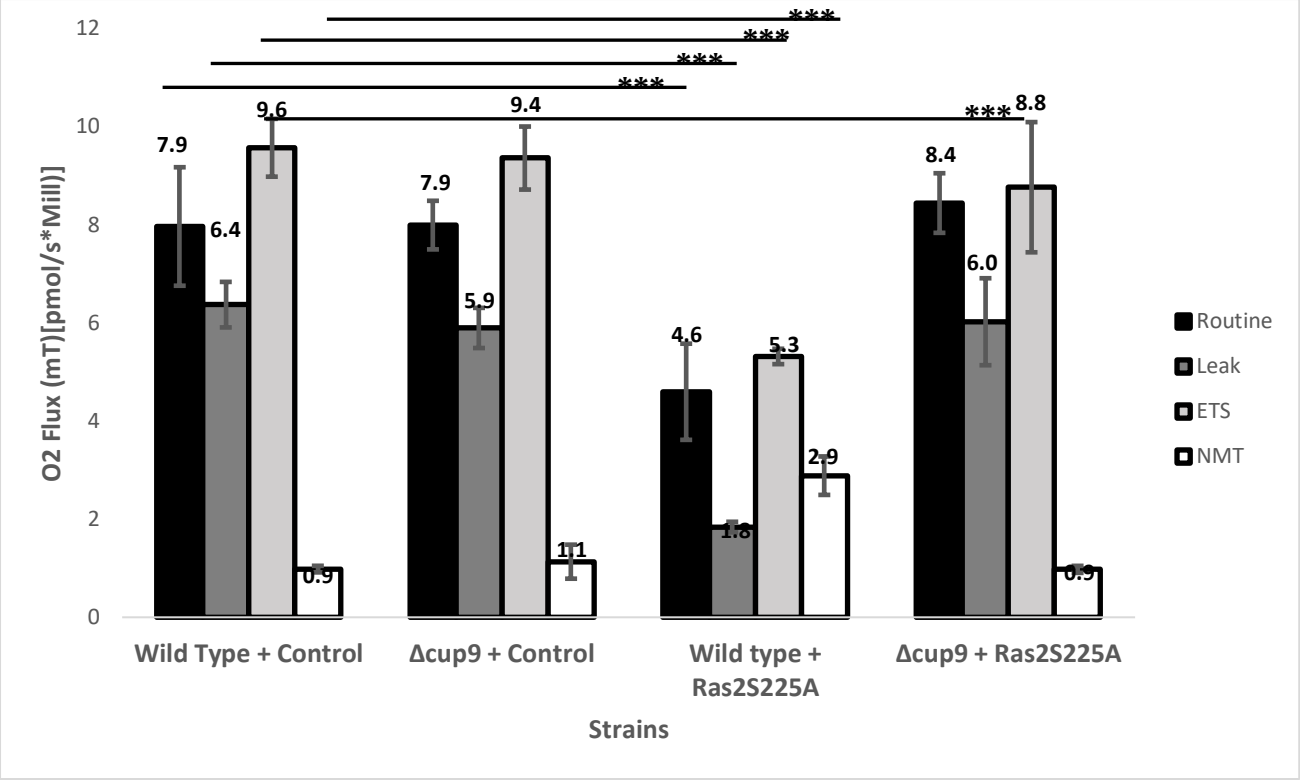

Figure 30. A bar chart representing the routine, leak, ETS and NMT O2 flux values for wild type and *Δcup9* cells overexpressing RAS2^{S225A} or an empty plasmid backbone control.
The data shown represents an average of three biological repeats and the error bars indicate the standard deviation.
A One-way ANOVA using a Tukey multiple comparison test was used to determine statistical significance. Routine, Leak, NMT and ETS of *Δcup9* control and *Δcup9* Ras2S225A are non-significant compared to the Wild type control (exception ETS of *Δcup9* Ras2S225A is significant compared to the wild type control). *** = adjusted p value ≤ 0.001.

No significant changes appeared in the wild type control when compared to the *Δcup9* control strain. However, a reduction in routine respiration could be observed in the wild type strain overexpression *RAS2^{S225A}* when compared to the wild type control and the *Δcup9* control strain (**Fig. 30**). This indicates that the *RAS2^{S225A}* mutant allele in wild type cells caused a significant decrease in routine respiration when compared to the wild type control. Moreover, a significant decrease in leak respiration could be found in the wild type strain overexpressing *RAS2^{S225A}* when compared to the wild type control strain (**Fig. 30**). Another significant decrease could be noted in the maximal capacity of the electron transport system (ETS) in wild type cell expressing the mutant *RAS2^{S225A}* allele when compared to the wild

type control (**Fig. 30**). This result suggests a reduction in the overall capacity of the ETS caused by the overexpression of *RAS2*^{S225A} (**Fig. 30**). Interestingly, the wild type strain overexpressing *RAS2*^{S225A} also showed an increased non-mitochondrial oxygen consumption (**Fig. 30**). Surprisingly, it seems the deletion of cup9 could rescue the respiration defects noted in the wild type *RAS2*^{S225A} strain (**Fig. 30**). Here, an increase in the routine, leak and ETS in the *Δcup9 RAS2*^{S225A} strain was visible when compared to the wild type *RAS2*^{S225A} strain. Also, a decrease in the NMT could be noted in the *Δcup9 RAS2*^{S225A} strain when compared to the wild type *RAS2*^{S225A} strain (**Fig. 30**).

3.7 Gene ontology analysis of RNA sequencing data

Based on the result seen in 3.6.1 we sought to investigate what differences in global gene expression may exist between the wild type control, *RAS2*^{S225A}, and *Δcup9 RAS2*^{S225A} cells. We hypothesised this may reveal why deletion of *CUP9* can rescue the growth defect and respiratory function of *RAS2*^{S225A} expressing cells. The analysis of significantly ($q \leq 0.05$) differently gene lists obtained from RNA Sequencing was performed in order to identify differently expressed genes and up and downregulated cellular pathways. The genes in the lists were ranked from the most upregulated to the most downregulated and were analysed using gene ontology within the Yeastmine platform.

Comparison of lists of up and downregulated genes revealed that three cellular pathways were upregulated in *Δcup9 RAS2*^{S225A} compared to *RAS2*^{S225A}; methionine biosynthesis, glutathione biosynthesis, and the Fe-S cluster assembly which are all involved in sulphur metabolic processes. Further analysis using yeast mine mapping genes onto known metabolic pathways revealed the specific genes upregulated in those pathways:

We found that the gene responsible for the rate limiting step for glutathione synthesis – *GSH1*- was upregulated. Furthermore, all genes of the cytosolic-nuclear Fe/S protein

biogenesis were upregulated and only three genes involved in the mitochondrial Fe/S protein biogenesis were upregulated (**Fig. 31**).

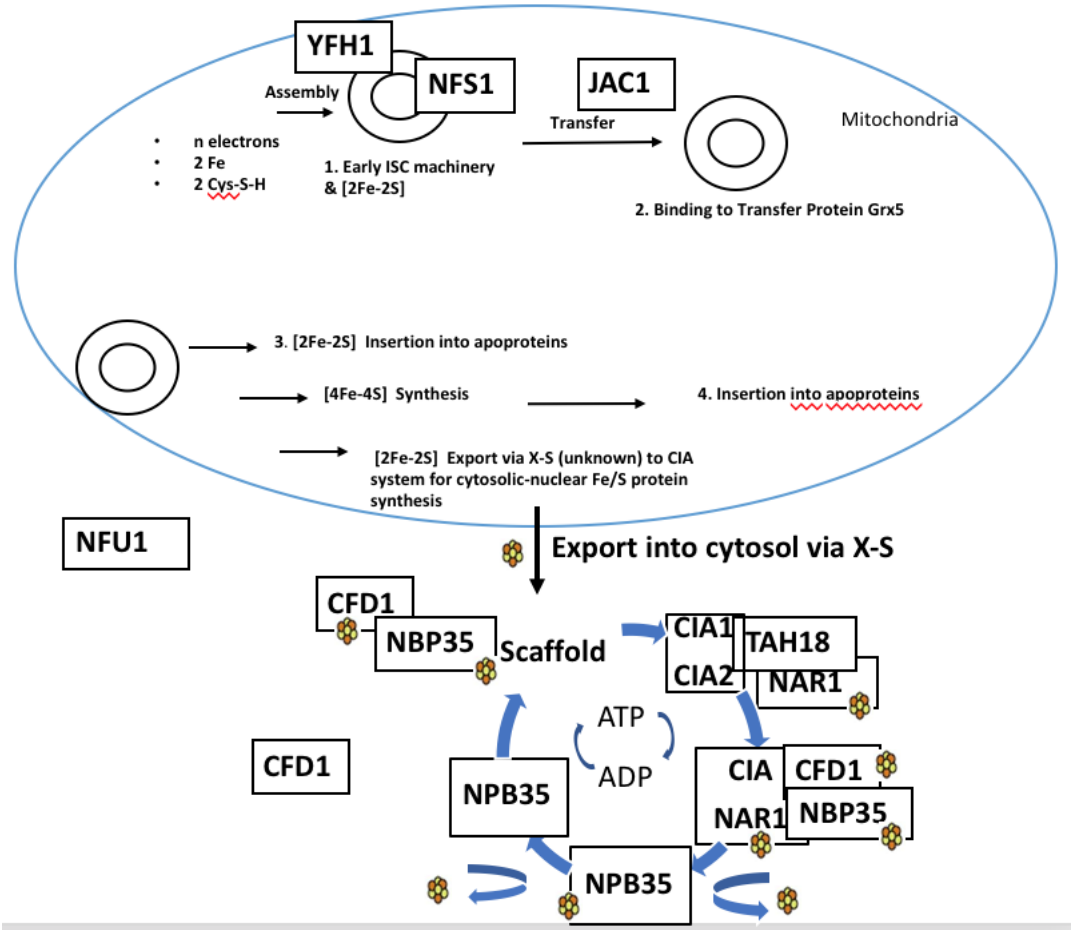

Figure 31. A schematic representing the Iron-Sulphur cluster assembly in *S. cerevisiae* highlighting up-regulated genes seen in the Gene Ontology analysis.
The Fe-S cluster assembly is a multistage process occurring in multiple compartments. The biogenesis of Fe-S proteins is essential for several cellular function including genome maintenance, energy conversation, protein translation, and antiviral response. The first steps of the biosynthesis of Fe-S proteins take place in the mitochondrion. Here, electrons, iron and cysteine are required to synthesise a [2Fe-2S] cluster on the early ISC (Iron-Sulphur Cluster Assembly) machinery. The early ISC is composed of the scaffold protein, Isu1, which requires sulphide, electrons, and iron. The cysteine desulferase complex Nfs1-Isd11-Acp1 provides the sulphide, electrons are obtained from the transfer chain NADPH-Arh1 and the ferredoxin Yah1, and the iron from the regulator or iron donor Yfh1. Following this assembly reaction, the cluster will bind to a transfer protein, the Hsp70 chaperone Ssq1, through Jac1 – a J-type co-chaperone. The [2Fe-2S] cluster is ultimately delivered to the monothiol glutaredoxin Grx5 (steps 1-2 in schematic). The cluster is then trafficked to the late ISC machinery for the synthesis of [4Fe-4S] clusters or to [2Fe-2S] targets such as apoproteins (3./4.). Some [2Fe-2S] clusters are also transported out of the mitochondrion via the *X-S* unknown component and delivered to the CIA (cytosolic Iron-Sulphur Protein Assembly) machinery in the cytosol for the maturation of nuclear and cytosolic Fe-S proteins.
The CIA system is a nucleotide-dependent cycle using the Cfd1-Nbp35 scaffold. Here, Nar1 and Cia1 interact with the scaffold complex. This enables the transfer of [2Fe-2S] clusters to Subset1 of cytosolic and nuclear FeS proteins. Following this, FeS cluster assembly in Subset II of cytosolic and nuclear FeS proteins is proposed to be facilitated by the dissociation of Nar1, Cia1, and Cfd1 releasing Nbp35. The cycle is closed and re-started when Apo-Cfd1 and apo-Nbp35 reform (Sharma *et al.*, 2010; Braymer and Lill, 2017)

For the methionine synthesis pathway, we could note that the genes at the last steps of this process were upregulated as presented in **Fig. 32** below. In order to investigate whether Ras2 hyperactivation could lead to changes in sulphur pathway processed, we also analysed Microarray Data where *PDE2* was deleted while 4 mM cAMP was added to mimic Ras2 activation**.** We found several genes in the methionine synthesis pathway were upregulated as well (**Fig. 32)**.

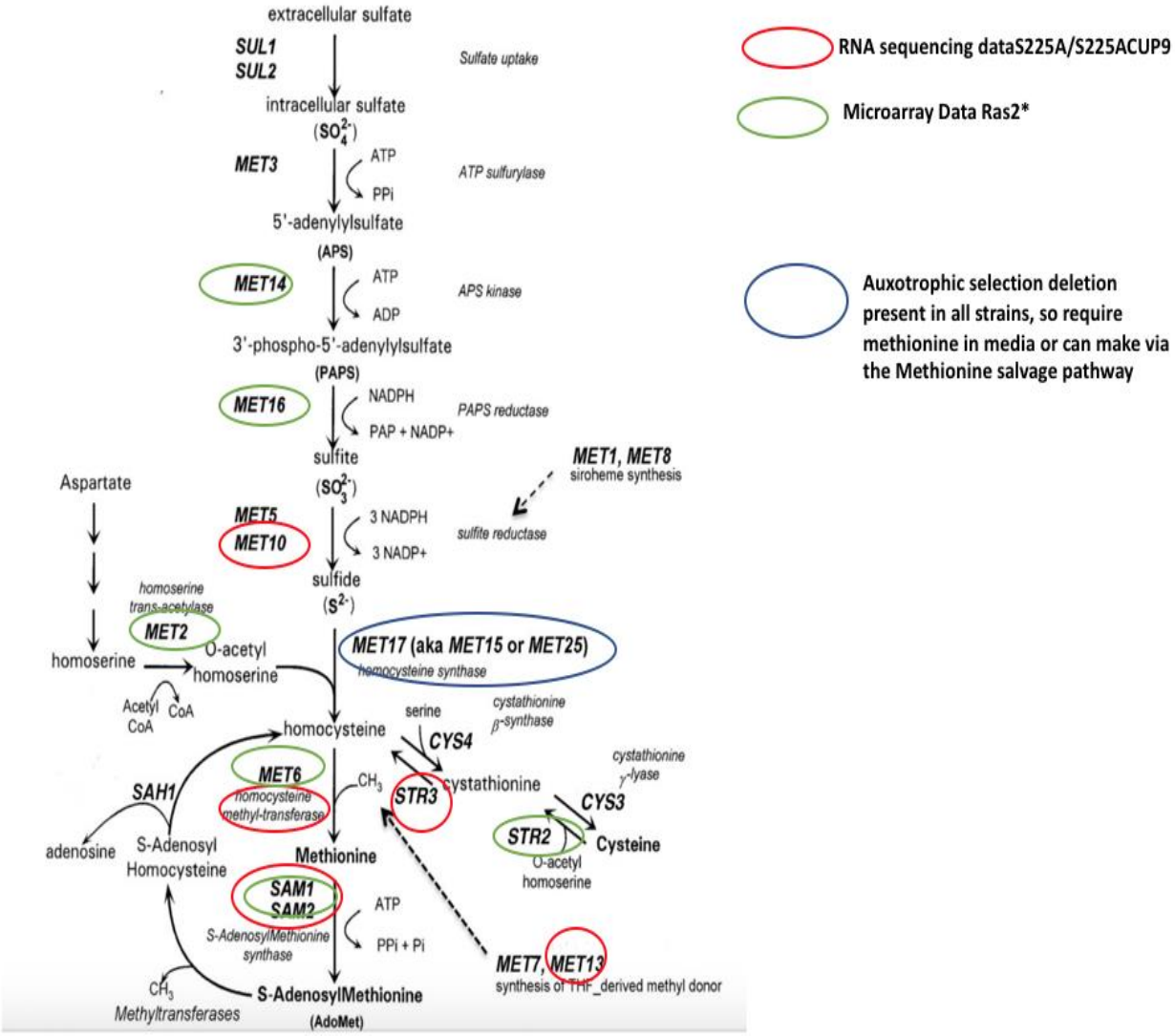

Figure 32. A schematic showing the methionine biosynthesis pathway and upregulated genes in *S. cerevisiae.*

Methionine is synthesised in *S. cerevisiae* through the methylation of homocysteine. Here, a methyl group from 5-methyl-THF is transferred to the thiol of homocysteine catalysed by the cobalamin-independent methionine synthase Met6p generating methionine.

3.8.1 Growth analysis of yeast cells overexpressing *RAS2, RAS2^{S225A}* or *RAS2^{S225E}* in methionine drop-out media

Upon receiving the results of the RNA sequencing analysis, we hypothesised that the deletion of *CUP9* let to an increase in methionine salvage in cells expressing *RAS2^{S225A}* thus restoring a metabolic defect that may be linked to the growth and viability phenotypes observed. The BY4741 wild type strain carried a *MET15* gene deletion and so is unable to grow in media lacking methionine. As *MET15* lies above the methionine salvage pathway we reasoned that deletion of *CUP9* may allow for growth in the MET-auxotrophic wild type *RAS2^{S225A}* strain. We therefore conducted a 24 hours growth assay of the MET-auxotrophic wild type and *Δcup9* strains overexpressing *RAS2, RAS2^{S225A}, RAS2^{S225E}* or an empty plasmid control in media where methionine was added back and media lacking methionine completely.
In the line with our hypothesis, no growth defects were found in the wild type strains overexpressing *RAS2^{S225A}* or *RAS2^{S225E}* when methionine was completely added back to the methionine drop out media. Those strains even showed a slightly increased final OD and log phase when compared to the wild type empty plasmid control (**Fig. 33**). However, a growth defect of the wild type overexpressing *RAS2* could be observed suggesting the importance of the amino acid in controlling growth (**Fig. 33**). Not surprisingly, the MET-auxotrophic wild type strains overexpressing *RAS2^{S225A}, RAS2^{S225E}* or an empty plasmid control could not grow in the media lacking methionine (**Fig. 33**). Remarkably though the MET-auxotrophic wild type strain overexpressing *RAS2* was able to grow with no significant differences when compared to the wild type strain overexpressing *RAS2* grown in media containing methionine (**Fig. 33**).

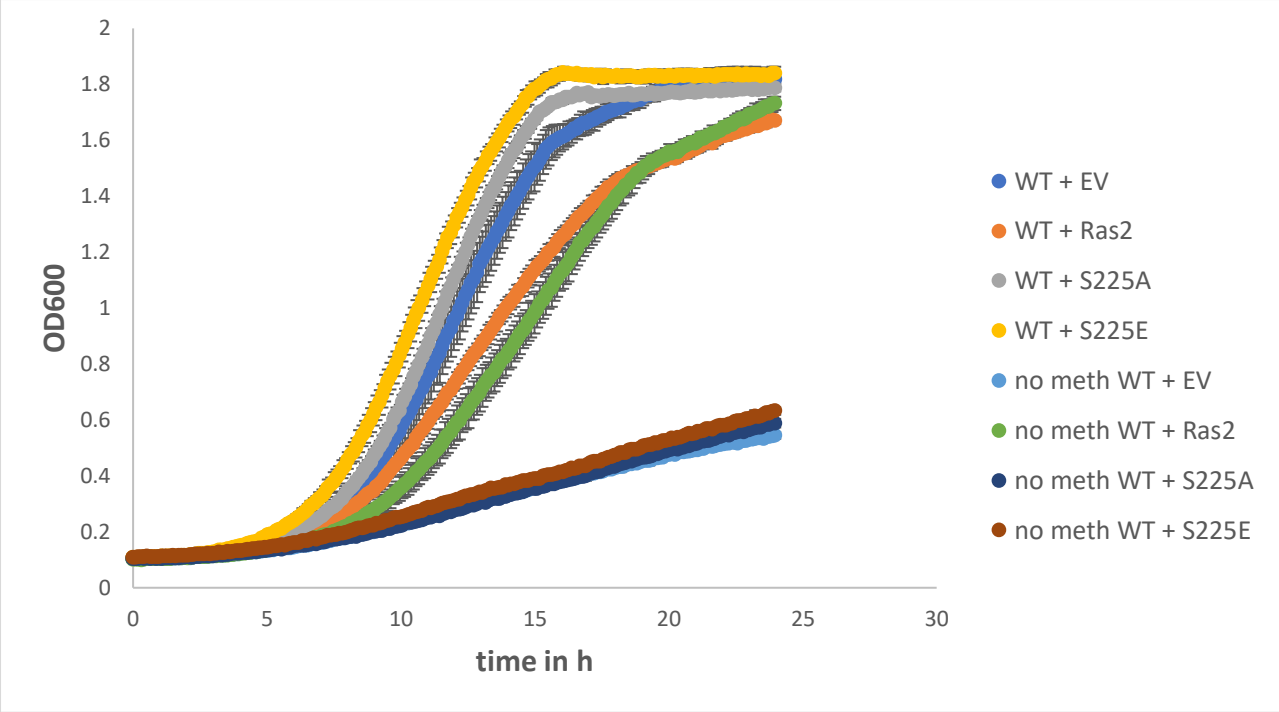

Figure 33. Growth analysis of *S. cerevisiae* wild type strains overexpressing *RAS2*, *RAS2*^{S225A}, *RAS2*^{S225E} or control cells in media lacking or containing methionine.
The growth analysis was conducted in SD-Met media and SD-Met media where methionine was completely added back (Material and Methods, Section 2.8.1) and represents an average of three biological repeats. The error bars display the standard deviation.

3.8.2 Growth analysis of yeast cells overexpressing *RAS2*, *RAS2*^{S225A} or *RAS2*^{S225E} in methionine drop-out media in the *Δcup9* background

When growing *Δcup9* strains overexpressing *RAS2*, *RAS2*^{S225A}, *RAS2*^{S225E} or an empty plasmid control in SD-Met media where methionine was completely added back, it was notable that *Δcup9* strains overexpressing *RAS2*^{S225A} or *RAS2*^{S225E} had an increased log phase and reached the final OD quicker than the *Δcup9* strains overexpressing *RAS2* or an empty plasmid control (**Fig. 34**). The *CUP9* deletion strains carrying the mutant alleles also seemed to have a slightly decreased lag phase compared to the control and *RAS2* strain (**Fig. 34**). No significant difference in growth between the *Δcup9* strains overexpressing *RAS2* or an empty plasmid control was detected (**Fig. 34**).

When growing the *Δcup9* strains overexpressing *RAS2*, *RAS2*^{S225A}, *RAS2*^{S225E} or an empty plasmid control in media lacking methionine, we could see that the deletion of *CUP9* allowed *RAS2*^{S225} mutants to grow, whereas the *Δcup9* strains overexpressing *RAS2* or an empty plasmid control were not growing (**Fig. 34**). Furthermore, the lag phase of *Δcup9* strains overexpressing *RAS2*^{S225} mutants was significantly increased and the log phase was slower compared to the wild type control strain grown in media containing methionine. The final OD of the wild type control strain grown in media containing methionine was not reached, however, it seems that the mutant strains grown in media lacking methionine did not yet reach stationary phase (**Fig. 34**). We suggest the final OD measured in the wild type control strain grown in media containing methionine could still be reached by the *RAS2*^{S225} mutants when growing for a longer period of time.

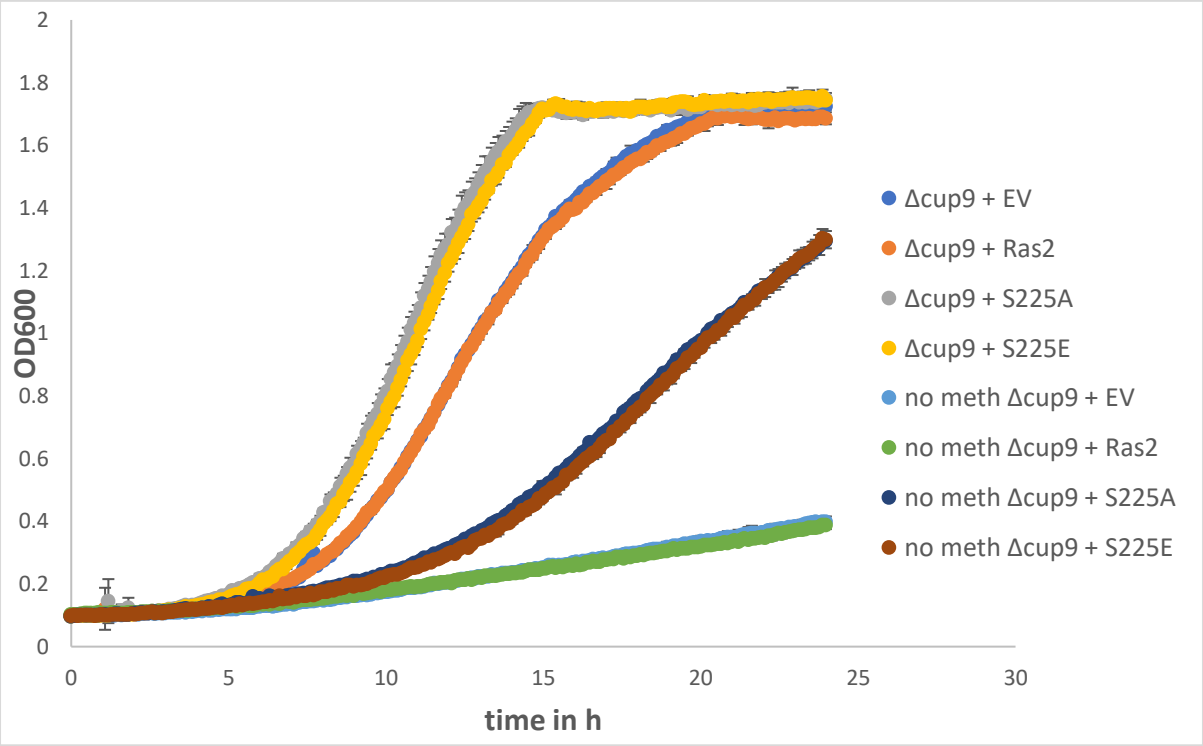

Figure 34. Growth analysis of *S. cerevisiae Δcup9* strains overexpressing *RAS2*, *RAS2*^{S225A}, *RAS2*^{S225E} or an empty plasmid control in media lacking or containing methionine.
The growth analysis was conducted in SD-Met media and SD-Met media where methionine was completely added back (Material and Methods, Section 2.8.1) and represents an average of three biological repeats. The error bars display the standard deviation.

3.9.1 Further investigation of the methionine biosynthesis pathway using growth analysis in supplemented media

Based on the RNA sequencing analysis showing upregulation of genes at the last steps of the methionine synthesis pathway, we hypothesised that an addition of substrates for those steps might help to overcome the growth and viability defects shown in the wild type strains overexpressing *RAS2*^{S225} mutants. We therefore investigated the effect of the addition S-AdenosylMethionine, L-Homocysteine, and S-AdenosylHomocysteine each at a concentration of 0.5 mM.

A toxic effect was seen when adding 0.5 mM S-AdenosylMethionine to the strains growing in SD-URA media (data not shown). The addition of 0.5 mM L-Homocysteine showed no effect on the growth of the wild type strains overexpressing *RAS2*, *RAS2*^{S225A}, *RAS2*^{S225E} or an empty plasmid control compared to the wild type strains overexpressing *RAS2*, *RAS2*^{S225A}, *RAS2*^{S225E} or an empty plasmid control grown in normal SD-URA media (**Fig. 35**).

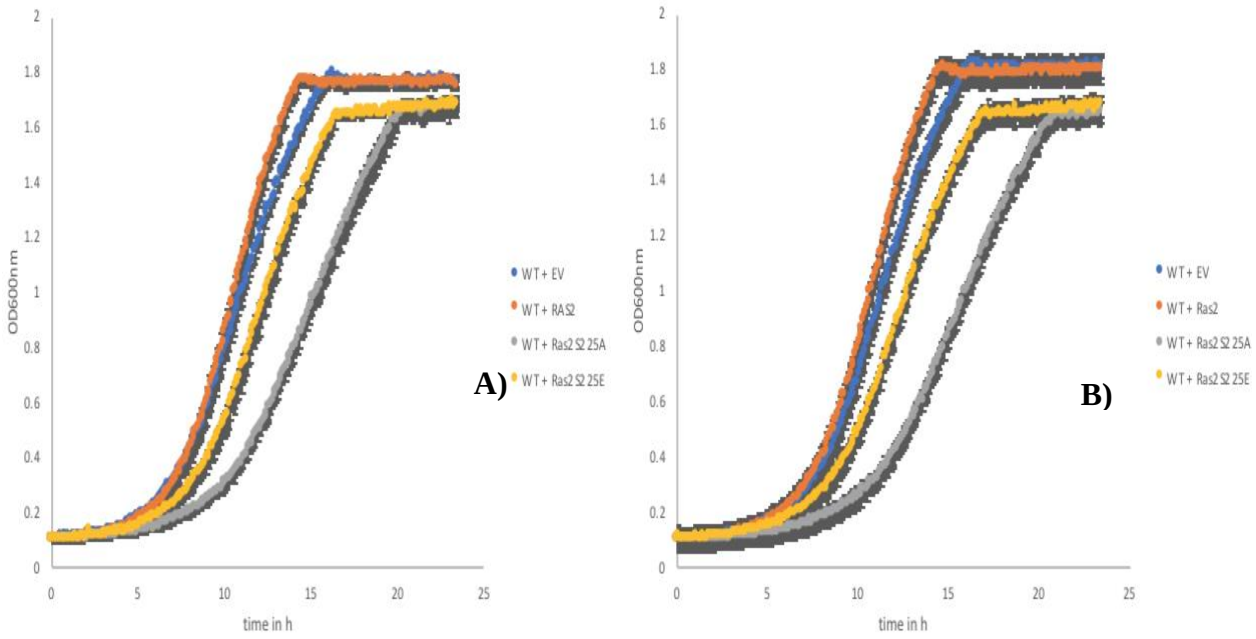

Figure 35. Growth analysis of *S. cerevisiae* wild type strains overexpressing *RAS2*, *RAS2*^{S225A}, *RAS2*^{S225E} or control cells in SD-URA media with 0.5 mM L-Homocysteine addition.
The growth analysis was conducted in SD-URA media for the controls (**A**) and SD-URA media with 0.5 mM L-Homocysteine addition (**B**) (Material and Methods, Section 2.8.1). The data shown represents an average of three biological repeats. The error bars display the standard deviation.

We then examined the effect of 0.5 mM S-AdenosylHomocysteine on the wild type strains overexpressing *RAS2*, *RAS2*^{S225A}, *RAS2*^{S225E} or an empty plasmid control. No significant effect on the growth of the wild type strains overexpressing *RAS2*, *RAS2*^{S225A}, *RAS2*^{S225E} or an empty plasmid control compared to the wild type strains overexpressing *RAS2*, *RAS2*^{S225A}, *RAS2*^{S225E} or an empty plasmid control grown in normal SD-URA media was detected. However, the wild type strains overexpressing the *RAS2*^{S225} mutations reached their final OD slower when compared to the wild type strain control grown in normal SD-URA media (**Fig. 36**).

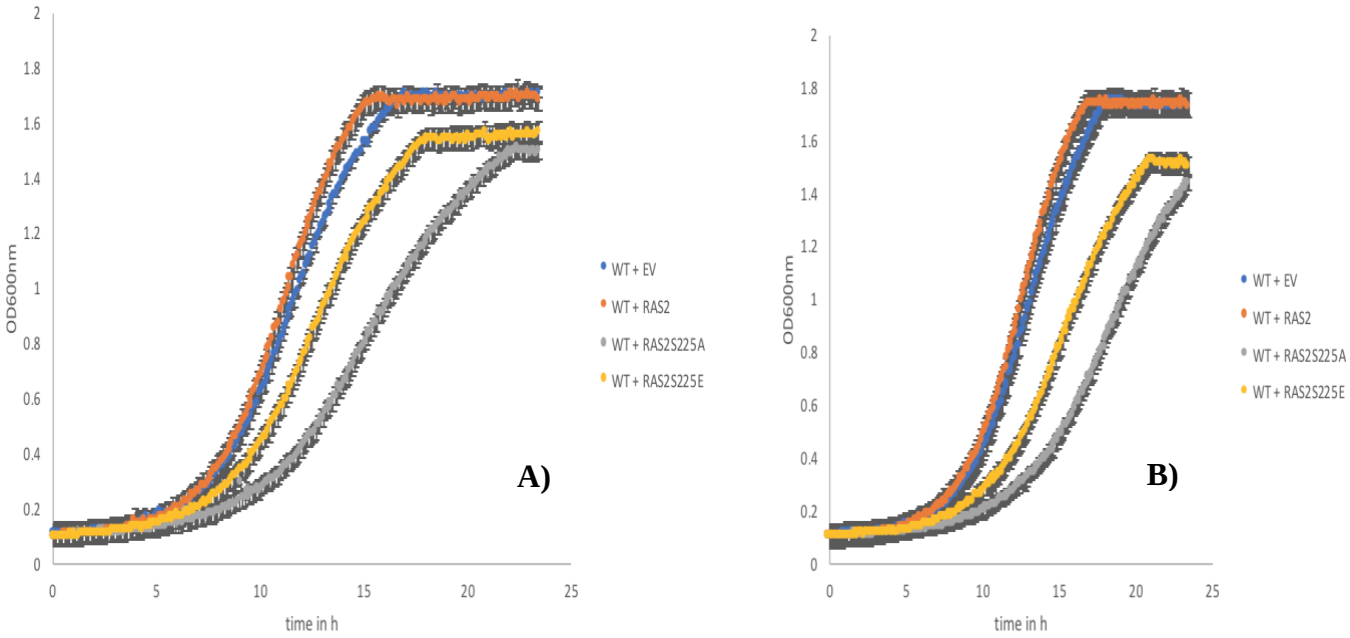

Figure 36. Growth analysis of *S. cerevisiae* wild type strains overexpressing *RAS2*, *RAS2*^{S225A}, *RAS2*^{S225E} or an empty plasmid control in SD-URA media with 0.5 mM S-AdenosylHomocysteine addition.
The growth analysis was conducted in SD-URA media for the controls (**A**) and SD-URA media with 0.5 mM S-AdenosylHomocysteine addition (**B**) (Material and Methods, Section 2.8.1). The data shown represents an average of three biological repeats. The error bars display the standard deviation.

Furthermore, neither the addition of 0.5 mM S-AdenosylHomocysteine nor L-Homocysteine was able to rescue the reduced viability or colony forming units seen in the wild type strains overexpressing the *RAS2*^{S225} mutants (**Fig. 37**, **38**).

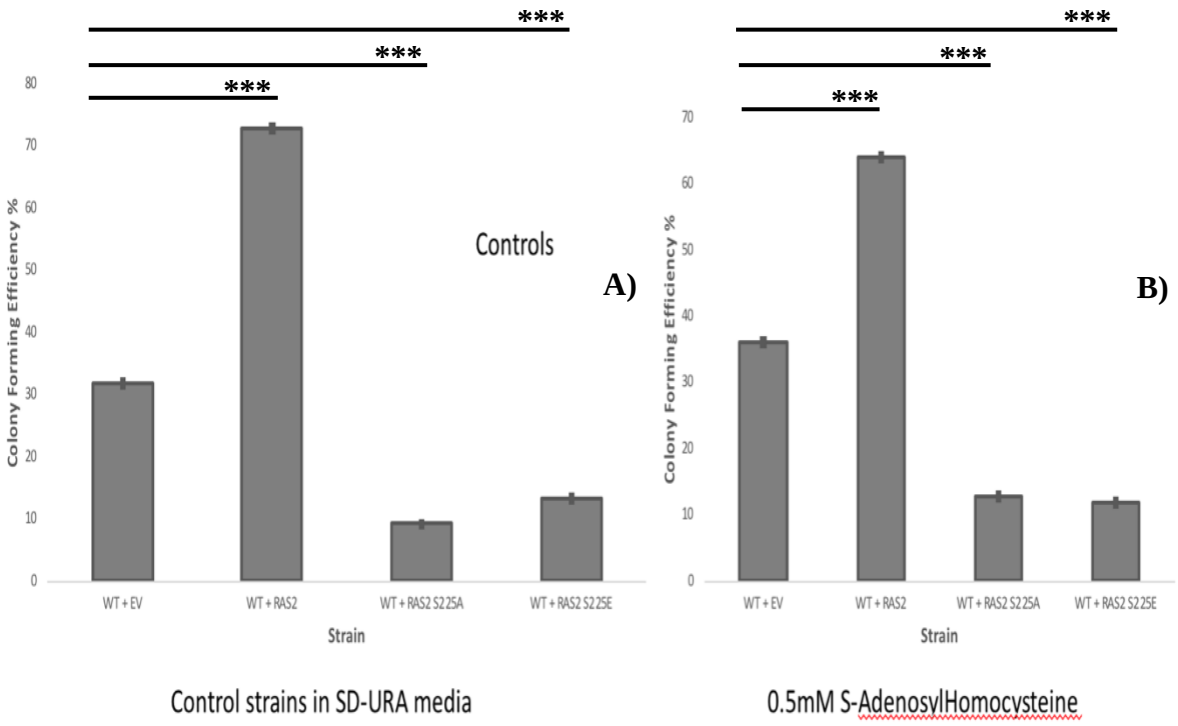

Figure 37. A colony forming efficiency assay of *S. cerevisiae* wild type cells overexpressing RAS2, RAS2S225A, RAS2S225E or an empty plasmid control grown in SD –URA media with 0.5 mM S-AdenosylHomocysteine addition.
A) Wild type control cells grown in SD-URA media
B) Wild type cells grown in SD-URA media supplemented with 0.5 mM S-AdensosylHomocysteine.
A One-way ANOVA using a Tukey multiple comparison test was used to determine statistical significance compared to the control. *** = adjusted p value ≤ 0.001.

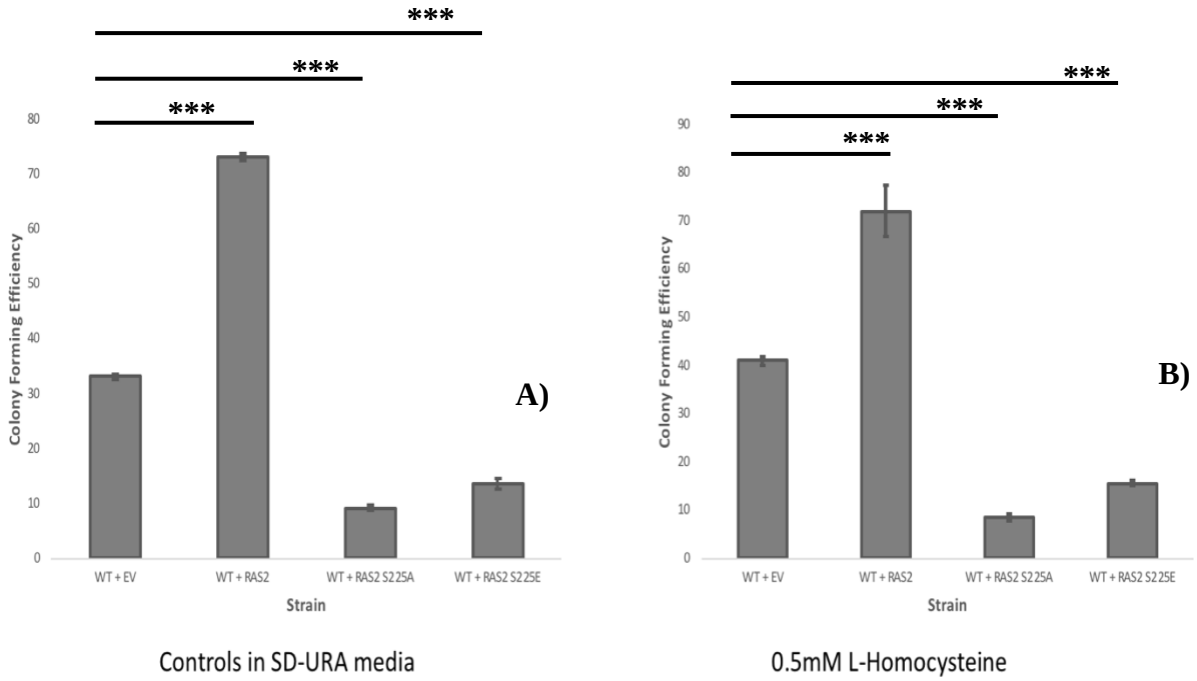

Figure 38. A colony forming efficiency assay of *S. cerevisiae* wild type cells overexpressing *RAS2*, *RAS2*^{S225A}, *RAS2*^{S225E} or an empty plasmid control grown in SD –URA media with 0.5 mM L-Homocysteine addition.
A) Wild type control cells grown in SD-URA media
B) Wild type cells grown in SD-URA media supplemented with 0.5 mM L-Homocysteine.
A One-way ANOVA using a Tukey multiple comparison test was used to determine statistical significance compared to the control. *** = adjusted p value ≤ 0.001.

3.10 Ferrozine sensitivity assay to investigate the upregulation of the Fe-S cluster assembly of yeast cells overexpressing *RAS2, RAS2*^{S225A} or *RAS2*^{S225E}

Based on the RNA sequencing analysis showing an upregulation of genes involved in the Fe-S cluster assembly, we investigated the effect of 0.25 mM ferrozine – an iron chelator – on wild type and *Δcup9* strains overexpressing *RAS2, RAS2*^{S225A}, *RAS2*^{S225E} or an empty plasmid control using a spotting assay as described in Material and Methods, Section 2.8.4.

On the control SD-URA plate a reduction in growth was visible in wild type cells overexpressing the *RAS2*^{S225} mutant alleles when compared to the control strain (**Fig. 39 A**). This was concordant with the phenotypes seen in the growth assay (**Fig. 22**) and the viability assay (**Fig. 26 A**). No significant reduction in growth could be detected in the wild type cells overexpressing the *RAS2*^{S225} mutant alleles using the integration system when compared to the control strain (**Fig. 39 B**). This was also concordant with the phenotypes seen in the

growth assay (**Fig. 22**) and the viability assay (**Fig. 26 A**). No significant reduction in growth was seen in the *Δcup9* strains overexpressing *RAS2, RAS2*^{S225A}, *RAS2*^{S225E} or an empty plasmid control when compared to the wild type strains overexpressing *RAS2, RAS2*^{S225A}, *RAS2*^{S225E} or an empty plasmid control (**Fig. 39 C**). A medium sensitivity to 0.25 mM ferrozine could be detected in the wild type strains overexpressing *RAS2, RAS2*^{S225A}, *RAS2*^{S225E} or an empty plasmid control (2µ system) when compared to their control SD-URA plate (**Fig. 39 A**). A slight sensitivity to 0.25 mM ferrozine was visible in the wild type strains overexpressing *RAS2, RAS2*^{S225A}, *RAS2*^{S225E} or an empty plasmid control (integration system) when compared to their control SD-URA plate (**Fig. 39 B**). A high sensitivity to 0.25 mM ferrozine was detected in the *Δcup9* strains overexpressing *RAS2, RAS2*^{S225A}, *RAS2*^{S225E} or an empty plasmid control when compared to their control plate (**Fig. 39 C**).

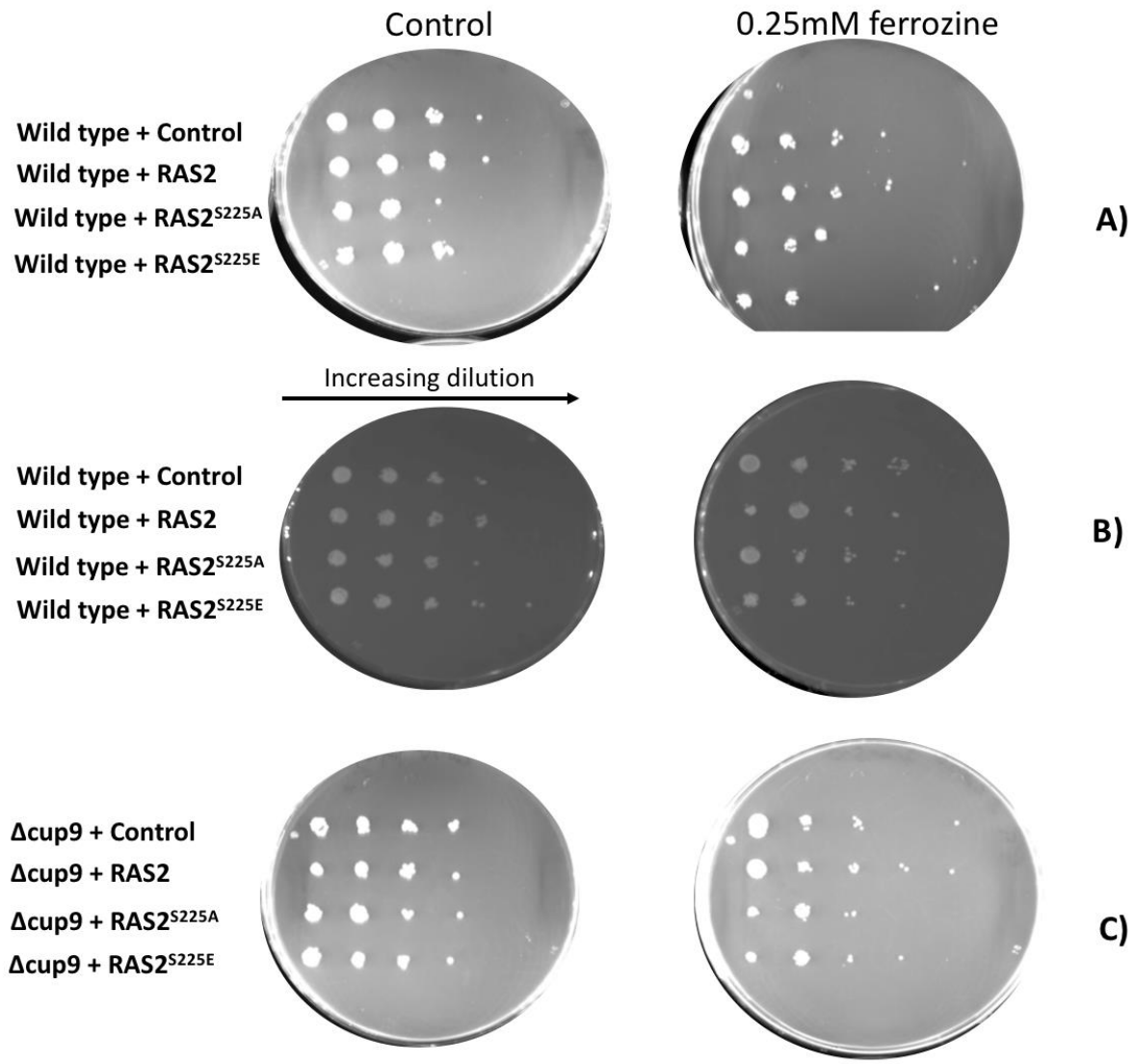

Figure 39. A spotting assay of wild type and *Δcup9* strains overexpressing *RAS2, RAS2^{S225A}, RAS2^{S225E}* or an empty plasmid control on 0.25 mM ferrozine agar plates.
A) Overexpression system: wild type strains overexpressing *RAS2, RAS2^{S225A}, RAS2^{S225E}* or an empty plasmid control on 0.25 mM ferrozine agar plates.
B) Integration system: wild type strains overexpressing *RAS2, RAS2^{S225A}, RAS2^{S225E}* or an empty plasmid control on 0.25 mM ferrozine agar plates.
C) *Δcup9* strains overexpressing *RAS2, RAS2^{S225A}, RAS2^{S225E}* or an empty plasmid control on 0.25 mM ferrozine agar plates.
All controls were plated onto SD-URA agar plates.

4. Discussion

In the present study we sought to further investigate the impact of modifying serine 225 of Ras2p, a known target for phosphorylation. We made use of two systems that allowed for differential levels of overexpression with the aim of mimicking the combinatorial effect of Ras mutation plus gene duplication that is often found to occur in cancer. In the present study, we therefore compared data from a plasmid overexpression system with data using a genome integration system. We demonstrate that while overexpression of Ras2 and mutant forms of Ras can be tolerated by the cell, the presence of increased copy number in combination with mutation leads to an altered cell fate.

4.1 Western blot analysis confirms expression of *ras2*, *ras2*^{S225A} and *ras2*^{S225E} alleles in *S. cerevisiae*

Western blot analysis confirmed that Ras2, Ras2^{S225A} and Ras2^{S225E} were overexpressed in both a wild type and *Δras2* background. The overexpression of either *RAS2*^{S225A} or *RAS2*^{S225E} using a single copy of the mutated gene led to an increase in Ras2p expression during stationary phase of growth when compared to the control and *RAS2* cells. This suggests that Serine^{225} has a putative role in controlling Ras2 protein expression or protein stability.

Ras degradation has been subject to alternative therapeutic approaches in fighting oncogenicity of Ras mutations (Nabet *et al.*, 2018; Röth *et al.*, 2020). Generally, protein degradation approaches utilise cellular proteolytic pathways, such as the ubiquitin proteasome system (UPS) (Röth, Fulcher and Sapkota, 2019). Degradation via the UPS occurs through the addition of ubiquitin chains onto the target protein. Three enzymes are responsible for this cascade: the ubiquitin-activating enzyme (E1), the ubiquitin-conjugating enzyme (E2), and the ubiquitin ligase (E3). While E1 is responsible for the ATP-dependent activation of the C-terminal glycine of ubiquitin, E2 allows conjugation of the activated

ubiquitin to its active site cysteine. E3 then enables the transfer of ubiquitin to substrate proteins targeting primarily their lysin residues (Pickart and Eddins, 2004; Roos-Mattjus and Sistonen, 2004). Ultimately poly-ubiquitylation then leads to the degradation of the target protein through the proteasome (Komander and Rape, 2012; Akutsu, Dikic and Bremm, 2016; Yau and Rape, 2016). Cancers frequently show mutated Ras proteins. Studies by (Zeng *et al.*, 2014) show that mutated Ras causes overexpression of the protein $NEDD_{4\text{-}1}$. Furthermore, PTEN (a phosphatase) degradation is promoted by inhibiting Ras ubiquitination through $NEDD_{4\text{-}1}$ ultimately resulting in tumorigenesis (Zeng *et al.*, 2014).

Furthermore, other studies have shown that H-Ras degradation through the proteasome occurs when the Wnt/ß-catenin signalling pathway is activated (Kim *et al.*, 2009; Cho *et al.*, 2016; Jeong, Ro and Choi, 2018). Here, prior to the degradation of H-Ras via the recruitment of ß-TrCP-E3 ligase, glycogen synthase kinase 3ß phosphorylates H-Ras. Abnormal Wnt/ß-catenin signalling inhibits this pathway increasing expression levels of Ras and Ras-induced colorectal cancer (Cha *et al.*, 2016; Cho *et al.*, 2016; Dohlman and Campbell, 2019).

Evidence exist that during nutritional depletion in the diauxic phase of growth, Ras2p is targeted for proteolysis to shut-down Ras/cAMP/PKA signalling. Cells lacking Whi2 – a growth regulation protein – fail to degrade or deactivate Ras2p when Ras2p is translated from the plasma membrane to the mitochondria during the diauxic phase of growth. Fundamental for vesicle trafficking is the actin cytoskeleton (Leadsham *et al.*, 2009).

We suggest that failure in ubiquitination of Ras2p, aberrant vesicle transport of Ras2p which might trap Ras2p in the vacuole preventing its degradation (Leadsham *et al.*, 2009), or improper localisation to the nuclear envelope leads to an increase in expression of Ras2p. However, overexpression of Ras2p seen in the integrated system might occur through another mechanism which requires further investigations. A study by (Englaender *et al.*, 2017)

showed that when integrated into the genome, the expression levels of the protein was dependent on its genomic integration location.

The higher values of the overall relative band intensities of the 2μ system was expected due to the different levels of gene copies in the two systems: overexpression vectors that contained a 2μ origin of replication and thus multiple copies, and genome integration vectors that, when inserted, will generate a single copy of the gene. However, to determine the reason for increased stability linked to serine225 mutation we would have to look at mRNA levels and stability (lifetime of Ras2 mRNA following arrest of transcription and monitoring mRNA levels by rtPCR or Northern Blot) as well as protein turnover (adding protein synthesis inhibitor such as cyclohexamide and monitoring loss of protein over time by western blot).

4.2 Mutation of serine 225 in Ras2 leads to mislocalisation and constitutive activity

During the logarithmic phase of growth wild type cells localised GTP-bound Ras to the plasma membrane and nucleus (Piper-brown, 2019). This localisation (Willumsen *et al.*, 1984; Colicelli, 2004) activates the cAMP/PKA pathway initiating both cell growth and proliferation (Tisi, Belotti and Martegani, 2014). In wild type cells overexpressing either $RAS2^{S225A}$ or $RAS2^{S225E}$, however, an increase in active Ras found at the nuclear envelop/ER was observed. During stationary phase of growth when nutrient availability is scarce, GTP-bound Ras was seen as a diffused cytoplasmic signal with some intracellular foci within the vacuole consistent with the shut-down of Ras activity. Interestingly, wild type cells overexpressing either $RAS2^{S225A}$ or $RAS2^{S225E}$ presented a nuclear envelop localisation of GTP-bound Ras. This was not observed in the control or the *RAS2* overexpression cells. Ras proteins are subject to posttranslational modifications (PTM) in order to localise to and

associate with membranes where they get activated (Wennerberg, Rossman and Der, 2005; Cox and Der, 2010). Here, the CAAX motif is sequentially processed (Hancock *et al.*, 1991). The first PTM is farnesylation via farnesyltransferase allowing loose interaction with endomembranes like the ER (Choy *et al.*, 1999). Furthermore, the Ras inhibitor 1 (Eri1) enables contact of GTP-bound Ras2 with the ER (Sobering *et al.*, 2003). Serine 225 mutations might disturb the PTM chain preventing further pivotal protein processing like prenylation and palmitoylation holding Ras2 at the ER, ultimately preventing Ras translocation to the plasma membrane leading to mislocalisation seen in (Piper-brown, 2019). However, Ras can be activated at the ER (Bivona *et al.*, 2003), and studies have shown that overexpression or hyperactivation of Ras triggers actin polymerization, resulting in a constantly activated cAMP/PKA pathway (Pratyusha *et al.*, 2018).

We hypothesise that aberrant activation of the cAMP/PKA pathway occurs due to mis-localisation and inappropriate activation of Ras in Serine 225 mutants in both logarithmic phase of growth and during nutrient depletion where Ras activity should be at its lowest and PKA signalling should be minimal.

Previous conducted work presented in this study was exclusively carried out in wild type cells. Therefore, we believe it would be useful to study the effect of the overexpression of either *RAS2, RAS2*^{S225A} or *RAS2*^{S225E} on the localisation of active Ras when endogenous wild type Ras2p is absent. Hence future investigations in a *Δras2* background should be conducted.

Future investigation involving the integration of Ras and mutant S225 into Eri1 deletion strains would be interesting. Eri1is a component of the ER-localized GPI-GnT complex which is inhibited by GTP-bound Ras2 (Sobering *et al.*, 2004). It would be interesting to see if enhanced loss of growth occurs when Ras is activated on the nuclear envelope/ER. Further investigations on RBD-GFP localisation in Eri1 deletion strain and in Ras integration strains

might elucidate if overexpression of Eri1 shuts down Ras in the nuclear envelope and rescues the phenotype.

4.3 Mutation of serine 225 in Ras2 leads to growth defects and loss of viability

Fundamental for the regulation and integration of cell growth, cell cycle progression and metabolic activity is the Ras/cAMP pathway (Reinders *et al.*, 1998; Thevelein and de Winde, 1999; Smets *et al.*, 2010; Conrad *et al.*, 2014; Steyfkens *et al.*, 2018). Aberrant activation of the Ras/cAMP pathway via activating mutations in the *RAS2* gene or mutations in *BCY1* lead to an incorrect diauxic re-programming of the cell during nutrient depletion (Colombo *et al.*, 1998; Kelliher *et al.*, 2018). Elevated cAMP levels lead to loss of viability during stationary phase due to the inability of cells to activate expression of genes enabling carbohydrate storage, oxidative phosphorylation and stress response and is strongly correlated with cell death (Colombo *et al.*, 1998; Kelliher *et al.*, 2018). On the other hand, decreased cAMP/PKA activity ceases growth and promotes quiescence transition (Thevelein and de Winde, 1999; Smets *et al.*, 2010).

However, we showed that overexpression of either $RAS2^{S225A}$ or $RAS2^{S225E}$ leads to enhanced PKA activity leading to a decrease in viability due to growth cessation rather than cell death. We suggest that the mislocalisation of active Ras to the nuclear envelope/ER opposed to the plasma membrane when either $RAS2^{S225A}$ or $RAS2^{S225E}$ is overexpressed, perturbs normal Ras signalling and activation of cAMP/PKA pathway dysregulating the cell cycle. Growth cessation may occur when effectors are activated that enable the expression of genes de-regulating the co-ordination of growth and environmental sensing (Piper-brown, 2019).

We could conclude that the overexpression of either $RAS2^{S225A}$ or $RAS2^{S225E}$ induced growth defects were dominant as the growth defects could also be observed when endogenous Ras2 was absent. However, when we repeated this experiment using a single copy of the mutated

gene, no growth defect was detected in either the wild type or the *Δras2* background. We suggest that this shows that both the mutation and overexpression is important to have measurable effects from the Serine^{225} mutations in yeast. This is concordant with findings of cancer studies suggesting that duplication of oncogenes was common in the manifestation of cancer (Burgess *et al.*, 2017).

4.4 Deletion of *CUP9* rescues the toxic effects of Ras2S225 mutation

The transcription of the gene *PTR2* encoding an integral membrane protein Ptr2p that translocates di/tri-peptides across the plasma membrane is regulated by its transcriptional repressor Cup9 (Perry *et al.*, 1994). Studies showed that the deletion of *CUP9* in *S. cerevisiae* led to no significant changes in life span or heat shock resistance (Fabrizio *et al.*, 2010). The di/tri-peptide transporter PTR2p is able to transport the broadest variety of dipeptides amongst other peptide transporters in *S. cerevisiae*. The deletion of *CUP9* enables unhindered expression of *PTR2* which has shown to allow for stable cell growth on numerous di/tri-peptides (Homann *et al.*, 2005).

Previous work (Piper-brown, 2019) showed that the deletion of *CUP9* could rescue the growth and viability defects of Ras2^{S225} mutations. We propose that an increase in *PTR2* expression when *CUP9* is deleted results in an increased peptide uptake enabling cells to re-enter the cell cycle allowing growth (Homann *et al.*, 2005). However, we also suggest that a link exists between Ras and nutrient availability to direct cell fate (Piper-brown, 2019). Previous studies have established mitochondrial sensitivity to Ras signalling through cAMP/PKA signalling and without cAMP/PKA signalling (Hlavata, 2003; Hlavatá *et al.*, 2008). Studies in lymphoid cells have shown that increased cAMP/PKA levels can promote mitochondrial dependent apoptosis through transcriptional changes (Zhang *et al.*, 2008). Others provided evidence that increased PKA activity is able to cause mitochondrial

dependent apoptosis. Here, especially the function of PKA subunit Tpk3p is important (Gourlay and Ayscough, 2006; Leadsham *et al.*, 2009). Tpk3p regulates mitochondrial activity through transcriptional control of various genes important in mitochondrial function e.g. genes involved in the election transport system. Down-regulation of genes via Tpk3p regulation that are important for respiration leads to a decrease in respiratory capacity (Leadsham and Gourlay, 2010). Increased PKA activity could explain the lower respiration capacity observed in our study in wild type cells overexpression $RAS2^{S225A}$. However, we believe cell cycle cessation occurs rather than cell apoptosis.

Furthermore, we showed that the deletion of *CUP9* restores Serine 225 induced respiratory defects which is supported by Fe-S assembly (Braymer and Lill, 2017)- a pathway upregulated in *CUP9* deletion strains. Gene ontology analysis revealed an upregulation of sulphur metabolic processes, including the upregulation of the rate limiting step in glutathione biosynthesis, the last steps of methionine biosynthesis, and the Fe-S cluster assembly – mainly the cytosolic part of the Fe-S synthesis.

It is well established that cell division requires both growth and metabolism (Ewald *et al.*, 2016; Palm and Thompson, 2017; Zhu and Thompson, 2019). However, if cell division can be actively promoted by metabolism remains unclear. Studies addressing this subject found an experimental system to study that cell division can be promoted by metabolism using a nuclear gene called $ABF2^{+}$ in *S. cerevisiae* which encodes a mitochondrial DNA maintenance protein called TFAM binding to and bending mitochondrial DNA (mtDNA). This protein is highly conserved in animals (Friddle *et al.*, 2004; Stigter, 2004). It was shown that moderate over-expression of Abf2p can increase the amount of mtDNA by 50-150 % as well as initiating a faster process of cell size increase, and DNA replication initiation in the nucleus (Zelenaya-Troitskaya *et al.*, 1998; Blank *et al.*, 2008, 2009).

Many cellular processes rely on sulphur metabolism and it is very well established that growth rate in yeast correlates with sulphur metabolic flux (Brosnan and Brosnan, 2006; Castrillo *et al.*, 2007). Sulphur metabolites such as glutathione which is the main redox buffer in cells, "peak" during the reductive phase (Murray, Beckmann and Kitano, 2007; Tu *et al.*, 2007). Unger and Hartwell, 1976, showed that yeast cells arrest before DNA replication is initiated when sulphur metabolism is disturbed. Recently a group (Blank *et al.*, 2009) has shown that an increased sulphur metabolic flux together with an increased reductive phase of the metabolic cycle could be observed in yeast cells with higher mtDNA levels. Furthermore, it was shown that cells with more mtDNA exhibit an enhanced growth rate when sulphur metabolic flux phenocopy was manipulated in wild type cells. Interestingly, initiation of DNA replication was accelerated in wild type cells where a hyperactive cystathionine-ß-synthase (CBS) allele was introduced (Blank *et al.*, 2009). In addition, it was found that the cell cycle regulates transcription of specific genes involved in sulphur metabolic pathways. The transcription of those genes had its highest level at the beginning of cell division (Spellman *et al.*, 1998).

We suggest that deletion of *CUP9* either restores the connection between the cell cycle and nutrition that Ras mutations break or re-instates the signal allowing cell cycle progression. Our hypothesis is that the observed rescue of growth occurs because of an increase in sulphur metabolic processes that are inhibited by aberrant signalling from the mutant Ras isoform.

4.5 *RAS2* overexpression allows MET- auxotrophic yeast to grow in media lacking methionine in a serine225 dependent manner and deletion of *CUP9* allows Ras2S225 mutants to grow in media lacking methionine

The amino acid methionine is pivotal for cell growth and development (Finkelstein, 1990). Methionine metabolism includes the methionine cycle generating methylation potential, the methionine salvage pathway which uses by-products of polyamine synthesis pathways to recycle methionine, and the transsulfuration pathway which is pivotal in controlling oxidation by producing cysteine and glutathione (Kaiser, 2020). Cancer cells are known to re-programme cellular metabolism. The "Hoffman effect" or methionine dependence presents another metabolic change acquired by cancer cells. Here, cancer cells are dependent on exogenous methionine and most of them are unable to grow in medium lacking methionine (Borrego *et al.*, 2016). Studies have shown that methionine dependence is supported by oncogenic H-Ras expression levels (Vanhamme and Szpirer, 1989).

However, we show that *RAS2* overexpression and *Δcup9* cells overexpressing $RAS2^{S225A}$, or $RAS2^{S225E}$ could overcome MET-auxotrophy and were able to grow in media lacking methionine. We hypothesise that wild type cells overexpressing *RAS2* and that loss of *CUP9* reactivates methionine salvage upregulating it to scavenge metabolites to generate higher levels of methionine re-establishing growth. We believe that $Serine^{225}$ mutations disrupt this process supressing sulphur metabolism leading to loss of growth and quiescence.

Interestingly, the growth defects caused in wild type cells with $Serine^{225}$ mutations were lost when these cells were grown in media where all the required methionine was added back. This is suggestive of an important role of the amino acid methionine in controlling growth which is supported by (Finkelstein, 1990).

4.6 AdoMET, AdoHomocysteine or L-homocysteine are not sufficient to rescue Ras225A induced cell cycle arrest

S-adenosyl methionine (AdoMet) and S-adenosyl Homocysteine (AdoHcy) are two key metabolic intermediates in the methionine metabolism. Many biological processes, such as metabolism, signal transduction, and gene expression rely on AdoMet-dependent transmethylation. Here, AdoMet is converted to AdoHcy which inhibits methyltransferase (Thomas and Surdin-Kerjan, 1997; Ogawa *et al.*, 2016). Recent studies indicate that an increased production of AdoMet can increase lifespan through AMP-activated protein kinase (AMPK) activation not only in *S. cerevisiae*, but also in worms and flies (Obata and Miura, 2015; Schosserer *et al.*, 2015; Ogawa *et al.*, 2016). If $Ras2^{S225}$ mutations did the opposite then this could be very relevant to correctly regulate cell growth.

We hypothesise that Ras signalling from wrong locations in the cells leads to low AdoMet synthesis which leads to low AMPK activity which in turn prevents cell growth thus connecting it to metabolic sensing (**Fig**. **40**). However, our data suggests that the addition of AdoMet, AdoHomocysteine or L-homocysteine were not sufficient to rescue Ras225A induced cell cycle arrest. We think that simply adding supplements does not achieve an effect as the correct balance of intermediates are needed for functioning metabolism.

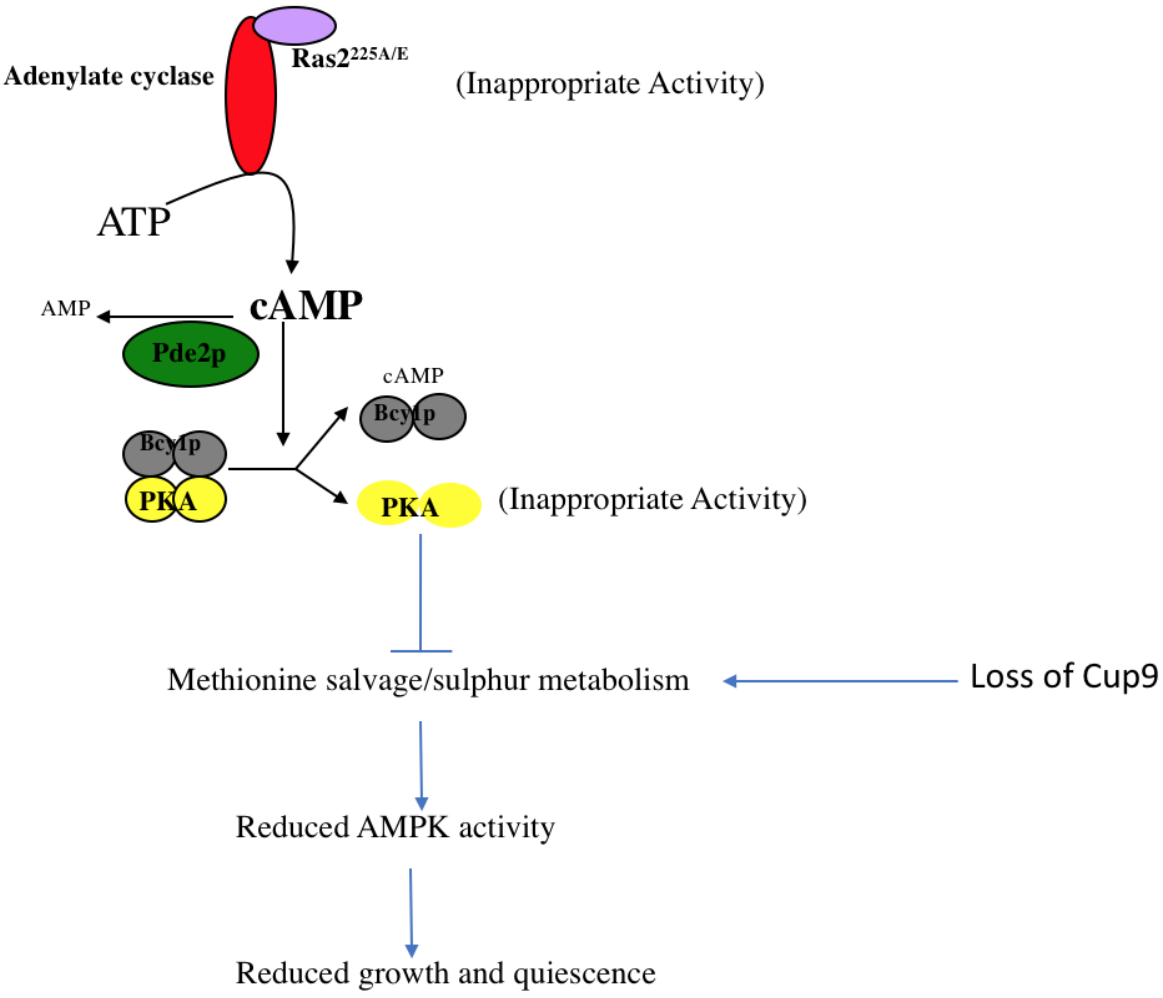

Figure 40. Our current Model how loss of *CUP9* reactivates methionine salvage and re-instates cell cycle through AdoMet and AMPK levels.

4.7 Importance of Fe-S pathway in growth

Studies investigating the cellular response to iron deficiency in *S. cerevisiae* focussing on changes in mRNA transcripts and protein levels indicate that the budding yeast responds to iron deficiency by either activating iron uptake systems, mobilising intracellular iron stores, or adjust metabolism to prevent iron depletion (Shakoury-Elizeh *et al.*, 2004; Puig, Askeland and Thiele, 2005; Philpott and Protchenko, 2008). The transcription factors, Aft1 and Aft2, in *S. cerevisiae* are responsible to activate transcription of genes which are necessary to respond

to iron deficiency (Waldron *et al.*, 2009). One of which is the haem-degrading enzyme with its corresponding gene, *HMX1*, targeted by Aft1 (Philpott and Protchenko, 2008). During iron deficiency, changed in glutamate synthesis occurs which may be responsible for the up-regulation of genes involved in amino acid and nitrogen uptake (Shakoury-Elizeh *et al.*, 2004). If some of those genes are down-regulated in the $RAS2^{S225}$ mutants, it might be that the $RAS2^{S225}$ mutation is severing the link between sulphur level sensing and action. However, only adding more intermediates to the media might not make a difference as metabolism requires the correct balance to function correctly. To investigate this further, it would be interesting to determine those genes by RNA sequencing analysis. In addition, test strips to see if hydrogen sulphide is produced could be used as this would indicate whether sulphur metabolism is not working. Furthermore, to test for specific iron sulphur incorporation into enzymes would be interesting to investigate.

4.8 Concluding marks

We demonstrated that both mutations and increase in oncogene copy number is important to have measurable effect of $Serine^{225}$ mutations. This is concordant with findings of cancer studies suggesting that duplication of oncogenes is common in the manifestation of cancer (Burgess *et al.*, 2017). We could also determine that the deletion of *CUP9* could rescue the toxic effects of $Ras2^{S225}$ mutant alleles including growth, viability, and respiratory defects. Furthermore, we show that overexpression of *RAS2* in wild type cells, and overexpression of $RAS2^{S225A}$ or $RAS2^{S225E}$ were able to overcome MET-auxotrophy which might represent the link between Ras2 activity, growth and nutrient sensing. However, due to time constraints this could not be investigated in detail. For future work, we therefore wish to further analyse Fe-S cluster assembly in the cytoplasm. Another possibility that explained the lack of cell

division linked to Fe-S is that DNA polymerase and helicase enzymes have Fe-S clusters. Deficiency or imbalance could lead to genome instability which we wish to test by adding DNA damaging agents, e.g. UV treatment or MMS addition.

Future work:

- Integrate Ras and mutant S225 into Eri1 deletion strains to activate Ras on the nuclear envelope/ER, and to see if enhanced loss of growth occurs
- Examine RBD-GFP localisation in Eri1 deletion strain and in Ras integration strains (does overexpression of ERi1 shut down Ras on the nuclear envelope and rescue phenotype?)
- Test which PKA subunit responsible for any of above that look interesting
- Investigate our model further in eukaryote multicellular model organisms, such as the nematode *C. elegans* to gain a better understanding of the Ras pathway and to strengthen or further investigate our model.
- COSMIC database of somatic mutations in cancer https://cancer.sanger.ac.uk/cosmic: There are some mutations in H-Ras that are close to the hypervariable region as 225. We speculate that the yeast models hold further validity and that some more work could be done in this area.

References:

Abdelkarim *et al.* (2019) 'The Hypervariable Region of K-Ras4B Governs Molecular Recognition and Function', *International Journal of Molecular Sciences*, 20(22), p. 5718. doi: 10.3390/ijms20225718.

Akutsu, M., Dikic, I. and Bremm, A. (2016) 'Ubiquitin chain diversity at a glance', *Journal of Cell Science*. doi: 10.1242/jcs.183954.

Alagramam, K., Naider, F. and Becker, J. M. (1995) 'A recognition component of the ubiquitin system is required for peptide transport in Saccharomyces cerevisiae', *Molecular Microbiology*, 15(2), pp. 225–234. doi: 10.1111/j.1365-2958.1995.tb02237.x.

Almoguera, C. *et al.* (1988) 'Most human carcinomas of the exocrine pancreas contain mutant c-K-ras genes', *Cell*, 53(4), pp. 549–554. doi: 10.1016/0092-8674(88)90571-5.

Anghileri, P. *et al.* (1999) 'Chromosome Separation and Exit from Mitosis in Budding Yeast: Dependence on Growth Revealed by cAMP-Mediated Inhibition', *Experimental Cell Research*, 250(2), pp. 510–523. doi: 10.1006/excr.1999.4531.

Apolloni, A. *et al.* (2000) 'H-ras but Not K-ras Traffics to the Plasma Membrane through the Exocytic Pathway', *Molecular and Cellular Biology*, 20(7), pp. 2475–2487. doi: 10.1128/MCB.20.7.2475-2487.2000.

Arnold, A. R., Grodick, M. A. and Barton, J. K. (2016) 'DNA Charge Transport: from Chemical Principles to the Cell', *Cell Chemical Biology*, 23(1), pp. 183–197. doi: 10.1016/j.chembiol.2015.11.010.

Athuluri-Divakar, S. K. *et al.* (2016) 'A Small Molecule RAS-Mimetic Disrupts RAS Association with Effector Proteins to Block Signaling', *Cell*, 165(3), pp. 643–655. doi: 10.1016/j.cell.2016.03.045.

Averous, J. *et al.* (2016) 'GCN2 contributes to mTORC1 inhibition by leucine deprivation through an ATF4 independent mechanism', *Scientific Reports*, 6(1), p. 27698. doi:

10.1038/srep27698.

Barbacid, M. (1987) ‘ras Genes’, *Annual Review of Biochemistry*, 56(1), pp. 779–827. doi: 10.1146/annurev.bi.56.070187.004023.

Baroni, M. D. *et al.* (1989) ‘Cell size modulation by CDC25 and RAS2 genes in Saccharomyces cerevisiae.’, *Molecular and Cellular Biology*, 9(6), pp. 2715–2723. doi: 10.1128/MCB.9.6.2715.

Baroni, M. D. *et al.* (1992) ‘cAMP-mediated increase in the critical cell size required for the G1 to S transition in Saccharomyces cerevisiae’, *Experimental Cell Research*, 201(2), pp. 299–306. doi: 10.1016/0014-4827(92)90277-F.

Baroni, M. D., Monti, P. and Alberghina, L. (1994) ‘Repression of growth-regulated Gl cyclin expression by cyclic AMP in budding yeast’, *Nature*, 371(6495), pp. 339–342. doi: 10.1038/371339a0.

Belotti, F. *et al.* (2012) ‘Localization of Ras signaling complex in budding yeast’, *Biochimica et Biophysica Acta (BBA) - Molecular Cell Research*, 1823(7), pp. 1208–1216. doi: 10.1016/j.bbamcr.2012.04.016.

Berlanga, J. J., Santoyo, J. and de Haro, C. (1999) ‘Characterization of a mammalian homolog of the GCN2 eukaryotic initiation factor 2alpha kinase’, *European Journal of Biochemistry*, 265(2), pp. 754–762. doi: 10.1046/j.1432-1327.1999.00780.x.

Bertram, P. G. *et al.* (2000) ‘Tripartite Regulation of Gln3p by TOR, Ure2p, and Phosphatases’, *Journal of Biological Chemistry*, 275(46), pp. 35727–35733. doi: 10.1074/jbc.M004235200.

Biou, V. and Cherfils, J. (2004) ‘Structural Principles for the Multispecificity of Small GTP-Binding Proteins †’, *Biochemistry*, 43(22), pp. 6833–6840. doi: 10.1021/bi049630u.

Bivona, T. G. *et al.* (2003) ‘Phospholipase Cγ activates Ras on the Golgi apparatus by means of RasGRP1’, *Nature*, 424(6949), pp. 694–698. doi: 10.1038/nature01806.

Bivona, T. G. *et al.* (2006) 'PKC Regulates a Farnesyl-Electrostatic Switch on K-Ras that Promotes its Association with Bcl-Xl on Mitochondria and Induces Apoptosis', *Molecular Cell*, 21(4), pp. 481–493. doi: 10.1016/j.molcel.2006.01.012.

Blank, H. M. *et al.* (2008) 'An Increase in Mitochondrial DNA Promotes Nuclear DNA Replication in Yeast', *PLoS Genetics*. Edited by O. Cohen-Fix, 4(4), p. e1000047. doi: 10.1371/journal.pgen.1000047.

Blank, H. M. *et al.* (2009) 'Sulfur Metabolism Actively Promotes Initiation of Cell Division in Yeast', *PLoS ONE*. Edited by P. Cobine, 4(11), p. e8018. doi: 10.1371/journal.pone.0008018.

Blasco, R. B. *et al.* (2011) 'c-Raf, but Not B-Raf, Is Essential for Development of K-Ras Oncogene-Driven Non-Small Cell Lung Carcinoma', *Cancer Cell*, 19(5), pp. 652–663. doi: 10.1016/j.ccr.2011.04.002.

Bodenmiller, B. *et al.* (2008) 'PhosphoPep—a database of protein phosphorylation sites in model organisms', *Nature Biotechnology*, 26(12), pp. 1339–1340. doi: 10.1038/nbt1208-1339.

Bodenmiller, B. *et al.* (2010) 'Phosphoproteomic Analysis Reveals Interconnected System-Wide Responses to Perturbations of Kinases and Phosphatases in Yeast', *Science Signaling*, 3(153), pp. rs4–rs4. doi: 10.1126/scisignal.2001182.

Boguski, M. S. and McCormick, F. (1993) 'Proteins regulating Ras and its relatives', *Nature*, 366(6456), pp. 643–654. doi: 10.1038/366643a0.

Boivin, D., Bilodeau, D. and Béliveau, R. (1996) 'Regulation of cytoskeletal functions by Rho small GTP-binding proteins in normal and cancer cells.', *Canadian journal of physiology and pharmacology*, 74(7), pp. 801–10. Available at: http://www.ncbi.nlm.nih.gov/pubmed/8946066.

Bonawitz, N. D. *et al.* (2007) 'Reduced TOR Signaling Extends Chronological Life Span via

Increased Respiration and Upregulation of Mitochondrial Gene Expression', *Cell Metabolism*, 5(4), pp. 265–277. doi: 10.1016/j.cmet.2007.02.009.

Borrego, S. L. *et al.* (2016) 'Metabolic changes associated with methionine stress sensitivity in MDA-MB-468 breast cancer cells', *Cancer & Metabolism*, 4(1), p. 9. doi: 10.1186/s40170-016-0148-6.

Botstein, D. and Fink, G. R. (2011) 'Yeast: An Experimental Organism for 21st Century Biology', *Genetics*, 189(3), pp. 695–704. doi: 10.1534/genetics.111.130765.

Bourne, H. R., Sanders, D. A. and McCormick, F. (1990) 'The GTPase superfamily: a conserved switch for diverse cell functions', *Nature*, 348(6297), pp. 125–132. doi: 10.1038/348125a0.

Bourne, H. R., Sanders, D. A. and McCormick, F. (1991) 'The GTPase superfamily: conserved structure and molecular mechanism', *Nature*, 349(6305), pp. 117–127. doi: 10.1038/349117a0.

Brauer, M. J. *et al.* (2008) 'Coordination of Growth Rate, Cell Cycle, Stress Response, and Metabolic Activity in Yeast', *Molecular Biology of the Cell*. Edited by T. Fox, 19(1), pp. 352–367. doi: 10.1091/mbc.e07-08-0779.

Braymer, J. J. and Lill, R. (2017) 'Iron–sulfur cluster biogenesis and trafficking in mitochondria', *Journal of Biological Chemistry*, 292(31), pp. 12754–12763. doi: 10.1074/jbc.R117.787101.

Bremner, R. and Balmain, A. (1990) 'Genetic changes in skin tumor progression: Correlation between presence of a mutant ras gene and loss of heterozygosity on mouse chromosome 7', *Cell*, 61(3), pp. 407–417. doi: 10.1016/0092-8674(90)90523-H.

Breviario, D. *et al.* (1986) 'Carbon source regulation of RAS1 expression in Saccharomyces cerevisiae and the phenotypes of ras2- cells.', *Proceedings of the National Academy of Sciences*, 83(12), pp. 4152–4156. doi: 10.1073/pnas.83.12.4152.

Broach, J. R. (2012) ‘Nutritional Control of Growth and Development in Yeast’, *Genetics*, 192(1), pp. 73–105. doi: 10.1534/genetics.111.135731.

Broek, D. *et al.* (1987) ‘The S. cerevisiae CDC25 gene product regulates the RAS/adenylate cyclase pathway’, *Cell*, 48(5), pp. 789–799. doi: 10.1016/0092-8674(87)90076-6.

Brosnan, J. T. and Brosnan, M. E. (2006) ‘The Sulfur-Containing Amino Acids: An Overview’, *The Journal of Nutrition*, 136(6), pp. 1636S-1640S. doi: 10.1093/jn/136.6.1636S.

Burgess, M. R. *et al.* (2017) ‘KRAS Allelic Imbalance Enhances Fitness and Modulates MAP Kinase Dependence in Cancer’, *Cell*, 168(5), pp. 817-829.e15. doi: 10.1016/j.cell.2017.01.020.

Busti, S. *et al.* (2010) ‘Glucose Signaling-Mediated Coordination of Cell Growth and Cell Cycle in Saccharomyces Cerevisiae’, *Sensors*, 10(6), pp. 6195–6240. doi: 10.3390/s100606195.

Cai, H. *et al.* (2007) ‘Differential Regulation and Substrate Preferences in Two Peptide Transporters of Saccharomyces cerevisiae’, *Eukaryotic Cell*, 6(10), pp. 1805–1813. doi: 10.1128/EC.00257-06.

Cameron, S. *et al.* (1988) ‘cAMP-independent control of sporulation, glycogen metabolism, and heat shock resistance in S. cerevisiae’, *Cell*, 53(4), pp. 555–566. doi: 10.1016/0092-8674(88)90572-7.

Cardenas, M. E. *et al.* (1999) ‘The TOR signaling cascade regulates gene expression in response to nutrients’, *Genes & Development*, 13(24), pp. 3271–3279. doi: 10.1101/gad.13.24.3271.

Casey, P. J. *et al.* (1989) ‘p21ras is modified by a farnesyl isoprenoid.’, *Proceedings of the National Academy of Sciences*, 86(21), pp. 8323–8327. doi: 10.1073/pnas.86.21.8323.

Castrillo, J. I. *et al.* (2007) ‘Growth control of the eukaryote cell: a systems biology study in yeast’, *Journal of Biology*, 6(2), p. 4. doi: 10.1186/jbiol54.

Cazzaniga, P. *et al.* (2008) 'Modeling and stochastic simulation of the Ras/cAMP/PKA pathway in the yeast Saccharomyces cerevisiae evidences a key regulatory function for intracellular guanine nucleotides pools', *Journal of Biotechnology*, 133(3), pp. 377–385. doi: 10.1016/j.jbiotec.2007.09.019.

Cha, P.-H. *et al.* (2016) 'Small-molecule binding of the axin RGS domain promotes β-catenin and Ras degradation', *Nature Chemical Biology*, 12(8), pp. 593–600. doi: 10.1038/nchembio.2103.

Chen, X. *et al.* (2009) 'Endogenous expression of HrasG12V induces developmental defects and neoplasms with copy number imbalances of the oncogene', *Proceedings of the National Academy of Sciences*, 106(19), pp. 7979–7984. doi: 10.1073/pnas.0900343106.

Cho, Y.-H. *et al.* (2016) 'KY1022, a small molecule destabilizing Ras via targeting the Wnt/β-catenin pathway, inhibits development of metastatic colorectal cancer', *Oncotarget*, 7(49), pp. 81727–81740. doi: 10.18632/oncotarget.13172.

Choy, E. *et al.* (1999) 'Endomembrane Trafficking of Ras', *Cell*, 98(1), pp. 69–80. doi: 10.1016/S0092-8674(00)80607-8.

Clark, S. G., McGrath, J. P. and Levinson, A. D. (1985) 'Expression of normal and activated human Ha-ras cDNAs in Saccharomyces cerevisiae', *Molecular and Cellular Biology*, 5(10), pp. 2746–2752. doi: 10.1128/mcb.5.10.2746-2752.1985.

Cobitz, A. R. *et al.* (1989) 'Phosphorylation of RAS1 and RAS2 proteins in Saccharomyces cerevisiae.', *Proceedings of the National Academy of Sciences*, 86(3), pp. 858–862. doi: 10.1073/pnas.86.3.858.

Cohen, P. (2002) 'The origins of protein phosphorylation', *Nature Cell Biology*, 4(5), pp. E127–E130. doi: 10.1038/ncb0502-e127.

Colicelli, J. (2004) 'Human RAS superfamily proteins and related GTPases.', *Science's STKE : signal transduction knowledge environment*, 2004(250). doi:

10.1126/stke.2502004re13.

Collisson, E. A. *et al.* (2012) 'A Central Role for RAF→MEK→ERK Signaling in the Genesis of Pancreatic Ductal Adenocarcinoma', *Cancer Discovery*, 2(8), pp. 685–693. doi: 10.1158/2159-8290.CD-11-0347.

Colombo, S. *et al.* (1998) 'Involvement of distinct G-proteins, Gpa2 and Ras, in glucose- and intracellular acidification-induced cAMP signalling in the yeast Saccharomyces cerevisiae', *EMBO Journal*, 17(12), pp. 3326–3341. doi: 10.1093/emboj/17.12.3326.

Colombo, S. *et al.* (2004) 'Activation State of the Ras2 Protein and Glucose-induced Signaling in Saccharomyces cerevisiae', *Journal of Biological Chemistry*, 279(45), pp. 46715–46722. doi: 10.1074/jbc.M405136200.

Conrad, M. *et al.* (2014) 'Nutrient sensing and signaling in the yeast Saccharomyces cerevisiae', *FEMS Microbiology Reviews*, 38(2), pp. 254–299. doi: 10.1111/1574-6976.12065.

Cox, A. D. *et al.* (2014) 'Drugging the undruggable RAS: Mission Possible?', *Nature Reviews Drug Discovery*, 13(11), pp. 828–851. doi: 10.1038/nrd4389.

Cox, A. D. and Der, C. J. (2010) 'Ras history', *Small GTPases*, 1(1), pp. 2–27. doi: 10.4161/sgtp.1.1.12178.

Cruz-Migoni, A. *et al.* (2019) 'Structure-based development of new RAS-effector inhibitors from a combination of active and inactive RAS-binding compounds', *Proceedings of the National Academy of Sciences*, 116(7), pp. 2545–2550. doi: 10.1073/pnas.1811360116.

Dobrowolski, S., Harter, M. and Stacey, D. W. (1994) 'Cellular ras activity is required for passage through multiple points of the G0/G1 phase in BALB/c 3T3 cells.', *Molecular and Cellular Biology*, 14(8), pp. 5441–5449. doi: 10.1128/MCB.14.8.5441.

Dohlman, H. G. and Campbell, S. L. (2019) 'Regulation of large and small G proteins by ubiquitination', *Journal of Biological Chemistry*, 294(49), pp. 18613–18623. doi:

10.1074/jbc.REV119.011068.

Downward, J. (2003) 'Targeting RAS signalling pathways in cancer therapy', *Nature Reviews Cancer*, 3(1), pp. 11–22. doi: 10.1038/nrc969.

Drebot, M. A. *et al.* (1990) 'Genetic assessment of stationary phase for cells of the yeast Saccharomyces cerevisiae', *Journal of Bacteriology*, 172(7), pp. 3584–3589. doi: 10.1128/jb.172.7.3584-3589.1990.

Du, F. *et al.* (2002) 'Pairs of dipeptides synergistically activate the binding of substrate by ubiquitin ligase through dissociation of its autoinhibitory domain', *Proceedings of the National Academy of Sciences*, 99(22), pp. 14110–14115. doi: 10.1073/pnas.172527399.

Edkins, S. and O'Meara, S. (2006) 'Recurrent KRAS codon 146 mutations in human colorectal cancer', *Cancer Biology & Therapy*, 5(8), pp. 928–932. doi: 10.4161/cbt.5.8.3251.

Van Ende, M., Wijnants, S. and Van Dijck, P. (2019) 'Sugar Sensing and Signaling in Candida albicans and Candida glabrata', *Frontiers in Microbiology*, 10. doi: 10.3389/fmicb.2019.00099.

Englaender, J. A. *et al.* (2017) 'Effect of Genomic Integration Location on Heterologous Protein Expression and Metabolic Engineering in E. coli', *ACS Synthetic Biology*, 6(4), pp. 710–720. doi: 10.1021/acssynbio.6b00350.

Etienne-Manneville, S. and Hall, A. (2002) 'Rho GTPases in cell biology', *Nature*, 420(6916), pp. 629–635. doi: 10.1038/nature01148.

Ewald, J. C. *et al.* (2016) 'The Yeast Cyclin-Dependent Kinase Routes Carbon Fluxes to Fuel Cell Cycle Progression', *Molecular Cell*, 62(4), pp. 532–545. doi: 10.1016/j.molcel.2016.02.017.

Fabrizio, P. *et al.* (2010) 'Genome-Wide Screen in Saccharomyces cerevisiae Identifies Vacuolar Protein Sorting, Autophagy, Biosynthetic, and tRNA Methylation Genes Involved in Life Span Regulation', *PLoS Genetics*. Edited by S. K. Kim, 6(7), p. e1001024. doi:

10.1371/journal.pgen.1001024.

Falcón, A. A. and Aris, J. P. (2003) 'Plasmid Accumulation Reduces Life Span in Saccharomyces cerevisiae', *Journal of Biological Chemistry*, 278(43), pp. 41607–41617. doi: 10.1074/jbc.M307025200.

Finkelstein, J. D. (1990) 'Methionine metabolism in mammals', *The Journal of Nutritional Biochemistry*, 1(5), pp. 228–237. doi: 10.1016/0955-2863(90)90070-2.

Fivaz, M. and Meyer, T. (2005) 'Reversible intracellular translocation of KRas but not HRas in hippocampal neurons regulated by Ca2+/calmodulin', *Journal of Cell Biology*, 170(3), pp. 429–441. doi: 10.1083/jcb.200409157.

Forrester, K. *et al.* (1987) 'Detection of high incidence of K-ras oncogenes during human colon tumorigenesis', *Nature*, 327(6120), pp. 298–303. doi: 10.1038/327298a0.

Foury, F. (1997) 'Human genetic diseases: a cross-talk between man and yeast', *Gene*, 195(1), pp. 1–10. doi: 10.1016/S0378-1119(97)00140-6.

Friddle, R. W. *et al.* (2004) 'Mechanism of DNA Compaction by Yeast Mitochondrial Protein Abf2p', *Biophysical Journal*, 86(3), pp. 1632–1639. doi: 10.1016/S0006-3495(04)74231-9.

Fujita-Yamaguchi, Y. *et al.* (1989) 'In vitro tyrosine phosphorylation studies on RAS proteins and calmodulin suggest that polylysine-like basic peptides or domains may be involved in interactions between insulin receptor kinase and its substrate.', *Proceedings of the National Academy of Sciences*, 86(19), pp. 7306–7310. doi: 10.1073/pnas.86.19.7306.

Fujiyama, A., Matsumoto, K. and Tamanoi, F. (1987) 'A novel yeast mutant defective in the processing of ras proteins: assessment of the effect of the mutation on processing steps.', *The EMBO journal*, 6(1), pp. 223–8. Available at: http://www.ncbi.nlm.nih.gov/pubmed/3556161.

G1 phase called START primarily regulates cell cycle progression (2014) *Scitable by nature*

education. Available at: https://www.nature.com/scitable/topicpage/eukaryotes-and-cell-cycle-14046014/.

Gibbs, J. B. *et al.* (1988) 'Purification of ras GTPase activating protein from bovine brain.', *Proceedings of the National Academy of Sciences*, 85(14), pp. 5026–5030. doi: 10.1073/pnas.85.14.5026.

Goffeau, A. *et al.* (1996) 'Life with 6000 Genes', *Science*, 274(5287), pp. 546–567. doi: 10.1126/science.274.5287.546.

Goldberg, D., Segal, M. and Levitzki, A. (1994) 'Cdc25 is not the signal receiver for glucose induced cAMP response in S. cerevisiae', *FEBS Letters*, 356(2–3), pp. 249–254. doi: 10.1016/0014-5793(94)01273-3.

Goodwin, J. S. *et al.* (2005) 'Depalmitoylated Ras traffics to and from the Golgi complex via a nonvesicular pathway', *Journal of Cell Biology*, 170(2), pp. 261–272. doi: 10.1083/jcb.200502063.

Gourlay, C. W. and Ayscough, K. R. (2006) 'Actin-Induced Hyperactivation of the Ras Signaling Pathway Leads to Apoptosis in Saccharomyces cerevisiae', *Molecular and Cellular Biology*, 26(17), pp. 6487–6501. doi: 10.1128/MCB.00117-06.

Gray, J. V. *et al.* (2004) '"Sleeping Beauty": Quiescence in Saccharomyces cerevisiae', *Microbiology and Molecular Biology Reviews*, 68(2), pp. 187–206. doi: 10.1128/MMBR.68.2.187-206.2004.

Gross, E., Goldberg, D. and Levitzki, A. (1992) 'Phosphorylation of the S. cerevisiae Cdc25 in response to glucose results in its dissociation from Ras', *Nature*, 360(6406), pp. 762–765. doi: 10.1038/360762a0.

Guaragnella, N. *et al.* (2014) 'The expanding role of yeast in cancer research and diagnosis: insights into the function of the oncosuppressors p53 and BRCA1/2', *FEMS Yeast Research*, 14(1), pp. 2–16. doi: 10.1111/1567-1364.12094.

Gysin, S. *et al.* (2011) 'Therapeutic Strategies for Targeting Ras Proteins', *Genes & Cancer*, 2(3), pp. 359–372. doi: 10.1177/1947601911412376.

Hancock, J. F. *et al.* (1989) 'All ras proteins are polyisoprenylated but only some are palmitoylated', *Cell*, 57(7), pp. 1167–1177. doi: 10.1016/0092-8674(89)90054-8.

Hancock, J. F. *et al.* (1991) 'A CAAX or a CAAL motif and a second signal are sufficient for plasma membrane targeting of ras proteins.', *The EMBO journal*, 10(13), pp. 4033–9. Available at: http://www.ncbi.nlm.nih.gov/pubmed/1756714.

Hartwell, L. H. (1974) 'Saccharomyces cerevisiae cell cycle.', *Bacteriological Reviews*, 38(2), pp. 164–198. doi: 10.1128/MMBR.38.2.164-198.1974.

He, B. *et al.* (1991) 'RAM2, an essential gene of yeast, and RAM1 encode the two polypeptide components of the farnesyltransferase that prenylates a-factor and Ras proteins.', *Proceedings of the National Academy of Sciences*, 88(24), pp. 11373–11377. doi: 10.1073/pnas.88.24.11373.

Head, J. and Johnston, S. R. (2004) 'New targets for therapy in breast cancer: Farnesyltransferase inhibitors', *Breast Cancer Research*, 6(6), p. 262. doi: 10.1186/bcr947.

Henis, Y. I., Hancock, J. F. and Prior, I. A. (2009) 'Ras acylation, compartmentalization and signaling nanoclusters (Review)', *Molecular Membrane Biology*, 26(1–2), pp. 80–92. doi: 10.1080/09687680802649582.

Herrmann, C. (2003) 'Ras–effector interactions: after one decade', *Current Opinion in Structural Biology*, 13(1), pp. 122–129. doi: 10.1016/S0959-440X(02)00007-6.

Herskowitz, I. (1988) 'Life cycle of the budding yeast Saccharomyces cerevisiae.', *Microbiological reviews*, 52(4), pp. 536–53. doi: 10.1128/mr.52.4.536-553.1988.

Hlavata, L. (2003) 'The oncogenic RAS2val19 mutation locks respiration, independently of PKA, in a mode prone to generate ROS', *The EMBO Journal*, 22(13), pp. 3337–3345. doi: 10.1093/emboj/cdg314.

Hlavatá, L. *et al.* (2008) 'Elevated Ras/protein kinase A activity in Saccharomyces cerevisiae reduces proliferation rate and lifespan by two different reactive oxygen species-dependent routes', *Aging Cell*, 7(2), pp. 148–157. doi: 10.1111/j.1474-9726.2007.00361.x.

Homann, O. R. *et al.* (2005) 'Harnessing Natural Diversity to Probe Metabolic Pathways', *PLoS Genetics*. Edited by S. Dutcher, 1(6), p. e80. doi: 10.1371/journal.pgen.0010080.

Island, M. D., Naider, F. and Becker, J. M. (1987) 'Regulation of dipeptide transport in Saccharomyces cerevisiae by micromolar amino acid concentrations', *Journal of Bacteriology*, 169(5), pp. 2132–2136. doi: 10.1128/jb.169.5.2132-2136.1987.

Jacquet, E. *et al.* (1994) 'Properties of the Catalytic Domain of CDC25, a Saccharomyces cerevisiae GDP/GTP Exchange Factor: Comparison of Its Activity on Full-Length and C-Terminal Truncated RAS2 Proteins', *Biochemical and Biophysical Research Communications*, 199(2), pp. 497–503. doi: 10.1006/bbrc.1994.1256.

Jeong, W.-J., Ro, E. J. and Choi, K.-Y. (2018) 'Interaction between Wnt/β-catenin and RAS-ERK pathways and an anti-cancer strategy via degradations of β-catenin and RAS by targeting the Wnt/β-catenin pathway', *npj Precision Oncology*, 2(1), p. 5. doi: 10.1038/s41698-018-0049-y.

Jian, D. *et al.* (2010) 'Feedback regulation of Ras2 guanine nucleotide exchange factor (Ras2-GEF) activity of Cdc25p by Cdc25p phosphorylation in the yeast Saccharomyces cerevisiae', *FEBS Letters*, 584(23), pp. 4745–4750. doi: 10.1016/j.febslet.2010.11.006.

Jin, X. *et al.* (2016) 'Nitrogen Starvation-induced Phosphorylation of Ras1 Protein and Its Potential Role in Nutrient Signaling and Stress Response', *Journal of Biological Chemistry*, 291(31), pp. 16231–16239. doi: 10.1074/jbc.M115.713206.

Johnson, D. C. *et al.* (2005) 'STRUCTURE, FUNCTION, AND FORMATION OF BIOLOGICAL IRON-SULFUR CLUSTERS', *Annual Review of Biochemistry*, 74(1), pp. 247–281. doi: 10.1146/annurev.biochem.74.082803.133518.

Jones, S., Vignais, M. L. and Broach, J. R. (1991) 'The CDC25 protein of Saccharomyces cerevisiae promotes exchange of guanine nucleotides bound to ras', *Molecular and Cellular Biology*, 11(5), pp. 2641–2646. doi: 10.1128/mcb.11.5.2641-2646.1991.

Jorgensen, P. (2002) 'Systematic Identification of Pathways That Couple Cell Growth and Division in Yeast', *Science*, 297(5580), pp. 395–400. doi: 10.1126/science.1070850.

Junttila, M. R. *et al.* (2010) 'Selective activation of p53-mediated tumour suppression in high-grade tumours', *Nature*, 468(7323), pp. 567–571. doi: 10.1038/nature09526.

Kaiser, P. (2020) 'Methionine Dependence of Cancer', *Biomolecules*, 10(4), p. 568. doi: 10.3390/biom10040568.

Kataoka, T. *et al.* (1984) 'Genetic analysis of yeast RAS1 and RAS2 genes', *Cell*, 37(2), pp. 437–445. doi: 10.1016/0092-8674(84)90374-X.

Kelliher, C. M. *et al.* (2018) 'Layers of regulation of cell-cycle gene expression in the budding yeast Saccharomyces cerevisiae', *Molecular Biology of the Cell*. Edited by M. J. Solomon, 29(22), pp. 2644–2655. doi: 10.1091/mbc.E18-04-0255.

Kerr, E. M. *et al.* (2016) 'Mutant Kras copy number defines metabolic reprogramming and therapeutic susceptibilities', *Nature*, 531(7592), pp. 110–113. doi: 10.1038/nature16967.

Kim, S.-E. *et al.* (2009) 'H-Ras is degraded by Wnt/β-catenin signaling via β-TrCP-mediated polyubiquitylation', *Journal of Cell Science*, 122(6), pp. 842–848. doi: 10.1242/jcs.040493.

Kingsbury, J. M., Sen, N. D. and Cardenas, M. E. (2015) 'Branched-Chain Aminotransferases Control TORC1 Signaling in Saccharomyces cerevisiae', *PLOS Genetics*. Edited by G. P. Copenhaver, 11(12), p. e1005714. doi: 10.1371/journal.pgen.1005714.

Kodaz, H. (2017) 'Frequency of RAS Mutations (KRAS, NRAS, HRAS) in Human Solid Cancer', *Eurasian Journal of Medicine and Oncology*. doi: 10.14744/ejmo.2017.22931.

KOLCH, W. (2000) 'Meaningful relationships: the regulation of the Ras/Raf/MEK/ERK pathway by protein interactions', *Biochemical Journal*, 351(2), pp. 289–305. doi:

10.1042/bj3510289.

Komander, D. and Rape, M. (2012) 'The Ubiquitin Code', *Annual Review of Biochemistry*, 81(1), pp. 203–229. doi: 10.1146/annurev-biochem-060310-170328.

Kraakman, L. *et al.* (1999) 'A Saccharomyces cerevisiae G-protein coupled receptor, Gpr1, is specifically required for glucose activation of the cAMP pathway during the transition to growth on glucose', *Molecular Microbiology*, 32(5), pp. 1002–1012. doi: 10.1046/j.1365-2958.1999.01413.x.

Kramer, K. *et al.* (2003) 'Isoprenylcysteine Carboxyl Methyltransferase Activity Modulates Endothelial Cell Apoptosis', *Molecular Biology of the Cell*. Edited by G. Guidotti, 14(3), pp. 848–857. doi: 10.1091/mbc.e02-07-0390.

Laude, A. J. and Prior, I. A. (2008) 'Palmitoylation and localisation of RAS isoforms are modulated by the hypervariable linker domain', *Journal of Cell Science*, 121(4), pp. 421–427. doi: 10.1242/jcs.020107.

Laurent, J. M. *et al.* (2016) 'Efforts to make and apply humanized yeast', *Briefings in Functional Genomics*, 15(2), pp. 155–163. doi: 10.1093/bfgp/elv041.

Leadsham, J. E. *et al.* (2009) 'Whi2p links nutritional sensing to actin-dependent Ras-cAMP-PKA regulation and apoptosis in yeast', *Journal of Cell Science*, 122(5), pp. 706–715. doi: 10.1242/jcs.042424.

Leadsham, J. E. and Gourlay, C. W. (2010) 'cAMP/PKA signaling balances respiratory activity with mitochondria dependent apoptosis via transcriptional regulation', *BMC Cell Biology*, 11(1), p. 92. doi: 10.1186/1471-2121-11-92.

Lemaire, K. *et al.* (2004) 'Glucose and Sucrose Act as Agonist and Mannose as Antagonist Ligands of the G Protein-Coupled Receptor Gpr1 in the Yeast Saccharomyces cerevisiae', *Molecular Cell*, 16(2), pp. 293–299. doi: 10.1016/j.molcel.2004.10.004.

Li, H.-Y., Cao, K. and Zheng, Y. (2003) 'Ran in the spindle checkpoint: a new function for a

versatile GTPase', *Trends in Cell Biology*, 13(11), pp. 553–557. doi: 10.1016/j.tcb.2003.09.003.

Li, Q. *et al.* (2011) 'Hematopoiesis and leukemogenesis in mice expressing oncogenic NrasG12D from the endogenous locus', *Blood*, 117(6), pp. 2022–2032. doi: 10.1182/blood-2010-04-280750.

Lill, R. *et al.* (1999) 'The Essential Role of Mitochondria in the Biogenesis of Cellular Iron-Sulfur Proteins', *Biological Chemistry*, 380(10). doi: 10.1515/BC.1999.147.

Lill, R. (2009) 'Function and biogenesis of iron–sulphur proteins', *Nature*, 460(7257), pp. 831–838. doi: 10.1038/nature08301.

Lito, P. *et al.* (2012) 'Relief of Profound Feedback Inhibition of Mitogenic Signaling by RAF Inhibitors Attenuates Their Activity in BRAFV600E Melanomas', *Cancer Cell*, 22(5), pp. 668–682. doi: 10.1016/j.ccr.2012.10.009.

Liu, W. N., Yan, M. and Chan, A. M. (2017) 'A thirty-year quest for a role of R-Ras in cancer: from an oncogene to a multitasking GTPase', *Cancer Letters*, 403, pp. 59–65. doi: 10.1016/j.canlet.2017.06.003.

Liu, X. *et al.* (2015) 'Reliable cell cycle commitment in budding yeast is ensured by signal integration', *eLife*, 4. doi: 10.7554/eLife.03977.

Lu, A. *et al.* (2009) 'A clathrin-dependent pathway leads to KRas signaling on late endosomes en route to lysosomes', *Journal of Cell Biology*, 184(6), pp. 863–879. doi: 10.1083/jcb.200807186.

Lynch, S. J. *et al.* (2015) 'The Differential Palmitoylation States of N-Ras and H-Ras Determine Their Distinct Golgi Subcompartment Localizations', *Journal of Cellular Physiology*, 230(3), pp. 610–619. doi: 10.1002/jcp.24779.

Madrid, M. *et al.* (2016) 'Multiple crosstalk between TOR and the cell integrity MAPK signaling pathway in fission yeast', *Scientific Reports*, 6(1), p. 37515. doi:

10.1038/srep37515.

Marshall, M. S. *et al.* (1987) 'Regulatory function of the Saccharomyces cerevisiae RAS C-terminus.', *Molecular and Cellular Biology*, 7(7), pp. 2309–2315. doi: 10.1128/MCB.7.7.2309.

Martinelli, E. *et al.* (2009) 'Anti-epidermal growth factor receptor monoclonal antibodies in cancer therapy', *Clinical & Experimental Immunology*, 158(1), pp. 1–9. doi: 10.1111/j.1365-2249.2009.03992.x.

Maurer, T. *et al.* (2012) 'Small-molecule ligands bind to a distinct pocket in Ras and inhibit SOS-mediated nucleotide exchange activity', *Proceedings of the National Academy of Sciences*, 109(14), pp. 5299–5304. doi: 10.1073/pnas.1116510109.

Memon, A. R. (2004) 'The role of ADP-ribosylation factor and SAR1 in vesicular trafficking in plants', *Biochimica et Biophysica Acta (BBA) - Biomembranes*, 1664(1), pp. 9–30. doi: 10.1016/j.bbamem.2004.04.005.

Milburn, M. V. *et al.* (1990) 'Molecular switch for signal transduction: Structural differences between active and inactive forms of protooncogenic ras proteins', *Science*, 247(4945), pp. 939–945. doi: 10.1126/science.2406906.

Mitchell, D. A. *et al.* (2012) 'The Erf4 Subunit of the Yeast Ras Palmitoyl Acyltransferase Is Required for Stability of the Acyl-Erf2 Intermediate and Palmitoyl Transfer to a Ras2 Substrate', *Journal of Biological Chemistry*, 287(41), pp. 34337–34348. doi: 10.1074/jbc.M112.379297.

Mitsuzawa, H. (1994) 'Increases in cell size at START caused by hyperactivation of the cAMP pathway in Saccharomyces cerevisiae', *Molecular and General Genetics MGG*, 243(2), pp. 158–165. doi: 10.1007/BF00280312.

Mizunuma, M. *et al.* (2013) 'Ras/cAMP-dependent Protein Kinase (PKA) Regulates Multiple Aspects of Cellular Events by Phosphorylating the Whi3 Cell Cycle Regulator in Budding

Yeast', *Journal of Biological Chemistry*, 288(15), pp. 10558–10566. doi: 10.1074/jbc.M112.402214.

Modrek, B. *et al.* (2009) 'Oncogenic Activating Mutations Are Associated with Local Copy Gain', *Molecular Cancer Research*, 7(8), pp. 1244–1252. doi: 10.1158/1541-7786.MCR-08-0532.

Mohammadi, S. *et al.* (2015) 'Scope and limitations of yeast as a model organism for studying human tissue-specific pathways', *BMC Systems Biology*. BMC Systems Biology, 9(1). doi: 10.1186/s12918-015-0253-0.

Mulcahy, L. S., Smith, M. R. and Stacey, D. W. (1985) 'Requirement for ras proto-oncogene function during serum-stimulated growth of NIH 3T3 cells', *Nature*, 313(5999), pp. 241–243. doi: 10.1038/313241a0.

Munirajan, A. K. *et al.* (1998) 'Detection of a rare point mutation at codon 59 and relatively high incidence of H-ras mutation in Indian oral cancer.', *International Journal of Oncology*. doi: 10.3892/ijo.13.5.971.

Murray, D. B., Beckmann, M. and Kitano, H. (2007) 'Regulation of yeast oscillatory dynamics', *Proceedings of the National Academy of Sciences*, 104(7), pp. 2241–2246. doi: 10.1073/pnas.0606677104.

Murugan, A. K. *et al.* (2009) 'Detection of two novel mutations and relatively high incidence of H-RAS mutations in Vietnamese oral cancer', *Oral Oncology*, 45(10), pp. e161–e166. doi: 10.1016/j.oraloncology.2009.05.638.

Murugan, A. K., Grieco, M. and Tsuchida, N. (2019) 'RAS mutations in human cancers: Roles in precision medicine', *Seminars in Cancer Biology*, 59, pp. 23–35. doi: 10.1016/j.semcancer.2019.06.007.

Nabet, B. *et al.* (2018) 'The dTAG system for immediate and target-specific protein degradation', *Nature Chemical Biology*, 14(5), pp. 431–441. doi: 10.1038/s41589-018-0021-

Nakafuku, M. *et al.* (1988) ‘Isolation of a second yeast Saccharomyces cerevisiae gene (GPA2) coding for guanine nucleotide-binding regulatory protein: studies on its structure and possible functions.’, *Proceedings of the National Academy of Sciences*, 85(5), pp. 1374–1378. doi: 10.1073/pnas.85.5.1374.

Nie, Z., Hirsch, D. S. and Randazzo, P. A. (2003) ‘Arf and its many interactors’, *Current Opinion in Cell Biology*, 15(4), pp. 396–404. doi: 10.1016/S0955-0674(03)00071-1.

Nikawa, J., Sass, P. and Wigler, M. (1987) ‘Cloning and characterization of the low-affinity cyclic AMP phosphodiesterase gene of Saccharomyces cerevisiae.’, *Molecular and Cellular Biology*, 7(10), pp. 3629–3636. doi: 10.1128/MCB.7.10.3629.

Normanno, N. *et al.* (2009) ‘Implications for KRAS status and EGFR-targeted therapies in metastatic CRC’, *Nature Reviews Clinical Oncology*, 6(9), pp. 519–527. doi: 10.1038/nrclinonc.2009.111.

Obata, F. and Miura, M. (2015) ‘Enhancing S-adenosyl-methionine catabolism extends Drosophila lifespan’, *Nature Communications*, 6(1), p. 8332. doi: 10.1038/ncomms9332.

Ogawa, T. *et al.* (2016) ‘Stimulating S -adenosyl-l-methionine synthesis extends lifespan via activation of AMPK’, *Proceedings of the National Academy of Sciences*, 113(42), pp. 11913–11918. doi: 10.1073/pnas.1604047113.

Olofsson, B. (1999) ‘Rho Guanine Dissociation Inhibitors’, *Cellular Signalling*, 11(8), pp. 545–554. doi: 10.1016/S0898-6568(98)00063-1.

Ostrem, J. M. *et al.* (2013) ‘K-Ras(G12C) inhibitors allosterically control GTP affinity and effector interactions’, *Nature*, 503(7477), pp. 548–551. doi: 10.1038/nature12796.

Ostrem, J. M. L. and Shokat, K. M. (2016) ‘Direct small-molecule inhibitors of KRAS: from structural insights to mechanism-based design’, *Nature Reviews Drug Discovery*, 15(11), pp. 771–785. doi: 10.1038/nrd.2016.139.

Palm, W. and Thompson, C. B. (2017) ‘Nutrient acquisition strategies of mammalian cells’, *Nature*, 546(7657), pp. 234–242. doi: 10.1038/nature22379.

Papageorge, A. G. *et al.* (1984) ‘Saccharomyces cerevisiae synthesizes proteins related to the p21 gene product of ras genes found in mammals.’, *Molecular and Cellular Biology*, 4(1), pp. 23–29. doi: 10.1128/MCB.4.1.23.

Peeters, K. *et al.* (2017) ‘Fructose-1,6-bisphosphate couples glycolytic flux to activation of Ras’, *Nature Communications*, 8(1), p. 922. doi: 10.1038/s41467-017-01019-z.

Pereira-Leal, J. B. and Seabra, M. C. (2001) ‘Evolution of the rab family of small GTP-binding proteins’, *Journal of Molecular Biology*, 313(4), pp. 889–901. doi: 10.1006/jmbi.2001.5072.

Pereira, C., Bessa, C., *et al.* (2012) ‘Contribution of Yeast Models to Neurodegeneration Research’, *Journal of Biomedicine and Biotechnology*, 2012, pp. 1–12. doi: 10.1155/2012/941232.

Pereira, C., Coutinho, I., *et al.* (2012) ‘New insights into cancer-related proteins provided by the yeast model’, *FEBS Journal*, 279(5), pp. 697–712. doi: 10.1111/j.1742-4658.2012.08477.x.

Perry, J. R. *et al.* (1994) ‘Isolation and characterization of a Saccharomyces cerevisiae peptide transport gene’, *Molecular and Cellular Biology*, 14(1), pp. 104–115. doi: 10.1128/mcb.14.1.104-115.1994.

Petranovic, D. *et al.* (2010) ‘Prospects of yeast systems biology for human health: integrating lipid, protein and energy metabolism’, *FEMS Yeast Research*, 10(8), pp. 1046–1059. doi: 10.1111/j.1567-1364.2010.00689.x.

Phan, V. T. *et al.* (2010) ‘The RasGAP Proteins Ira2 and Neurofibromin Are Negatively Regulated by Gpb1 in Yeast and ETEA in Humans’, *Molecular and Cellular Biology*, 30(9), pp. 2264–2279. doi: 10.1128/MCB.01450-08.

Philpott, C. C. and Protchenko, O. (2008) ‘Response to Iron Deprivation in Saccharomyces cerevisiae’, *Eukaryotic Cell*, 7(1), pp. 20–27. doi: 10.1128/EC.00354-07.

Pickart, C. M. and Eddins, M. J. (2004) ‘Ubiquitin: structures, functions, mechanisms’, *Biochimica et Biophysica Acta (BBA) - Molecular Cell Research*, 1695(1–3), pp. 55–72. doi: 10.1016/j.bbamcr.2004.09.019.

Piper-brown, E. (2019) ‘Kent Academic Repository PhD in Cell Biology’.

Powers, S. *et al.* (1984) ‘Genes in S. cerevisiae encoding proteins with domains homologous to the mammalian ras proteins’, *Cell*, 36(3), pp. 607–612. doi: 10.1016/0092-8674(84)90340-4.

Pratyusha, V. A. *et al.* (2018) ‘Ras hyperactivation versus overexpression: Lessons from Ras dynamics in Candida albicans’, *Scientific Reports*, 8(1), p. 5248. doi: 10.1038/s41598-018-23187-8.

Prior, I. A. and Hancock, J. F. (2012) ‘Ras trafficking, localization and compartmentalized signalling’, *Seminars in Cell & Developmental Biology*, 23(2), pp. 145–153. doi: 10.1016/j.semcdb.2011.09.002.

Prior, I. A., Lewis, P. D. and Mattos, C. (2012) ‘A Comprehensive Survey of Ras Mutations in Cancer’, *Cancer Research*, 72(10), pp. 2457–2467. doi: 10.1158/0008-5472.CAN-11-2612.

Puig, S., Askeland, E. and Thiele, D. J. (2005) ‘Coordinated Remodeling of Cellular Metabolism during Iron Deficiency through Targeted mRNA Degradation’, *Cell*, 120(1), pp. 99–110. doi: 10.1016/j.cell.2004.11.032.

Qiu, Y. *et al.* (2021) ‘Targeting RAS phosphorylation in cancer therapy: Mechanisms and modulators’, *Acta Pharmaceutica Sinica B*. doi: 10.1016/j.apsb.2021.02.014.

Quevedo, C. E. *et al.* (2018) ‘Small molecule inhibitors of RAS-effector protein interactions derived using an intracellular antibody fragment’, *Nature Communications*, 9(1), p. 3169.

doi: 10.1038/s41467-018-05707-2.

Rak, A. (2003) ‘Structure of Rab GDP-Dissociation Inhibitor in Complex with Prenylated YPT1 GTPase’, *Science*, 302(5645), pp. 646–650. doi: 10.1126/science.1087761.

Rasheed, S., Gardner, M. B. and Huebner, R. J. (1978) ‘In vitro isolation of stable rat sarcoma viruses’, *Proceedings of the National Academy of Sciences*, 75(6), pp. 2972–2976. doi: 10.1073/pnas.75.6.2972.

Rebsamen, M. *et al.* (2015) ‘SLC38A9 is a component of the lysosomal amino acid sensing machinery that controls mTORC1’, *Nature*, 519(7544), pp. 477–481. doi: 10.1038/nature14107.

Reinders, A. *et al.* (1998) ‘Saccharomyces cerevisiae cAMP-dependent protein kinase controls entry into stationary phase through the Rim15p protein kinase’, *Genes & Development*, 12(18), pp. 2943–2955. doi: 10.1101/gad.12.18.2943.

Relógio, A. *et al.* (2014) ‘Ras-Mediated Deregulation of the Circadian Clock in Cancer’, *PLoS Genetics*. Edited by F. Levi, 10(5), p. e1004338. doi: 10.1371/journal.pgen.1004338.

Ridley, A. J. (2001) ‘Rho GTPases and cell migration.’, *Journal of cell science*, 114(Pt 15), pp. 2713–22. Available at: http://www.ncbi.nlm.nih.gov/pubmed/11683406.

Robinson, L. *et al.* (1987) ‘CDC25: a component of the RAS-adenylate cyclase pathway in Saccharomyces cerevisiae’, *Science*, 235(4793), pp. 1218–1221. doi: 10.1126/science.3547648.

Rocks, O. (2005) ‘An Acylation Cycle Regulates Localization and Activity of Palmitoylated Ras Isoforms’, *Science*, 307(5716), pp. 1746–1752. doi: 10.1126/science.1105654.

Rocks, O. *et al.* (2010) ‘The Palmitoylation Machinery Is a Spatially Organizing System for Peripheral Membrane Proteins’, *Cell*, 141(3), pp. 458–471. doi: 10.1016/j.cell.2010.04.007.

Rodenhuis, S. *et al.* (1987) ‘Mutational Activation of the K- ras Oncogene’, *New England Journal of Medicine*, 317(15), pp. 929–935. doi: 10.1056/NEJM198710083171504.

Rodriguez-Viciana, P., Sabatier, C. and McCormick, F. (2004) 'Signaling Specificity by Ras Family GTPases Is Determined by the Full Spectrum of Effectors They Regulate', *Molecular and Cellular Biology*, 24(11), pp. 4943–4954. doi: 10.1128/MCB.24.11.4943-4954.2004.

Rolland, F. *et al.* (2000) 'Glucose-induced cAMP signalling in yeast requires both a G-protein coupled receptor system for extracellular glucose detection and a separable hexose kinase-dependent sensing process', *Molecular Microbiology*, 38(2), pp. 348–358. doi: 10.1046/j.1365-2958.2000.02125.x.

Roos-Mattjus, P. and Sistonen, L. (2004) 'The ubiquitin-proteasome pathway', *Annals of Medicine*, 36(4), pp. 285–295. doi: 10.1080/07853890310016324.

Röth, S. *et al.* (2020) 'Targeting Endogenous K-RAS for Degradation through the Affinity-Directed Protein Missile System', *Cell Chemical Biology*, 27(9), pp. 1151-1163.e6. doi: 10.1016/j.chembiol.2020.06.012.

Röth, S., Fulcher, L. J. and Sapkota, G. P. (2019) 'Advances in targeted degradation of endogenous proteins', *Cellular and Molecular Life Sciences*, 76(14), pp. 2761–2777. doi: 10.1007/s00018-019-03112-6.

Roy, S. *et al.* (2005) 'Individual Palmitoyl Residues Serve Distinct Roles in H-Ras Trafficking, Microlocalization, and Signaling', *Molecular and Cellular Biology*, 25(15), pp. 6722–6733. doi: 10.1128/MCB.25.15.6722-6733.2005.

Rubio-Texeira, M. *et al.* (2010) 'Saccharomyces cerevisiae plasma membrane nutrient sensors and their role in PKA signaling', *FEMS Yeast Research*, 10(2), pp. 134–149. doi: 10.1111/j.1567-1364.2009.00587.x.

Russell, J. J. *et al.* (2017) *Non-model model organisms*, *BMC Biology*. BMC Biology. doi: 10.1186/s12915-017-0391-5.

Santangelo, G. M. (2006) 'Glucose Signaling in Saccharomyces cerevisiae', *Microbiology and Molecular Biology Reviews*, 70(1), pp. 253–282. doi: 10.1128/MMBR.70.1.253-

282.2006.

Sass, P. *et al.* (1986) ‘Cloning and characterization of the high-affinity cAMP phosphodiesterase of Saccharomyces cerevisiae.’, *Proceedings of the National Academy of Sciences*, 83(24), pp. 9303–9307. doi: 10.1073/pnas.83.24.9303.

Scheffzek, K. *et al.* (1996) ‘Crystal structure of the GTPase-activating domain of human p120GAP and implications for the interaction with Ras’, *Nature*, 384(6609), pp. 591–596. doi: 10.1038/384591a0.

Scheffzek, K. (1997) ‘The Ras-RasGAP Complex: Structural Basis for GTPase Activation and Its Loss in Oncogenic Ras Mutants’, *Science*, 277(5324), pp. 333–338. doi: 10.1126/science.277.5324.333.

Scheid, M. P. and Woodgett, J. R. (2001) ‘Phosphatidylinositol 3′ Kinase Signaling in Mammary Tumorigenesis’, *Journal of Mammary Gland Biology and Neoplasia*, 6, pp. 83–99. doi: 10.1023/A:1009520616247.

Schlichting, I. *et al.* (1990) ‘Time-resolved X-ray crystallographic study of the conformational change in Ha-Ras p21 protein on GTP hydrolysis’, *Nature*, 345(6273), pp. 309–315. doi: 10.1038/345309a0.

Schmick, M. *et al.* (2014) ‘KRas Localizes to the Plasma Membrane by Spatial Cycles of Solubilization, Trapping and Vesicular Transport’, *Cell*, 157(2), pp. 459–471. doi: 10.1016/j.cell.2014.02.051.

Schmidt, W. K. *et al.* (1998) ‘Endoplasmic reticulum membrane localization of Rce1p and Ste24p, yeast proteases involved in carboxyl-terminal CAAX protein processing and amino-terminal a-factor cleavage’, *Proceedings of the National Academy of Sciences*, 95(19), pp. 11175–11180. doi: 10.1073/pnas.95.19.11175.

Schneper, L. *et al.* (2004) ‘The Ras/Protein Kinase A Pathway Acts in Parallel with the Mob2/Cbk1 Pathway To Effect Cell Cycle Progression and Proper Bud Site Selection’,

Eukaryotic Cell, 3(1), pp. 108–120. doi: 10.1128/EC.3.1.108-120.2004.

Schomerus, C., Munder, T. and Küntzel, H. (1990) 'Site-directed mutagenesis of the Saccharomyces cerevisiae CDC25 gene: effects on mitotic growth and cAMP signalling', *Molecular and General Genetics MGG*, 223(3), pp. 426–432. doi: 10.1007/BF00264449.

Schosserer, M. *et al.* (2015) 'Methylation of ribosomal RNA by NSUN5 is a conserved mechanism modulating organismal lifespan', *Nature Communications*, 6(1), p. 6158. doi: 10.1038/ncomms7158.

Schulze, W. X., Deng, L. and Mann, M. (2005) 'Phosphotyrosine interactome of the ErbB-receptor kinase family', *Molecular Systems Biology*, 1(1). doi: 10.1038/msb4100012.

Seabra, M. C. and Wasmeier, C. (2004) 'Controlling the location and activation of Rab GTPases', *Current Opinion in Cell Biology*, 16(4), pp. 451–457. doi: 10.1016/j.ceb.2004.06.014.

Shakoury-Elizeh, M. *et al.* (2004) 'Transcriptional Remodeling in Response to Iron Deprivation in Saccharomyces cerevisiae', *Molecular Biology of the Cell*, 15(3), pp. 1233–1243. doi: 10.1091/mbc.e03-09-0642.

Shamji, A. F., Kuruvilla, F. G. and Schreiber, S. L. (2000) 'Partitioning the transcriptional program induced by rapamycin among the effectors of the Tor proteins', *Current Biology*, 10(24), pp. 1574–1581. doi: 10.1016/S0960-9822(00)00866-6.

Sharifpoor, S. *et al.* (2011) 'A quantitative literature-curated gold standard for kinase-substrate pairs', *Genome Biology*, 12(4), p. R39. doi: 10.1186/gb-2011-12-4-r39.

Sharma, A. K. *et al.* (2010) 'Cytosolic Iron-Sulfur Cluster Assembly (CIA) System: Factors, Mechanism, and Relevance to Cellular Iron Regulation', *Journal of Biological Chemistry*, 285(35), pp. 26745–26751. doi: 10.1074/jbc.R110.122218.

Shi, R. *et al.* (2021) 'Biogenesis of Iron–Sulfur Clusters and Their Role in DNA Metabolism', *Frontiers in Cell and Developmental Biology*, 9. doi:

10.3389/fcell.2021.735678.

Smets, B. *et al.* (2010) 'Life in the midst of scarcity: adaptations to nutrient availability in Saccharomyces cerevisiae', *Current Genetics*, 56(1), pp. 1–32. doi: 10.1007/s00294-009-0287-1.

Sobering, A. K. *et al.* (2003) 'A Novel Ras Inhibitor, Eri1, Engages Yeast Ras at the Endoplasmic Reticulum', *Molecular and Cellular Biology*, 23(14), pp. 4983–4990. doi: 10.1128/MCB.23.14.4983-4990.2003.

Sobering, A. K. *et al.* (2004) 'Yeast Ras Regulates the Complex that Catalyzes the First Step in GPI-Anchor Biosynthesis at the ER', *Cell*, 117(5), pp. 637–648. doi: 10.1016/j.cell.2004.05.003.

Soh, J. *et al.* (2009) 'Oncogene Mutations, Copy Number Gains and Mutant Allele Specific Imbalance (MASI) Frequently Occur Together in Tumor Cells', *PLoS ONE*. Edited by I. O.-L. Ng, 4(10), p. e7464. doi: 10.1371/journal.pone.0007464.

Song, S.-P. *et al.* (2013) 'Ras palmitoylation is necessary for N-Ras activation and signal propagation in growth factor signalling', *Biochemical Journal*, 454(2), pp. 323–332. doi: 10.1042/BJ20121799.

Spellman, P. T. *et al.* (1998) 'Comprehensive Identification of Cell Cycle–regulated Genes of the Yeast Saccharomyces cerevisiae by Microarray Hybridization', *Molecular Biology of the Cell*. Edited by G. R. Fink, 9(12), pp. 3273–3297. doi: 10.1091/mbc.9.12.3273.

Stehling, O. *et al.* (2012) 'MMS19 Assembles Iron-Sulfur Proteins Required for DNA Metabolism and Genomic Integrity', *Science*, 337(6091), pp. 195–199. doi: 10.1126/science.1219723.

Stehling, O. *et al.* (2013) 'Human CIA2A-FAM96A and CIA2B-FAM96B Integrate Iron Homeostasis and Maturation of Different Subsets of Cytosolic-Nuclear Iron-Sulfur Proteins', *Cell Metabolism*, 18(2), pp. 187–198. doi: 10.1016/j.cmet.2013.06.015.

Stehling, O. and Lill, R. (2013) ‘The Role of Mitochondria in Cellular Iron-Sulfur Protein Biogenesis: Mechanisms, Connected Processes, and Diseases’, *Cold Spring Harbor Perspectives in Biology*, 5(8), pp. a011312–a011312. doi: 10.1101/cshperspect.a011312.

Stephen, A. G. *et al.* (2014) ‘Dragging Ras Back in the Ring’, *Cancer Cell*, 25(3), pp. 272–281. doi: 10.1016/j.ccr.2014.02.017.

Steyfkens, F. *et al.* (2018) ‘Multiple Transceptors for Macro- and Micro-Nutrients Control Diverse Cellular Properties Through the PKA Pathway in Yeast: A Paradigm for the Rapidly Expanding World of Eukaryotic Nutrient Transceptors Up to Those in Human Cells’, *Frontiers in Pharmacology*, 9. doi: 10.3389/fphar.2018.00191.

Stigter, D. (2004) ‘Packaging of single DNA molecules by the yeast mitochondrial protein Abf2p: reinterpretation of recent single molecule experiments’, *Biophysical Chemistry*, 110(1–2), pp. 171–178. doi: 10.1016/j.bpc.2004.01.012.

Stolze, B. *et al.* (2015) ‘Comparative analysis of KRAS codon 12, 13, 18, 61 and 117 mutations using human MCF10A isogenic cell lines’, *Scientific Reports*, 5(1), p. 8535. doi: 10.1038/srep08535.

Stracka, D. *et al.* (2014) ‘Nitrogen Source Activates TOR (Target of Rapamycin) Complex 1 via Glutamine and Independently of Gtr/Rag Proteins’, *Journal of Biological Chemistry*, 289(36), pp. 25010–25020. doi: 10.1074/jbc.M114.574335.

Sung, P. J. *et al.* (2013) ‘Phosphorylated K-Ras limits cell survival by blocking Bcl-xL sensitization of inositol trisphosphate receptors’, *Proceedings of the National Academy of Sciences*, 110(51), pp. 20593–20598. doi: 10.1073/pnas.1306431110.

Tanaka, K *et al.* (1990) ‘IRA2, a second gene of Saccharomyces cerevisiae that encodes a protein with a domain homologous to mammalian ras GTPase-activating protein.’, *Molecular and Cellular Biology*, 10(8), pp. 4303–4313. doi: 10.1128/MCB.10.8.4303.

Tanaka, Kazuma *et al.* (1990) ‘S. cerevisiae genes IRA1 and IRA2 encode proteins that may

be functionally equivalent to mammalian ras GTPase activating protein', *Cell*, 60(5), pp. 803–807. doi: 10.1016/0092-8674(90)90094-U.

Tanaka, K., Matsumoto, K. and Toh-E, A. (1989) 'IRA1, an inhibitory regulator of the RAS-cyclic AMP pathway in Saccharomyces cerevisiae.', *Molecular and Cellular Biology*, 9(2), pp. 757–768. doi: 10.1128/MCB.9.2.757.

Tate, J. J. *et al.* (2009) 'Rapamycin-induced Gln3 Dephosphorylation Is Insufficient for Nuclear Localization', *Journal of Biological Chemistry*, 284(4), pp. 2522–2534. doi: 10.1074/jbc.M806162200.

Tate, J. J. *et al.* (2010) 'Distinct Phosphatase Requirements and GATA Factor Responses to Nitrogen Catabolite Repression and Rapamycin Treatment in Saccharomyces cerevisiae', *Journal of Biological Chemistry*, 285(23), pp. 17880–17895. doi: 10.1074/jbc.M109.085712.

Tate, J. J. and Cooper, T. G. (2003) 'Tor1/2 Regulation of Retrograde Gene Expression in Saccharomyces cerevisiae Derives Indirectly as a Consequence of Alterations in Ammonia Metabolism', *Journal of Biological Chemistry*, 278(38), pp. 36924–36933. doi: 10.1074/jbc.M301829200.

Tenreiro, S. *et al.* (2013) 'Harnessing the power of yeast to unravel the molecular basis of neurodegeneration', *Journal of Neurochemistry*, 127(4), pp. 438–452. doi: 10.1111/jnc.12271.

Thevelein, J. M. *et al.* (2000) 'Nutrient-induced signal transduction through the protein kinase A pathway and its role in the control of metabolism, stress resistance, and growth in yeast', *Enzyme and Microbial Technology*, 26(9–10), pp. 819–825. doi: 10.1016/S0141-0229(00)00177-0.

Thevelein, J. M. and de Winde, J. H. (1999) 'Novel sensing mechanisms and targets for the cAMP-protein kinase A pathway in the yeast Saccharomyces cerevisiae', *Molecular Microbiology*, 33(5), pp. 904–918. doi: 10.1046/j.1365-2958.1999.01538.x.

Thomas, D. and Surdin-Kerjan, Y. (1997) ‘Metabolism of sulfur amino acids in Saccharomyces cerevisiae’, *Microbiology and Molecular Biology Reviews*, 61(4), pp. 503–532. doi: 10.1128/mmbr.61.4.503-532.1997.

Ting, P. Y. *et al.* (2015) ‘Tyrosine phosphorylation of RAS by ABL allosterically enhances effector binding’, *The FASEB Journal*, 29(9), pp. 3750–3761. doi: 10.1096/fj.15-271510.

Tisi, R., Belotti, F. and Martegani, E. (2014) ‘Yeast as a Model for Ras Signalling’, in, pp. 359–390. doi: 10.1007/978-1-62703-791-4_23.

Toda, T. *et al.* (1985) ‘In yeast, RAS proteins are controlling elements of adenylate cyclase’, *Cell*, 40(1), pp. 27–36. doi: 10.1016/0092-8674(85)90305-8.

Tokiwa, G. *et al.* (1994) ‘Inhibition of Gl cyclin activity by the Ras/cAMP pathway in yeast’, *Nature*, 371(6495), pp. 342–345. doi: 10.1038/371342a0.

Tonini, M. L. *et al.* (2018) ‘Branched late-steps of the cytosolic iron-sulphur cluster assembly machinery of Trypanosoma brucei’, *PLOS Pathogens*. Edited by N. J. Garg, 14(10), p. e1007326. doi: 10.1371/journal.ppat.1007326.

Trahey, M. and McCormick, F. (1987) ‘A cytoplasmic protein stimulates normal N-ras p21 GTPase, but does not affect oncogenic mutants’, *Science*, 238(4826), pp. 542–545. doi: 10.1126/science.2821624.

Tsaousis, A. D. *et al.* (2014) ‘Evolution of the Cytosolic Iron-Sulfur Cluster Assembly Machinery in Blastocystis Species and Other Microbial Eukaryotes’, *Eukaryotic Cell*, 13(1), pp. 143–153. doi: 10.1128/EC.00158-13.

Tu, B. P. *et al.* (2007) ‘Cyclic changes in metabolic state during the life of a yeast cell’, *Proceedings of the National Academy of Sciences*, 104(43), pp. 16886–16891. doi: 10.1073/pnas.0708365104.

Unger, M. W. and Hartwell, L. H. (1976) ‘Control of cell division in Saccharomyces cerevisiae by methionyl-tRNA’, *Proceedings of the National Academy of Sciences*, 73(5), pp.

1664–1668. doi: 10.1073/pnas.73.5.1664.

Vanhamme, L. and Szpirer, C. (1989) ‘Spontaneous and 5-azacytidine-induced revertants of methionine-dependent tumor-derived and H-ras-1-transformed cells’, *Experimental Cell Research*, 181(1), pp. 159–168. doi: 10.1016/0014-4827(89)90190-0.

Varshavsky, A. (1996) ‘The N-end rule: functions, mysteries, uses.’, *Proceedings of the National Academy of Sciences*, 93(22), pp. 12142–12149. doi: 10.1073/pnas.93.22.12142.

Varshavsky, A. (1997) ‘The N-end rule pathway of protein degradation’, *Genes to Cells*, 2(1), pp. 13–28. doi: 10.1046/j.1365-2443.1997.1020301.x.

Vetter, I. R. (2001) ‘The Guanine Nucleotide-Binding Switch in Three Dimensions’, *Science*, 294(5545), pp. 1299–1304. doi: 10.1126/science.1062023.

De Virgilio, C. and Loewith, R. (2006) ‘The TOR signalling network from yeast to man’, *The International Journal of Biochemistry & Cell Biology*, 38(9), pp. 1476–1481. doi: 10.1016/j.biocel.2006.02.013.

Vlastaridis, P. *et al.* (2017) ‘Estimating the total number of phosphoproteins and phosphorylation sites in eukaryotic proteomes’, *GigaScience*, 6(2). doi: 10.1093/gigascience/giw015.

Waldron, K. J. *et al.* (2009) ‘Metalloproteins and metal sensing’, *Nature*, 460(7257), pp. 823–830. doi: 10.1038/nature08300.

Wang, S. *et al.* (2015) ‘Lysosomal amino acid transporter SLC38A9 signals arginine sufficiency to mTORC1’, *Science*, 347(6218), pp. 188–194. doi: 10.1126/science.1257132.

Wang, X.-W. (2014) ‘Targeting mTOR network in colorectal cancer therapy’, *World Journal of Gastroenterology*, 20(15), p. 4178. doi: 10.3748/wjg.v20.i15.4178.

Weis, K. (2003) ‘Regulating Access to the Genome’, *Cell*, 112(4), pp. 441–451. doi: 10.1016/S0092-8674(03)00082-5.

Welsch, M. E. *et al.* (2017) ‘Multivalent Small-Molecule Pan-RAS Inhibitors’, *Cell*, 168(5),

pp. 878-889.e29. doi: 10.1016/j.cell.2017.02.006.

Wennerberg, K., Rossman, K. L. and Der, C. J. (2005) 'The Ras superfamily at a glance', *Journal of Cell Science*, 118(5), pp. 843–846. doi: 10.1242/jcs.01660.

Whistler, J. L. and Rine, J. (1997) 'Ras2 and Ras1 Protein Phosphorylation in Saccharomyces cerevisiae', *Journal of Biological Chemistry*, 272(30), pp. 18790–18800. doi: 10.1074/jbc.272.30.18790.

Wiles, A. M. *et al.* (2006) 'Nutrient regulation of oligopeptide transport in Saccharomyces cerevisiae', *Microbiology*, 152(10), pp. 3133–3145. doi: 10.1099/mic.0.29055-0.

Williams, V. L., Cohen, P. R. and Stewart, D. J. (2011) 'Sorafenib-induced premalignant and malignant skin lesions', *International Journal of Dermatology*, 50(4), pp. 396–402. doi: 10.1111/j.1365-4632.2010.04822.x.

Willumsen, B. M. *et al.* (1984) 'The p21 ras C-terminus is required for transformation and membrane association', *Nature*, 310(5978), pp. 583–586. doi: 10.1038/310583a0.

WU, S. *et al.* (1996) 'Structural insights into the function of the Rab GDI superfamily', *Trends in Biochemical Sciences*, 21(12), pp. 472–476. doi: 10.1016/S0968-0004(96)10062-1.

Xue, Y., Batlle, M. and Hirsch, J. P. (1998) 'GPR1 encodes a putative G protein-coupled receptor that associates with the Gpa2p Gα subunit and functions in a Ras-independent pathway', *The EMBO Journal*, 17(7), pp. 1996–2007. doi: 10.1093/emboj/17.7.1996.

Yan, J. *et al.* (1998) 'Ras Isoforms Vary in Their Ability to Activate Raf-1 and Phosphoinositide 3-Kinase', *Journal of Biological Chemistry*, 273(37), pp. 24052–24056. doi: 10.1074/jbc.273.37.24052.

Yau, R. and Rape, M. (2016) 'The increasing complexity of the ubiquitin code', *Nature Cell Biology*, 18(6), pp. 579–586. doi: 10.1038/ncb3358.

Yin, C. *et al.* (2019) 'Pharmacological Targeting of STK19 Inhibits Oncogenic NRAS-Driven Melanomagenesis', *Cell*, 176(5), pp. 1113-1127.e16. doi: 10.1016/j.cell.2019.01.002.

Young, A., Lou, D. and McCormick, F. (2013) 'Oncogenic and Wild-type Ras Play Divergent Roles in the Regulation of Mitogen-Activated Protein Kinase Signaling', *Cancer Discovery*, 3(1), pp. 112–123. doi: 10.1158/2159-8290.CD-12-0231.

Yung, Y. *et al.* (1997) 'Detection of ERK activation by a novel monoclonal antibody', *FEBS Letters*, 408(3), pp. 292–296. doi: 10.1016/S0014-5793(97)00442-0.

Zaman, S. *et al.* (2008) 'How Saccharomyces Responds to Nutrients', *Annual Review of Genetics*, 42(1), pp. 27–81. doi: 10.1146/annurev.genet.41.110306.130206.

Zaman, S. *et al.* (2009) 'Glucose regulates transcription in yeast through a network of signaling pathways', *Molecular Systems Biology*, 5(1), p. 245. doi: 10.1038/msb.2009.2.

Zelenaya-Troitskaya, O. *et al.* (1998) 'Functions of the high mobility group protein, Abf2p, in mitochondrial DNA segregation, recombination and copy number in Saccharomyces cerevisiae.', *Genetics*, 148(4), pp. 1763–76. Available at: http://www.ncbi.nlm.nih.gov/pubmed/9581629.

Zeng, T. *et al.* (2014) 'Impeded Nedd4-1-Mediated Ras Degradation Underlies Ras-Driven Tumorigenesis', *Cell Reports*, 7(3), pp. 871–882. doi: 10.1016/j.celrep.2014.03.045.

Zerial, M. and McBride, H. (2001) 'Rab proteins as membrane organizers', *Nature Reviews Molecular Cell Biology*, 2(2), pp. 107–117. doi: 10.1038/35052055.

Zhang, L. *et al.* (2008) 'Gene Expression Signatures of cAMP/Protein Kinase A (PKA)-promoted, Mitochondrial-dependent Apoptosis', *Journal of Biological Chemistry*, 283(7), pp. 4304–4313. doi: 10.1074/jbc.M708673200.

Zhu, J. and Thompson, C. B. (2019) 'Metabolic regulation of cell growth and proliferation', *Nature Reviews Molecular Cell Biology*, 20(7), pp. 436–450. doi: 10.1038/s41580-019-0123-5.

Appendices

Appendix 1. Sequence alignments of wild type *RAS2*^{S225A}

Query: protein sequence submitted

Subject: matching gene bank sequence

```
Sequence ID: gi|296147667|NM_001182936.1 Length: 969
Range 1: 1 to 959

Score:1755 bits(950), Expect:0.0,
Identities:956/959(99%),  Gaps:0/959(0%), Strand: Plus/Plus

Query  117   ATGCCTTTGAACAAGTCGAACATAAGAGAGTACAAGCTAGTCGTCGTTGGTGGTGGTGGT  176
             ||||||||||||||||||||||||||||||||||||||||||||||||||||||||||||
Sbjct  1     ATGCCTTTGAACAAGTCGAACATAAGAGAGTACAAGCTAGTCGTCGTTGGTGGTGGTGGT  60

Query  177   GTTGGTAAATCTGCTTTGACCATACAATTGACCCAATCGCACTTTGTAGATGAATACGAT  236
             ||||||||||||||||||||||||||||||||||||||||||||||||||||||||||||
Sbjct  61    GTTGGTAAATCTGCTTTGACCATACAATTGACCCAATCGCACTTTGTAGATGAATACGAT  120

Query  237   CCCACAATTGAGGATTCATACAGGAAGCAAGTGGTGATTGATGATGAAGTGTCTATATTG  296
             ||||||||||||||||||||||||||||||||||||||||||||||||||||||||||||
Sbjct  121   CCCACAATTGAGGATTCATACAGGAAGCAAGTGGTGATTGATGATGAAGTGTCTATATTG  180

Query  297   GACATTTTGGATACTGCAGGGCAGGAAGAATACTCTGCTATGAGGGAACAATACATGCGC  356
             ||||||||||||||||||||||||||||||||||||||||||||||||||||||||||||
Sbjct  181   GACATTTTGGATACTGCAGGGCAGGAAGAATACTCTGCTATGAGGGAACAATACATGCGC  240

Query  357   AACGGCGAAGGATTCCTATTGGTTTACTCTATAACGTCCAAGTCGTCTCTTGATGAGCTT  416
             ||||||||||||||||||||||||||||||||||||||||||||||||||||||||||||
Sbjct  241   AACGGCGAAGGATTCCTATTGGTTTACTCTATAACGTCCAAGTCGTCTCTTGATGAGCTT  300

Query  417   ATGACTTACTATCAACAGATATTGAGAGTCAAAGATACCGACTATGTTCCAATTGTGGTT  476
             ||||||||||||||||||||||||||||||||||||||||||||||||||||||||||||
Sbjct  301   ATGACTTACTATCAACAGATATTGAGAGTCAAAGATACCGACTATGTTCCAATTGTGGTT  360

Query  477   GTTGGTAACAAATCTGATTTAGAAAACGAAAAACAGGTCTCTTACCAGGACGGGTTGAAC  536
             ||||||||||||||||||||||||||||||||||||||||||||||||||||||||||||
Sbjct  361   GTTGGTAACAAATCTGATTTAGAAAACGAAAAACAGGTCTCTTACCAGGACGGGTTGAAC  420

Query  537   ATGGCAAAGCAAATGAACGCTCCTTTCTTGGAGACATCTGCTAAGCAAGCAATCAACGTG  596
             ||||||||||||||||||||||||||||||||||||||||||||||||||||||||||||
Sbjct  421   ATGGCAAAGCAAATGAACGCTCCTTTCTTGGAGACATCTGCTAAGCAAGCAATCAACGTG  480

Query  597   GAAGAGGCGTTTTACACTCTAGCACGTTTAGTTAGAGACGAAGGCGGCAAGTACAACAAG  656
             ||||||||||||||||||||||||||||||||||||||||||||||||||||||||||||
Sbjct  481   GAAGAGGCGTTTTACACTCTAGCACGTTTAGTTAGAGACGAAGGCGGCAAGTACAACAAG  540

Query  657   ACTTTGACGGAAAATGACAACTCCAAGCAAACTTCTCAAGATACAAAAGGGAGCGGTGCC  716
             ||||||||||||||||||||||||||||||||||||||||||||||||||||||||||||
Sbjct  541   ACTTTGACGGAAAATGACAACTCCAAGCAAACTTCTCAAGATACAAAAGGGAGCGGTGCC  600

Query  717   AACTCTGTGCCTAGAAATAGCGGTGGCCACAGGAAGATGAGCAATGCTGCCAACGGTAAA  776
             ||||||||||||||||||||||||||||||||||||||||||||||||||||||||||||
Sbjct  601   AACTCTGTGCCTAGAAATAGCGGTGGCCACAGGAAGATGAGCAATGCTGCCAACGGTAAA  660

Query  777   AATGTGAACAGTGCCACAACTGTCGTGAATGCCAGGAATGCAAGCATAGAGAGTAAGACA  836
             ||||||||||||  ||||||||||||||||||||||||||||||||||||||||||||||
Sbjct  661   AATGTGAACAGTAGCACAACTGTCGTGAATGCCAGGAATGCAAGCATAGAGAGTAAGACA  720

Query  837   GGGTTGGCAGGCAACCAGGCGACAAATGGTAAGACACAAACTGATCGCACCAATATAGAC  896
             ||||||||||||||||||||||||||||||||||||||||||||||||||||||||||||
Sbjct  721   GGGTTGGCAGGCAACCAGGCGACAAATGGTAAGACACAAACTGATCGCACCAATATAGAC  780

Query  897   AATTCCACGGGCCAAGCTGGTCAGGCCAACGCTCAAAGCGCTAATACGGTTAATAATCGT  956
             ||||||||||||||||||||||||||||||||||||||||||||||||||||||||||||
Sbjct  781   AATTCCACGGGCCAAGCTGGTCAGGCCAACGCTCAAAGCGCTAATACGGTTAATAATCGT  840

Query  957   GTAAATAATAATAGTAAGGCCGGTCAAGTTTCAAATGCTAAACAGGCTAGGAAGCAGCAA  1016
             ||||||||||||||||||||||||||||||||||||||||||||||||||||||||||||
Sbjct  841   GTAAATAATAATAGTAAGGCCGGTCAAGTTTCAAATGCTAAACAGGCTAGGAAGCAGCAA  900

Query  1017  GCTGCACCCGGCGGTAACACCAGTGAAGCCTCCAAGAGCGGACCGGGTGGCTGTTGTAT  1075
             ||||||||||||||||||||||||||||||||||||||||||| ||||||||||||||||
Sbjct  901   GCTGCACCCGGCGGTAACACCAGTGAAGCCTCCAAGAGCGGATCGGGTGGCTGTTGTAT  959
```

Appendix 2. Sequence alignments of wild type *RAS2*^{S225E}
Query: protein sequence submitted
Subject: matching gene bank sequence

Query: CLJ977_16479778_16479778 Query ID: lcl|Query_18749 Length: 1244

>Saccharomyces cerevisiae S288C Ras family GTPase RAS2 (RAS2), partial mRNA
Sequence ID: gi|296147667|NM_001182936.1 Length: 969
Range 1: 1 to 969

Score:1773 bits(960), Expect:0.0,
Identities:967/970(99%), Gaps:2/970(0%), Strand: Plus/Plus

```
Query  118   ATGCCTTTGAACAAGTCGAACATAAGAGAGTACAAGCTAGTCGTCGTTGGTGGTGGTGGT  177
             ||||||||||||||||||||||||||||||||||||||||||||||||||||||||||||
Sbjct  1     ATGCCTTTGAACAAGTCGAACATAAGAGAGTACAAGCTAGTCGTCGTTGGTGGTGGTGGT  60

Query  178   GTTGGTAAATCTGCTTTGACCATACAATTGACCCAATCGCACTTTGTAGATGAATACGAT  237
             ||||||||||||||||||||||||||||||||||||||||||||||||||||||||||||
Sbjct  61    GTTGGTAAATCTGCTTTGACCATACAATTGACCCAATCGCACTTTGTAGATGAATACGAT  120

Query  238   CCCACAATTGAGGATTCATACAGGAAGCAAGTGGTGATTGATGATGAAGTGTCTATATTG  297
             ||||||||||||||||||||||||||||||||||||||||||||||||||||||||||||
Sbjct  121   CCCACAATTGAGGATTCATACAGGAAGCAAGTGGTGATTGATGATGAAGTGTCTATATTG  180

Query  298   GACATTTTGGATACTGCAGGGCAGGAAGAATACTCTGCTATGAGGGAACAATACATGCGC  357
             ||||||||||||||||||||||||||||||||||||||||||||||||||||||||||||
Sbjct  181   GACATTTTGGATACTGCAGGGCAGGAAGAATACTCTGCTATGAGGGAACAATACATGCGC  240

Query  358   AACGGCGAAGGATTCCTATTGGTTTACTCTATAACGTCCAAGTCGTCTCTTGATGAGCTT  417
             ||||||||||||||||||||||||||||||||||||||||||||||||||||||||||||
Sbjct  241   AACGGCGAAGGATTCCTATTGGTTTACTCTATAACGTCCAAGTCGTCTCTTGATGAGCTT  300

Query  418   ATGACTTACTATCAACAGATATTGAGAGTCAAAGATACCGACTATGTTCCAATTGTGGTT  477
             ||||||||||||||||||||||||||||||||||||||||||||||||||||||||||||
Sbjct  301   ATGACTTACTATCAACAGATATTGAGAGTCAAAGATACCGACTATGTTCCAATTGTGGTT  360

Query  478   GTTGGTAACAAATCTGATTTAGAAAACGAAAAACAGGTCTCTTACCAGGACGGGTTGAAC  537
             ||||||||||||||||||||||||||||||||||||||||||||||||||||||||||||
Sbjct  361   GTTGGTAACAAATCTGATTTAGAAAACGAAAAACAGGTCTCTTACCAGGACGGGTTGAAC  420

Query  538   ATGGCAAAGCAAATGAACGCTCCTTTCTTGGAGACATCTGCTAAGCAAGCAATCAACGTG  597
             ||||||||||||||||||||||||||||||||||||||||||||||||||||||||||||
Sbjct  421   ATGGCAAAGCAAATGAACGCTCCTTTCTTGGAGACATCTGCTAAGCAAGCAATCAACGTG  480

Query  598   GAAGAGGCGTTTTACACTCTAGCACGTTTAGTTAGAGACGAAGGCGGCAAGTACAACAAG  657
             ||||||||||||||||||||||||||||||||||||||||||||||||||||||||||||
Sbjct  481   GAAGAGGCGTTTTACACTCTAGCACGTTTAGTTAGAGACGAAGGCGGCAAGTACAACAAG  540

Query  658   ACTTTGACGGAAAATGACAACTCCAAGCAAACTTCTCAAGATACAAAAGGGAGCGGTGCC  717
             ||||||||||||||||||||||||||||||||||||||||||||||||||||||||||||
Sbjct  541   ACTTTGACGGAAAATGACAACTCCAAGCAAACTTCTCAAGATACAAAAGGGAGCGGTGCC  600

Query  718   AACTCTGTGCCTAGAAATAGCGGTGGCCACAGGAAGATGAGCAATGCTGCCAACGGTAAA  777
             ||||||||||||||||||||||||||||||||||||||||||||||||||||||||||||
Sbjct  601   AACTCTGTGCCTAGAAATAGCGGTGGCCACAGGAAGATGAGCAATGCTGCCAACGGTAAA  660

Query  778   AATGTGAACAGTGAG-ACAACTGTCGTGAATGCCAGGAATGCAAGCATAGAGAGTAAGAC  836
             |||||||||||| || ||||||||||||||||||||||||||||||||||||||||||||
Sbjct  661   AATGTGAACAGT-AGCACAACTGTCGTGAATGCCAGGAATGCAAGCATAGAGAGTAAGAC  719

Query  837   AGGGTTGGCAGGCAACCAGGCGACAAATGGTAAGACACAAACTGATCGCACCAATATAGA  896
             ||||||||||||||||||||||||||||||||||||||||||||||||||||||||||||
Sbjct  720   AGGGTTGGCAGGCAACCAGGCGACAAATGGTAAGACACAAACTGATCGCACCAATATAGA  779

Query  897   CAATTCCACGGGCCAAGCTGGTCAGGCCAACGCTCAAAGCGCTAATACGGTTAATAATCG  956
             ||||||||||||||||||||||||||||||||||||||||||||||||||||||||||||
Sbjct  780   CAATTCCACGGGCCAAGCTGGTCAGGCCAACGCTCAAAGCGCTAATACGGTTAATAATCG  839

Query  957   TGTAAATAATAATAGTAAGGCCGGTCAAGTTTCAAATGCTAAACAGGCTAGGAAGCAGCA  1016
             ||||||||||||||||||||||||||||||||||||||||||||||||||||||||||||
Sbjct  840   TGTAAATAATAATAGTAAGGCCGGTCAAGTTTCAAATGCTAAACAGGCTAGGAAGCAGCA  899

Query  1017  AGCTGCACCCGGCGGTAACACCAGTGAAGCCTCCAAGAGCGGACCGGGTGGCTGTTGTAT  1076
             |||||||||||||||||||||||||||||||||||||||||||| ||||||||||||||||
Sbjct  900   AGCTGCACCCGGCGGTAACACCAGTGAAGCCTCCAAGAGCGGATCGGGTGGCTGTTGTAT  959

Query  1077  TATAAGTTAA  1086
             ||||||||||
Sbjct  960   TATAAGTTAA  969
```